

**AIRCRAFT MEASUREMENTS OF THE  
IMPACTS OF POLLUTION AEROSOLS  
ON CLOUDS AND PRECIPITATION OVER  
THE SIERRA NEVADA**

**APPENDICES TO THE FINAL REPORT**

*Prepared For:*

**California Energy Commission**  
Public Interest Energy Research Program

*Prepared By:*

Woodley Weather Consultants and The  
Hebrew University of Jerusalem



Arnold Schwarzenegger  
*Governor*

**PIER PROJECT REPORT APPENDICES**

February 2008  
CEC-500-2008-015-AP





**Prepared By:**

Dr. William L. Woodley, President  
Woodley Weather Consultants  
11 White Fir Court  
Littleton, Colorado 80127

and

Dr. Daniel Rosenfeld, Professor  
Department of Atmospheric Sciences  
The Hebrew University of Jerusalem  
Jerusalem, Israel

Commission Contract No. 500-02-004, UC MR-042

**Prepared For:**

Public Interest Energy Research (PIER) Program  
**California Energy Commission**

Guido Franco

**Contract Manager**

Kelly Birkinshaw

**Program Area Lead**

**Energy-Related Environmental Research**

Ken Koyama

**Acting Office Manager**

**Energy Systems Research**

Martha Krebs

**Deputy Director**

**ENERGY RESEARCH & DEVELOPMENT DIVISION**

Melissa Jones

**Executive Director**

## DISCLAIMER

This report was prepared as the result of work sponsored by the California Energy Commission. It does not necessarily represent the views of the Energy Commission, its employees or the State of California. The Energy Commission, the State of California, its employees, contractors and subcontractors make no warrant, express or implied, and assume no legal liability for the information in this report; nor does any party represent that the uses of this information will not infringe upon privately owned rights. This report has not been approved or disapproved by the California Energy Commission nor has the California Energy Commission passed upon the accuracy or adequacy of the information in this report.



## **Table of Contents**

- Appendix A. Worldwide Evidence for the Effect of Aerosols on Clouds and Precipitation
- Appendix B. Operational Documentation of the SUPRECIP-2 Program
- Appendix C. The SOAR Research Aircraft During SUPRECIP-2
- Appendix D. The Satellite Methodology Used in the Research Effort
- Appendix E. Presentation of Flight Tracks and Plotted Data for Flights of the Cloud Physics and Aerosol Aircraft



## **Appendix A**

### **Worldwide Evidence for the Effect of Aerosols on Clouds and Precipitation**



# Appendix A

## Worldwide Evidence for the Effect of Aerosols on Clouds and Precipitation

### 1.0 Introduction

Research on the effects of aerosols on clouds and precipitation over the California Sierra Nevada has been conducted over the past five years by the authors with the support of the Public Interest Energy Research (PIER) Program of the California Energy Commission (Energy Commission). It has taken place in the context of a larger investigation by the authors on the effects of aerosols worldwide. Upon considering the totality of the evidence presented herein, the case to be made for aerosol effects in California becomes stronger and more credible. It is important, therefore, to first present an overview of the results of the total worldwide investigations in order to put the PIER results into the appropriate context. This is done here, beginning with physical principles and ending with a summary of the results of the global investigations.

### 1.1. Physical Principles

Clouds exist because of dynamical and microphysical interactions. When moist air rises due to forcing mechanisms, such as surface convergence and/or heating, frontal lifting, and orographic uplift, it cools to the point of condensation. The drops condensed from the vapor form on aerosol particulates are called cloud condensation nuclei (CCN), which come in various sizes and concentrations. The CCN aerosols typically are a small fraction of the total atmospheric aerosols. If cooling continues within the cloud to temperatures below 0°C, ice may be nucleated on aerosols called ice nuclei (IN). There was a time when dynamical processes were viewed as more important than cloud microphysics, but now a more balanced view prevails as scientists have come to the realization of the great importance of aerosols, especially pollution aerosols, to cloud microphysical processes, for studies of the global climate and for studies of the effects of air pollution on clouds and precipitation. For example, most investigations of climate change have focused on the role of greenhouse gases in global warming and on the role of atmospheric aerosols in cooling the atmosphere by reflecting some of the incoming solar radiation back to space (i.e., global dimming) (Stanhill and Cohen, 2001). Thus, atmospheric aerosols are thought to serve as a counterbalance to global warming due to the greenhouse gases.

Pollution aerosols play other important roles. Several hours after emission from their sources some of the aerosols mature chemically to CCN, depending mainly on their size with little sensitivity to their original chemical composition and origin (Dusek et al., 2006). These CCN aerosols are activated at super saturations typically found in clouds. Gunn and Phillips (1957) have already shown in cloud chamber studies that adding high concentrations of air pollution aerosols to clouds nucleates larger number concentrations of smaller drops that are then slower to coalesce and precipitate than in clouds having low concentrations of CCN aerosols. This effect was observed later by aircraft measurements in polluted clouds mainly over the

otherwise pristine ocean (e.g., Squires, 1958). This was manifested best by ship tracks, which are produced by the CCN aerosols in the effluent from the ship stacks. These tracks are strips of polluted clouds with reduced drop size, as evident from the appearance of the ship tracks mainly in the 3.7  $\mu\text{m}$  reflectance of satellite imagery (e.g., Coakley et al., 1987). Ship tracks appear conspicuous also in the visible when the ambient clouds are so pristine that they become broken and sometime almost completely disappear due to rainout, whereas the ship track clouds remain solid because the aerosol particles from the ship stack suppress the precipitation (Rosenfeld et al., 2006).

The development of microphysical rendering of multi-spectral satellite imagery (Rosenfeld and Lensky, 1998) made it possible to identify ship track features in clouds over land originating from forest fires and from major urban areas, called here "pollution tracks". The launching of the Tropical Rainfall Measuring Satellite (TRMM) (TRMM, 1997) in late 1997 allowed detection of the pollution tracks by the Visible and Infra Red Sensor (VIRS) and measuring the precipitation in the clouds by the Precipitation Radar. Using TRMM, it was shown that precipitation was completely shutoff in tropical clouds having top temperatures  $\geq -10^{\circ}\text{C}$  after having been contaminated by smoke from forest fires in Indonesia (Rosenfeld, 1999) and in the Amazon (Rosenfeld and Woodley, 2003; Andreae et al., 2004). Similar effects were observed by TRMM for clouds contaminated by rural agricultural fires and by the burning of low grade fuels in India (Rosenfeld et al., 2002), and from urban and industrial air pollution in Australia (Rosenfeld, 2000).

Similar suppressive effects of aerosols on the precipitation from deep convective clouds were not anticipated because they reached heights where the clouds developed precipitation. Furthermore, cloud simulations suggest (Khain et al., 2005, Teller and Levin, 2006) that the delay of the onset of precipitation might even invigorate the clouds and lead to overall greater convective overturning and, hence enhanced precipitation, in spite of the reduction in precipitation efficiency (i.e., decreased fraction of condensates that fall as precipitation).

## **1.2. Quantifying the Effect of Aerosols on Orographic Precipitation**

Precipitation-forming processes in shallow orographic clouds having short-living cloud elements are most vulnerable to the effects of pollution aerosols, but the effects are difficult to quantify. Relating trends in the amount of precipitation to the aerosols is not a simple matter, because changes in the global and regional circulation patterns can have strong effects on the local precipitation amounts. This concern hampered efforts to tie directly and quantitatively the effects of anthropogenic aerosols on precipitation amounts. A way to resolve this problem is by relating the precipitation between two adjacent areas, where the precipitation in what is called the control area is little affected by the anthropogenic aerosols, while there is a basis to expect that the precipitation in the target area is affected by these aerosols. In such case, changes in the ratio of target/control precipitation can be related to changes in the aerosols. This requires that the precipitation in the target and control areas is highly correlated, which means that other factors causing variability in the precipitation amounts affect similarly the two areas and have little impact on the ratio between them.

Givati and Rosenfeld (2004) demonstrated that orographic clouds, which form as air is forced upward when passing over topographic barriers, are much more susceptible to suppression of precipitation by air pollution aerosols than clouds forming over the plains. Therefore, precipitation amounts from orographic clouds are often sensitive to the aerosols. For example, Borys et al., (2003) have shown that the addition of as little as  $1\text{-}\mu\text{g m}^{-3}$  of sulfate aerosols to a clean background can reduce the orographic snowfall rate in the Colorado Rocky Mountains by up to 50%, due to suppression of the riming of ice crystals with the smaller cloud droplets. Consequently, trends in the orographic precipitation enhancement factor ( $R_o$ ), which is the ratio between the hill and the upwind plains precipitation, can be used to quantify the effect of the trend in the aerosols on the hill precipitation during the considered period. This is so because the lifetime of the clouds over the hills is limited to the time that the air rises over the upwind slope of the hill. The descending air on the downwind side of the hill forces evaporation of the remaining cloud water that was not precipitated on the upwind slope. The limited available time for conversion of cloud water to precipitation at the upwind slope means that aerosol-induced slowing of that rate would also mean a net reduction of the overall precipitation amount there.

In contrast, the lifetimes of clouds that form over the plains are not restricted to such an extent. Convective clouds typically start to mature and decay as a result of the development of the downdraft, which in turn is initiated by the falling precipitation from the cloud. When the conversion rate of cloud water into precipitation is slowed by added pollution aerosols, this mechanism provides added time for the precipitation-forming processes in clouds over the plains. This effect was simulated to be working in deep warm-based convective clouds (Khain et al., 2005). During the cold season the clouds over the plains are not likely to be thermally driven by surface heating, but rather forced by synoptic features. By their nature, such features are long living, so that the conversion rate of cloud water to precipitation is rarely a limiting factor in the precipitation amounts.

Givati and Rosenfeld (2004) applied this methodology to assess the impact of anthropogenic aerosols on the orographic precipitation enhancement factor ( $R_o$ ). They documented  $R_o$  decreases of 10% to 25% in Israel and over the central and southern Sierra Nevada, downwind of the major coastal urban areas there. This is the point at which WWC became involved in its research effort for the PIER. As a consequence of its PIER contract support, WWC determined (Woodley et al., 2007) that the losses in precipitation were manifested also as losses in stream flows from the polluted regions of the Sierra as contrasted with no changes in the stream flows from the more pristine northern regions of the Sierra. It was determined also that the Pacific decadal oscillation (PDO) and the Southern Oscillation index (SOI) (Allan et al., 1991; Dettinger et al., 2004) cannot explain the observed trends in  $R_o$  (Rosenfeld and Givati, 2006). In addition, it was demonstrated that the quantitative satellite methodology developed by members of the WWC research team could be used to identify the regions that were being affected most detrimentally by the pollution. These satellite assessments were verified by aircraft measurements made during the SUPRECIP effort as described herein. This was done by establishing a direct link between the pollution aerosols and the suppressed precipitation-forming processes in the clouds.

Pollution effects on clouds and precipitation are not limited to California. Rosenfeld and Givati (2006) expanded their study to the whole western United States, where they showed that Ro remained stable over hills in the more pristine areas in northern California and Oregon but decreased again to the east of the densely populated and industrialized Seattle area. Similar effects were observed not only in the Pacific coastal areas, but also well inland. Precipitation was decreased by 18% over the mountains to the east of Salt Lake City, Utah, but it remained unchanged at the southern extension of the same mountain range (Rosenfeld and Givati, 2006; Griffith et al., 2005). Similar effects were found during easterly winds over the eastern slope of the Rocky Mountains downwind (i.e., to the west) of Denver and Colorado Springs (Jirak and Cotton, 2006). These decreasing trends in Ro could not be related to changes in atmospheric circulations such as the El Niño/La Niña or the Pacific Decadal Oscillations (Rosenfeld and Givati, 2006). Although the trends of aerosols are available only since 1988, aerosol measurements from the Interagency Monitoring of Protected Visual Environments (IMPROVE) aerosol monitoring network show that negative trends in Ro at stations having IMPROVE observations are associated with elevated concentrations of fine aerosols (particulate matter less than 2.5  $\mu\text{m}$  in diameter [ $\text{PM}_{2.5}$ ]). The  $\text{PM}_{2.5}$  showed stability or some increase in the areas where their levels were elevated and decreasing trends of Ro were noted. Strong decreasing trends of the coarse aerosols ( $\text{PM}_{10}$ – $\text{PM}_{2.5}$ ) were noted, especially in the areas with elevated levels of  $\text{PM}_{2.5}$ . The decreasing trend in coarse aerosols (which may act to initiate and enhance precipitation), in conjunction with the constancy and/or increases of the small aerosols (which frequently suppress precipitation), may explain the continuing decreases in orographic precipitation during the last two decades despite the improvement in conventional air quality. These results are summarized in Figure 1.

Numerical model simulations played a major role in the research effort for PIER that resulted in a paper by Lynn et al. (2006) strengthening the plausibility of the mechanism proposed by Givati and Rosenfeld (2004) for the suppression of precipitation in the California Sierra Nevada. Spectral (bin) microphysics was coupled to the Weather Research Forecast (WRF) model to investigate the effect of aerosols (i.e., air pollution) on precipitation in the Sierra Nevada Mountains. Two-dimensional simulations were produced using either maritime (“clean-air”) or continental (“dirty-air”) aerosols. The simulation with clean air produced more precipitation on the upwind mountain slope than the simulation with continental aerosols. After three hours of simulation time, the simulation with maritime aerosols produced about 30% more precipitation over the length of the mountain slope than the simulation with continental aerosols. This is illustrated in Figure 2.

Sensitivity tests demonstrated the importance of relative humidity and vertical velocity on cloud microphysical structure and precipitation amount. Greater differences in precipitation amounts between simulations with clean and dirty air were obtained when ice microphysical processes were included in the model simulations. Overall the modeled pattern of precipitation loss agrees fairly well with the losses that have been documented (Figure 3).

## Trends of orographic precipitation linked to the trends in aerosols

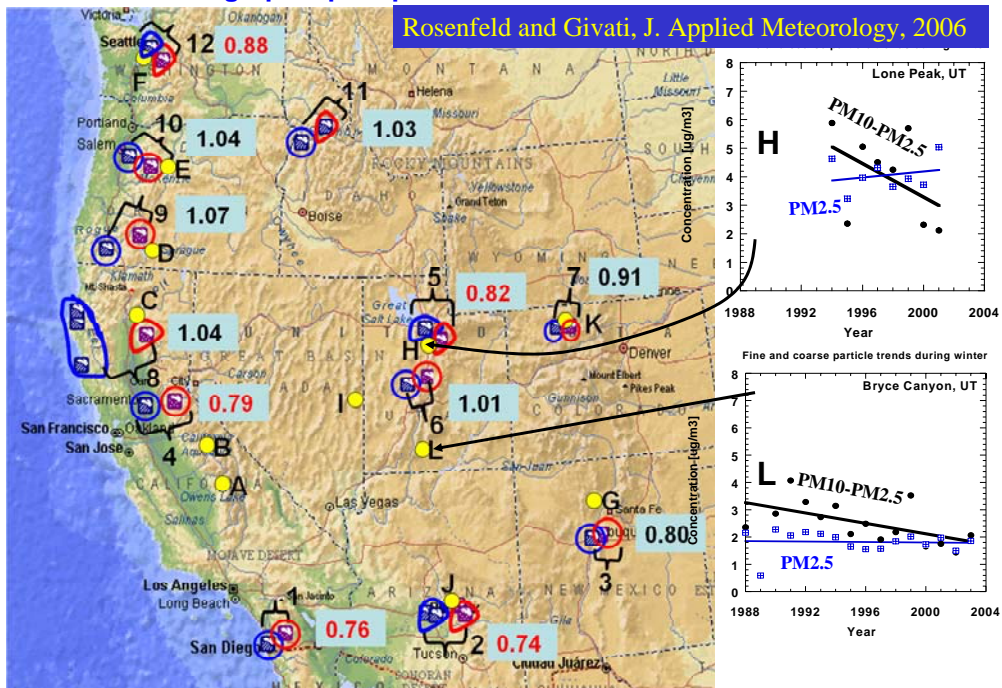
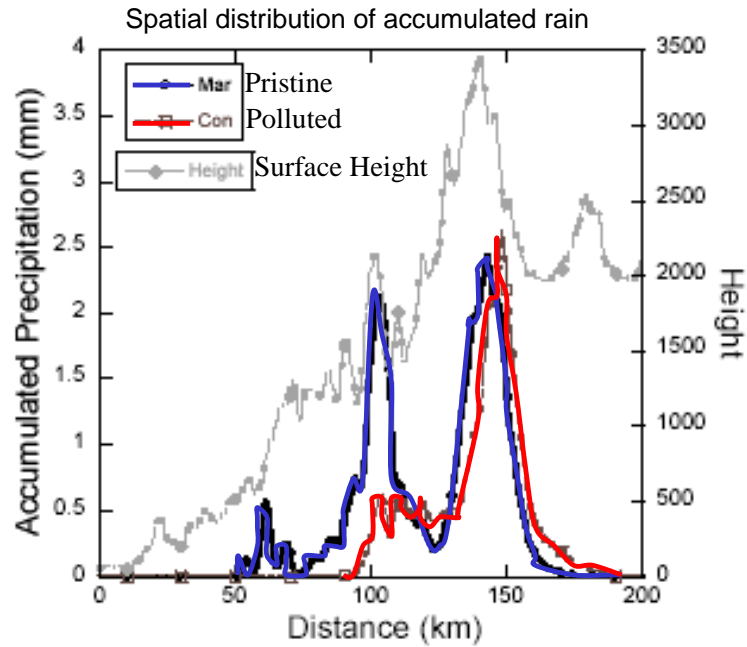


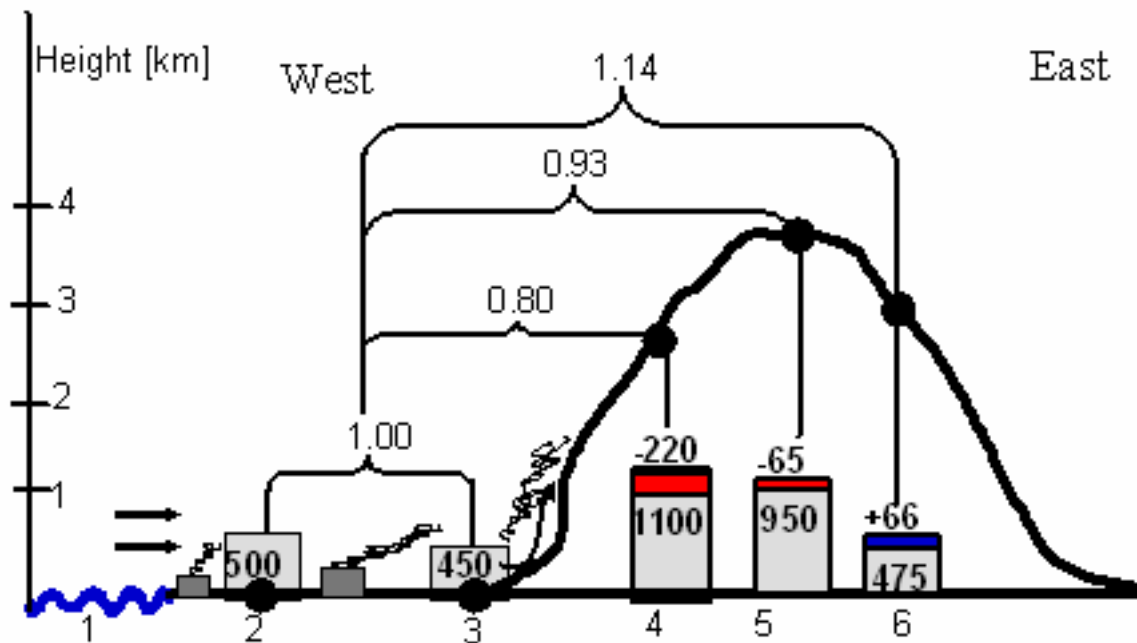
Figure 1. Summary map of the locations of the rain gauges, aerosol monitoring stations, and the main results of the orographic precipitation analyses. Rain gauge pairs are marked with a blue circle for the low station and a red circle for the downwind hilly station. Clusters of gauges are shown by an irregular enclosure. The station pairs are numbered. The fractional change of the winter (October–May) orographic enhancement factor of the high rain gauge(s) with respect to the low rain gauge(s) that was indicated during the measurement period is shown near each pair. The red numbers are smaller than 1.00 with a statistical significance of  $P < 0.05$ ;  $P$  is the statistical significance that corresponds to the Student's  $t$  test statistic, which measures the probability that there is no trend. The locations of the IMPROVE aerosol monitoring stations are shown in the yellow circles. One can see that for the stations shown the fine aerosols (PM<sub>2.5</sub>) have shown a slight increase since 1988 when measurements began while the coarse aerosols (PM<sub>10</sub>–PM<sub>2.5</sub>) have decreased in this time period. Although it cannot be viewed as proof, this is still more observational evidence that aerosols affect the orographic precipitation.

## Explicit 2D cloud simulations of cross section of the Sierra Nevada



Source: B. Lynn, A. Khain, D. Rosenfeld, and W. L. Woodley. 2007. "Effects of Aerosols on Precipitation from Orographic Clouds." *Journal of Geophysical Research* 112, D10225, doi:10.1029/2006JD007537,

**Figure 2. Model-simulated accumulated precipitation on the mountain slope for three hours for both the Maritime-Control (blue) and Continental-Control (red) permutations. A plot of the topography is also shown.**



Source: Givati and Rosenfeld. Applied Meteorology. 2004.

**Figure 3. Topographic cross section of the central Sierra Nevada showing the effects of urban air pollution on precipitation as the clouds move from west to east across the mountains.**

Thus, the totality of the evidence from the research performed by WWC for PIER that involves extensive precipitation and stream flow analyses, quantitative satellite measurements and numerical modeling makes a strong case for the loss of precipitation and stream flows in the California Sierra Nevada due to the generation of anthropogenic pollutants and their ingestion into Sierra clouds. Additional recent research in California and elsewhere has made the case even stronger.

Most recently, Rosenfeld et. al (2007a) used a unique dataset of observations of precipitation, visibility, and winds since 1954 at the top of Mount Hua, China (32°23'N, 109°54'E, 2160 m) to study the effects of pollutants on precipitation using visibility as a proxy for the atmospheric aerosol burden. They found that the ratio between the precipitation at Mount Hua and at the nearby lowland rain gauges decreased during the measurement period by about 20%. The decrease was greater for shorter visibility distances and for stronger winds at the mountaintop. This observation is consistent with the shorter lifetime available for conversion of the cloud water to precipitation when the cloud parcels pass faster and live for a shorter time due to stronger wind speeds across the mountain barrier. The decrease in  $R_o$  over Mount Hua occurred mainly for light and moderate rain days with little change in the probability for days with rain > 30 millimeters (mm) at the mountain top. These additional analyses provide physical fingerprints of the processes and support the hypothesis that the trend of increasing air pollution aerosol concentrations is responsible for the observed decreasing trend of the

orographic precipitation by slowing the conversion of cloud water into precipitation in the short living orographic cloud elements. It is the first time that a proxy to CCN concentrations in the free troposphere—the visibility at the top of Mount Hua at a height of 2160 meters (m) above sea level—has been shown to be directly correlated with the decreasing trend of Ro.

This study in China replicates the results of decreasing trends of Ro by 15%–20% that were already documented previously (Givati and Rosenfeld, 2004 and 2005; Rosenfeld and Givati, 2006; Griffith et al., 2005; Jirak et al., 2006). In addition, the suppression of orographic precipitation downwind of pollution sources has been documented in Australia, South Africa, Portugal, Israel, France, Switzerland, Morocco, Canada, Greece, and Spain. All of these findings, which are based on the analysis of precipitation records, strengthen greatly the credibility of results that have been obtained for California. The China study goes much further, because it has provided the physical fingerprints of the physical processes. It supports the hypothesis that the trend of increasing air pollution aerosol concentrations is responsible for the observed decreasing trend of the orographic precipitation by slowing down the conversion of cloud water to precipitation in the short-living orographic cloud elements.

The global findings make it obvious that there is a problem in polluted regions of the world where orographic precipitation makes a significant contribution to the regional water supply. This realization provides a strong rationale for further investigation, especially for evidence that the precipitation losses result in losses of the surface water supply, as has been shown for California. Rosenfeld et al. (2007b) recently documented the losses of surface water due to pollution to help explain the decreasing trends in the water that is available for consumption from the Lake of Galilee and in the outflow from the main springs of the Jordan River with respect to the nearby rainfall. The loss of more than  $10^8$  cubic meters ( $m^3$ )  $year^{-1}$  (more than 6% of the national water consumption in Israel) is caused by a decreasing trend in the orographic enhancement factor on the topographic barriers that serve as the main catchment areas. As shown by Givati and Rosenfeld (2005) this decreasing trend has been mitigated partially by cloud seeding in Israel for rain enhancement, but apparently the air pollution effects have dominated, causing a net loss of orographic precipitation there. Much of the water resources in this semi-arid area results from orographic precipitation. Therefore, this is an issue having major economic and societal implications, not only for the study area in Israel but for many other densely populated parts of the world where the livelihood of the inhabitants depends on water resulting from orographic precipitation, which might be compromised by the air pollution produced by the very people who depend on that water.

At this juncture it is important to emphasize that the precipitation from orographic clouds is not just sensitive to the detrimental impact of pollution aerosols. This means that seeding the same clouds with aerosols that are engineered to accelerate the conversion of cloud water into precipitation can enhance the precipitation, especially under the conditions where the water losses due to air pollution are the greatest. This already has been shown to be the case in Israel (Givati and Rosenfeld, 2005). Experimental randomized glaciogenic cloud seeding in northern Israel, which was reported to enhance rainfall there by 13%–16% (Gagin and Neumann, 1974 and 1981), has continued operationally since 1975. Givati and Rosenfeld (2005) analyzed the orographic enhancement factor over the hills of northern Israel for the whole period of 1950–

2002, during which  $R_o$  decreased by 15%, in spite of the reported positive seeding effect over the hills there. When separating the time series to seeded and unseeded conditions they found that the trend line of  $R_o$  was shifted upward by 12%–14% for the seeded rain time series compared to the unseeded time series. Thus, the opposite effects of air pollution and seeding appear to have nearly canceled each other in recent years, leading to the false impression that cloud seeding is no longer effective. However, the findings suggest that if the operational seeding were to stop,  $R_o$  would decrease further by about 12%–14%. The sensitivity of  $R_o$  to both seeding and pollution effects was greatest in the areas with the greatest natural orographic enhancement factor and practically nonexistent in areas where  $R_o$  is near unity. This suggests that the orographic clouds in Israel are highly sensitive to air pollution and to cloud seeding, each acting oppositely on the orographic precipitation. This is in agreement with the large susceptibility of precipitation from such short-living shallow clouds to aerosols.

Although the concentrations of IN active at  $-20^{\circ}\text{C}$  become larger in more polluted air masses, the finding that precipitation is suppressed by the air pollution suggests that the detrimental effects of the CCN pollution aerosols overpower the potential positive effects of the IN particles in the air pollution. This is consistent with the indication that the rain suppression due to air pollution in northern Israel overpowers the rain enhancement due to glaciogenic cloud seeding there (Givati and Rosenfeld, 2005). If it were not for the seeding, however, the losses of precipitation would be even greater than they are.

Glaciogenic cloud seeding to augment the Sierra snow pack has been underway in California for at least the last 60 years. Based on the experience in Israel, it is quite possible that the seeding in California has mitigated some of the pollution-induced losses of precipitation in the Sierra since it began around 1950. This should be investigated further.

Examination of the precipitation records over the twentieth century revealed that the detrimental effect of the pollution has not improved with time, despite the decreasing levels of standard measures of air pollution in places such as California. This is explained by the constancy of the very small aerosols that account for the bulk of the CCN concentrations. A major source of very small ( $< 0.1 \mu\text{m}$  diameter) aerosols, which are as efficient as CCN biomass smoke particles, is diesel engines (Lammel and Novakov, 1995). A diesel car produces several orders of magnitude more such particles per mile than a gasoline car with the same fuel consumption (Pierson and Rachaczek, 1984; Williams et al., 1989; Lowenthal et al., 1994; Weingartner et al., 1997; Maricq. et al., 1999). The consumption of diesel fuel in transportation has been increasing in California at twice the rate of gasoline since 1980, and consequently so has the production of these small CCN aerosols, which are not reflected in any of the standard air quality measures. Furthermore, these small and numerous particles have the greatest potential for precipitation suppression. In contrast, the larger ( $> 1 \mu\text{m}$ ) pollution particles could actually induce large drops and enhance precipitation, but these are the particles that have been eliminated most effectively from the emissions.

A different perspective on this problem has been presented in a paper by Kirchstetter et al. (2007) who summarized black carbon observations for the period 1967 through 2003 for the San Francisco Bay Area. Assuming that the BC observations are primarily a manifestation of the

effluent from diesel engines, the authors provide plots showing a sharp decrease in BC particulates even though diesel usage has increased in that period of observation. They ascribe this decrease to more stringent environmental controls and to improved diesel fuels and engines. More work is needed to reconcile these results with those of the SUPRECIP effort.

The totality of the evidence from the many investigations into the effect of pollution aerosols on clouds and precipitation indicate the following:

- Urban and industrialized regions of the world produce pollution aerosols that are most ubiquitous in submicron sizes, because the efforts to remove pollutants have been most effective for larger particle sizes.
- The smallest aerosols acting as cloud condensation nuclei (CCN) are the most suppressive of precipitation-forming processes in clouds.
- CCN pollution aerosols can act to invigorate long-living convective clouds or suppress the formation of precipitation in shallow orographic clouds that have short-living cloud elements. In the former case the CCN promote the transport of larger quantities of cloud water in the form of tiny cloud droplets upward to colder temperatures where the cloud water can freeze, releasing the latent of fusion to the cloudy air that invigorates the cloud. In the latter instance, the CCN act in the manner discussed extensively herein to suppress droplet sizes, coalescence, and precipitation.
- The winter orographic precipitation enhancement factor (Ro) has been decreasing at many locations in the world, including California, most of the Western United States, Australia, South Africa, Portugal, Israel, France, Switzerland, Morocco, China, Canada, Greece, and Spain. The Ro results for South Africa and Portugal are given in Figures 4 and 5.
- Although both absolute precipitation amounts and the precipitation enhancement factor are affected by fluctuations in the atmospheric circulation patterns, such as those associated with the Pacific decadal oscillation (PDO) and the Southern Oscillation index (SOI), these climatic fluctuations cannot explain the observed trends in the orographic precipitation enhancement factor.
- Although the trends of aerosols are available in the United States only since 1988, aerosol measurements from the Interagency Monitoring of Protected Visual Environments (IMPROVE) aerosol monitoring network show that the negative trends in the orographic precipitation enhancement factor are associated with elevated concentrations of fine aerosols (particulate matter less than 2.5  $\mu\text{m}$  in diameter).
- The research that WWC has done for PIER has shown that the regions of precipitation loss in California have higher concentrations of CCN pollution aerosols than more pristine areas and that there is a direct link between the CCN aerosols and the altered cloud structures including suppressed droplet growth and precipitation.
- Recent research involving Mount Hua in China has shown a direct link between reduced visibilities on the mountain, which are a manifestation of the presence of pollution

aerosols, and the loss of precipitation there as manifested by long-term decreases in the orographic precipitation enhancement factor.

- The regions of decreased orographic precipitation enhancement factor in California and Israel have been shown to be regions of decreased stream flows and decreased spring outflows, respectively. Thus, the regions of decreased precipitation enhancement factor are regions experiencing real losses in surface water. This is likely the case in the other regions of the world having comparable decreases in the orographic precipitation enhancement factor.
- Glaciogenic cloud seeding for precipitation enhancement has worked to offset the losses due to pollution in Israel. Consequently, long-term cloud seeding over the Sierra in California may have acted over the years to compensate for the precipitation losses in the polluted portions of the Sierra. This is a matter for further investigation.

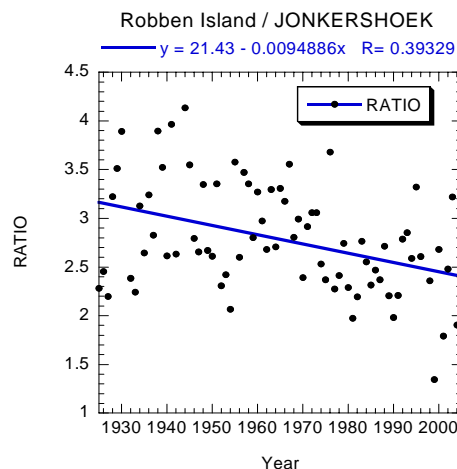


**Figure 4. Map of the southern tip of South Africa (top) showing the pair of stations for which the trend of the precipitation orographic enhancement factor ( $R_o$ ) was calculated. The mountain station was Jonkershoek and the upwind lowland station was Robben Island. The scatter plot and best fit line for the ratio of precipitation at Jonkershoek to Robben Island is given in the bottom panel of the figure.**



The ratio between Portoalegra (600 m) to Lisboa  
Ending / Starting ratio = 1.17 / 1.35 = 0.86

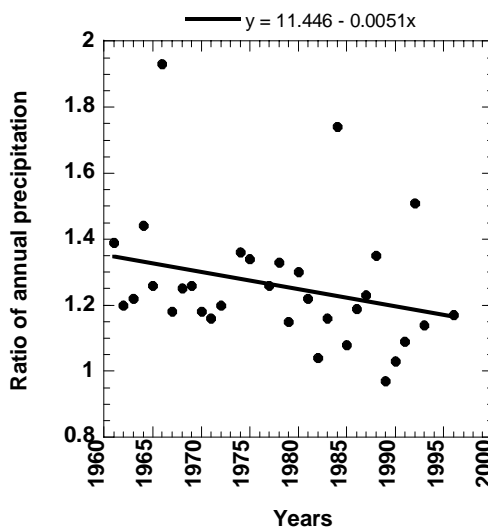


Figure 5. Map of western Portugal (top) showing the pair of stations for which the trend of the orographic factor was calculated. The mountain station was Porto Alegre and the upwind lowland station was Lisbon. The scatter plot and best fit line for the ratio of precipitation at Porto Alegre to Lisbon is given in the bottom panel of the figure.

Despite this strong collective evidence for the suppressive effects of CCN pollution aerosols on clouds and precipitation, it does not prove that sub-micron pollution aerosols are systematically compromising California's water supply. Considering the ramifications for California, obtaining such proof was the major motivation for the SUPRECIP Program.

# **Appendix B**

## **Operational Documentation of the SUPRECIP-2 Program**



## Appendix B

### Operational Documentation of the SUPRECIP Program

#### 1.0 Background

Following the publication of many of the recent findings cited above, a research effort called the Suppression of Precipitation (SUPRECIP) Experiment was conducted to make in situ aircraft measurements of the polluting aerosols, the composition of the clouds ingesting them, and the way the precipitation-forming processes are affected. SUPRECIP was conducted during February and March of 2005 (SUPRECIP-1) and 2006 (SUPRECIP-2). A Cheyenne II, turbo-prop, cloud physics research aircraft was used in SUPRECIP-1 and both the Cheyenne and an additional Cessna 340 aerosol aircraft were flown in SUPRECIP-2. These aircraft were used to measure atmospheric aerosols in pristine and polluted clouds and the impact of the aerosols on cloud-base microstructure, on the evolution with height of the cloud drop-size distribution and on the development of precipitation under warm and mixed-phase processes. They were used also to validate the multi-spectral satellite inferences of cloud structure and the effect of pollutants on cloud processes, especially the suppression of precipitation. This research effort is funded by the PIER (Public Interest Energy Research) Program of the California Energy Commission.

The instruments and respective data sets taken by the aerosol and cloud physics airplanes are given in Tables 1 and 2, respectively. These aircraft flights documented the aerosols and orographic clouds downwind of the densely populated areas in the central Sierra Nevada and contrasted them with the aerosols and clouds downwind of the sparsely populated areas in the northern Sierra Nevada.

The weather during SUPRECIP-1 was highly anomalous for the entire U.S. West Coast, consisting of dry conditions in the Pacific Northwest and flooding rains in Southern California. A high-pressure blocking pattern at the surface and aloft—and the resulting split in the jet-stream flow when it encountered the block—forced some of the weather disturbances to the north and northeast into Canada and Alaska, while some traveled southeastward under the blocking high to the Central and Southern California coast. This persistent region of low pressure under the block produced southerly and southeasterly winds and long periods of middle and high clouds over the Central and Northern Sierra for most of the project. The desired orographic clouds produced by the usual westerly winds into the Sierra were a rarity during SUPRECIP-1, and the program was extended through the first week in March 2005 in the hope of obtaining orographic storm events. Although the weather was a disappointment during SUPRECIP-1, much was learned in documenting the effect of pollutants on cloud microstructure and in validating the satellite inferences of cloud structure using the aircraft measurements and the concurrent radar depictions.

## 2.0 Purpose

An obvious focus of the overall investigation of the effect of pollution on Sierra Nevada winter precipitation ultimately must be on the nature and source of the pollutants that are apparently decreasing the orographic component of the precipitation over the portions of the Sierra Nevada that are climatologically downwind of known pollution sources such as the San Francisco Bay Area and Southern California, including Los Angeles and San Diego. The pollution aerosols are apparently tiny cloud condensation nuclei (CCN) that result in a very narrow spectrum of small drops that inhibits precipitation-forming coalescence processes and ultimately the riming of ice crystals in the clouds. A program, called the Suppression of Precipitation (SUPRECIP) Experiment was conducted to provide the needed documentation, using research aircraft during February and March in 2005 and in 2006 from Sacramento, California. The program documented the number, sizes, and concentrations of ingested aerosols and the resulting internal cloud microphysical structure.

The initial year of SUPRECIP was conducted under the umbrella of Woodley Weather Consultants (WWC), which specializes in weather modification studies, with the participation of other specialists in the field:

1. Prof. Daniel Rosenfeld of the Hebrew University of Jerusalem in Jerusalem, Israel. Professor Rosenfeld is known worldwide for his pioneering studies of the effects of pollutants on clouds.
2. The Seeding Operations and Atmospheric Research (SOAR) program, which is managed by the Sandy Land Underground Water Conservation District in Plains, Texas. SOAR provided the Cheyenne II, turbo-prop, cloud-physics aircraft; a pilot (Dr. David Prentice M.D. in 2005 and Mr. Gary Walker in 2006); and flight meteorologist Duncan Axisa.
3. Dr. Don Collins of the Atmospheric Aerosol Research Group within the Department of Atmospheric Sciences at Texas A&M University.

The use of the cloud physics aircraft made it possible to document differences in cloud microstructure associated with differences in CCN, measured by the airborne CCN counter, that were visibly related to air pollution. It was determined further that these differences were related visibly to the satellite retrievals, which were validated by the aircraft measurements. This is crucial, because previously only the satellite retrievals were available as indicators of the apparent negative effect of pollution on Sierra precipitation. Thus, the new aircraft measurements have validated the satellite inferences of cloud microstructure by showing the negative impact of pollutants on cloud processes and precipitation, thereby making the linkages much more credible. Pollution is certainly affecting Sierra clouds and precipitation detrimentally. Through the aircraft and satellite measurements in SUPRECIP it has been noted that much of the Sierra precipitation was produced by surprisingly shallow pristine clouds. This suggests that pollution will act detrimentally on such clouds and may help explain the long-term losses in Sierra orographic precipitation.

The totality of the contract work by WWC for the California Energy Commission through the initial year of SUPRECIP produced the following overall results:

- Strong observational evidence, obtained from aircraft and satellite platforms, shows that cloud microstructures have been altered, the net orographic component of Sierra Nevada precipitation has been diminished and the resulting stream flows have been reduced—primarily downwind of major urban and industrial areas. These changes have been most pronounced since 1945 and continue to the present. Little change has been noted in more pristine areas, especially over the northern Sierra.
- The changes above have been noted over much of the Western United States.
- These changes apparently have been produced by the ingestion of fine ( $< 1 \mu\text{m}$  diameter) particles, acting as hygroscopic CCN produced in the urban/industrial areas, which make the clouds microphysically inefficient in the formation of precipitation-sized drops and ice particles.
- Model simulations support the relationship between the pollutants and the suppressed net precipitation and runoff.
- Demonstration that the apparent changes in cloud microphysical properties and precipitation, as noted in the processed satellite imagery, correspond to “real” changes in cloud structure, as documented by aircraft measurements.
- The documented changes in cloud properties are apparently due to anthropogenic pollutants generated locally in California.

Although the results from the initial year of SUPRECIP supported the view that pollution is suppressing California orographic precipitation, further investigation was needed, because it was impossible to characterize the problem in only a five-week measurement program. The weather was highly anomalous for the entire U.S. West Coast during the measurement program. Because of a high-pressure blocking pattern at the surface and aloft and the resulting split in the jet-stream flow, the usual Pacific storms were shunted far to the south of Sacramento. Thus, the typical Sierra orographic clouds, produced by westerly winds into the Sierra and thought to be most sensitive to the effects of pollution, were rare during SUPRECIP.

SUPRECIP was continued for a second year as SUPRECIP-2 to focus on the orographic storm events in the Sierra Nevada that were lacking in 2005. Specifically, it was crucial to document the ingestion of the pollution aerosols by the orographic clouds as they formed and moved uphill. The satellite imagery already says that this is taking place and the precipitation measurements show the long-term effects of the pollution. It was nearly impossible in 2005 to systematically “map” the pollution aerosols at low to mid levels in urban and downwind areas with the Cheyenne II cloud physics aircraft while it was in instrument flight rules (IFR) flight. Because of this, a second aircraft (a Cessna 340 II) was used in SUPRECIP-2 to carry cloud nucleus (CN) and CCN counters to map aerosols during visual flight rules (VFR) flight. More attention was focused on the details of the pollution “footprint” as to the sources, kinds, and concentrations of the pollution aerosols and on what portions of the Sierra should be most affected by them. With this plan the Cessna 340 low-level aircraft mapped the pollution aerosols upwind of the coast, over the urban/industrial areas and downwind while the Cheyenne II cloud physics aircraft flew above to document their effects on the clouds ingesting them. The

two specially instrumented research aircraft were provided by the Seeding Operations & Atmospheric Research (SOAR) group, which specializes in conducting scientific weather modification research and operations. Photographs of these aircraft, along with documentation of the instruments that they carried in SUPRECIP-2, are given in Appendix C.

### **3.0 SUPRECIP-2 Program Overview**

The SUPRECIP-2 personnel and aircraft arrived at the Sacramento Executive Airport in late January 2006. The first flight day was on February 2, 2006, when the Cessna 340 aircraft conducted its first test flight. The last flights took place on March 14, 2006. During the 43 days of SUPRECIP-2 (i.e., February 1 through March 15, 2006) there was a flight of at least one project aircraft on 21 of the 43 days. Only one of the project aircraft flew on 4 of the 21 flight days. Flights of both project aircraft were made on the remaining 17 days. Since arriving in Sacramento, 53 research missions were flown on the 21 flight days—25 by the Cheyenne II cloud physics aircraft (named “Cloud 1”) and 28 by the Cessna 340 aerosol aircraft (named “Cloud 2”). A little over half (27 of 53) of the research missions were flown in March 2006. After a slow beginning with mostly unsuitable weather during February 2006, the weather improved greatly for the purposes of SUPRECIP-2, resulting in 10 flight days in March 2006. Only 47 minutes of flight time remained out of a total allotment of 110 hours at the outset of the program. A summary of the flights and the weather is provided in Table 1. Appendix C details the aircraft and their instrumentation systems. An assessment of the quality of the collected aircraft data is presented in Table 2 of that appendix. Important information for the SUPRECIP-2 flight days is also provided in Appendix C.

Concurrent with the SUPRECIP-2 operations was the operation of The National Oceanic and Atmospheric Administration’s (NOAA’s) Hydrometeorology Testbed (HMT) program, which is designed to bridge the wide chasm and to shorten the long lag time that exists currently between new research findings by its laboratory and university affiliates and NOAA Operations by the National Weather Service and its River Forecast Centers. Specifically, NOAA’s HMT is a program to accelerate the transfer of new technologies (e.g., observing instruments, numerical forecast models, and scientific techniques) whereby researchers and operational forecasters join forces in an operational setting to demonstrate, test, and evaluate the usefulness of new tools. The plan calls for the implementation of the HMT incrementally in different regions of the United States. The initial field year of the HMT was in Northern California, beginning on November 30, 2005, and extending through March 7, 2006, with primary emphasis on the North Fork of the American River Basin (ARB).

The SUPRECIP-2 operational area included the HMT area of interest so that the data exchange, on which there already is agreement in principle, will benefit the analyses for both programs. The ARB HMT has been divided into 14 Intensive Operating Periods (IOPs), which were typically 36 hours duration. Table 2 lists the periods. IOP-13, which encompasses March 2 and 3, 2006, already has been given first priority for an exchange of data and analyses.

The ARB HMT period was quite wet. December 2005 was about three times wetter than normal, and March 2006 had roughly twice normal precipitation. Figure 1 presents time plots of the

daily precipitation (water equivalent in the case of snow) for Sacramento International Airport and Blue Canyon in the Sierra. Note that the biggest storm was on New Year's Day, 2006, which is included in IOP-4. About 6 inches of precipitation was measured on this day and 9.58 inches was measured during IOP-4.

The weather during SUPRECIP-2 on February 1 and 2 consisted of a moist WNW flow of air over Northern California with showers and enhanced precipitation over the mountains. There was a prolonged period of ridging from February 3 to 14, and this was followed by weaker ridging from February 19 to 25. There was no precipitation during the period of ridging. A strong trough and cold front passed through the area on February 26 to 28. March 1 was a "between troughs" day, and a new trough and front approached the area on March 2. The cold front passed through the project area on March 3, and it was clear and cool on March 4. Yet another cold front approached the area on March 5 bringing rain by afternoon. Frontal and trough passage took place on March 6 and March 7, respectively. Another trough was approaching the project area on March 8, and this deep upper trough was over the area on March 9 through March 11, bringing snow levels down to about 1000 ft mean sea level (MSL). The deep upper trough passed the area on March 12. By March 13 another trough and front were approaching the project area, and frontal and trough passage took place on March 14. Clearing took place on March 15. There were many flight opportunities during the period.

**Table 1. SUPRECIP-2 Flight and Weather Summary**

Date	CLOUD PHYSICS			AEROSOL			Comments (purpose of flight)	Weather conditions
	Flight #	Eng. Start/Flight duration	Shutdown/Cum. Hours	Flight #	Eng. Start/Flight duration	Shutdown/Cum. Hours		
02-02-2006				1	23:00	01:35	Flight test CCN counter, TSI cloud particle counter (CPC) and set valve flow for inlet system.	Strong WNW moist flow with showers especially over the mountains
					2:35	2:35		
02-03-2006	1	22:20	23:30	2	22:27	23:39	Flight test cloud physics aircraft (CIP, FSSP, CDP). Continue flight testing CCN and CPC.	clearing conditions with low SC under overcast thin cirrus
		1:10	1:10		1:12	3:47		
02-04-2006	2	21:10	23:40	3	21:10	23:55	Research flight. Sacramento area to SE near Linden VOR then N and NNW to the west of the Sierra foothills over the Sierra.	Weak morning frontal passage clearing in afternoon.
		2:30	3:40		2:45	6:32		
02-05-2006								Cool & clear, no flights
02-06-2006								Broken to overcast cirrus clouds
02-07-2006								No flights strong ridging
02-08-2006				4	22:55	00:49	To adjust the intake flows on the two aerosol instruments and to make aerosol measurements over the Blodgett Forest Research Station	Strong ridge aloft, light winds, hazy
					1:54	8:26		

**Table 1. (continued)**

02-09-2006									Strong ridge persists, warm with light winds, no flights
02-10-2006	3	23:33 0:57	00:30 4:37	5	23:33 3:00	02:33 11:26	Intercomparison measurements of TSI CPC and temperature probes on both aircraft. Aerosol aircraft continues with CPC measurements.		
02-11-2006									Ridging conditions. No suitable clouds.
02-12-2006									Ridging conditions. No suitable clouds.
02-13-2006									Ridging conditions. No suitable clouds.
02-14-2006									Ridging conditions. No suitable clouds.
02-15-2006	4	18:07 1:58	20:05 6:35	6	18:10 3:15	21:25 14:41	Planned cloud physics flight and aerosol flight over the northern and central Sierra foothills.		Cumulus clouds over mountains. Small Cb clouds and snowshowers. Cold aloft.
02-16-2006	5			7	22:10 2:20	00:30 17:01	Planned cloud physics flight and aerosol flight over the northern Sierra foothills, starting with a formation flight to Blodgett. Flight continued to the central valley and the coastal range.		Few showers, cold trough approaching
02-17-2006	6			8	22:57 1:13	00:10 18:14	Planned cloud physics flight and aerosol flight over the northern Sierra foothills, starting with a formation flight to Blodgett. Flight continued to the central valley and the coastal range.		Showers with upper cold low

**Table 1. (continued)**

02-18-2006	7		9	18:12	21:33	Planned aerosol flight starting towards Blodgett and continuing towards Monterey and San Francisco bay.	Showers with upper cold low	
02-19-2006	8					No flights	Clearing as upper cold low moves away	
02-20-2006	9					No flights	Mostly clear and cool, few clouds over the Sierra, slow warming	
02-21-2006						No flights	Weak ridging aloft, no clouds	
02-21-2006		21:20		23:22		no flight	Maintenance flight	
02-21-2006		2:02		10:57			No flights	Weak ridging, clear, cool and hazy
02-22-2006						No flights	Weak ridging, clear, cool and hazy	
02-23-2006						No flights	Weak ridging, clear, cool and hazy	
02-24-2006						No flights	Increasing high clouds, hazy	
02-25-2006		no flight		22:11	22:44	Check the inlet flow with a TSI flow meter and instruments running.	Patchy high clouds, hazy	
				0:34	22:09			
02-25-2006		no flight		01:04	01:54	Instrument Flight Rules check.		
				0:50	22:59			

**Table 1. (continued)**

02-26-2006	6	18:40	20:14	10	20:20	22:15	Planned aerosol flight starting towards Blodgett and continuing towards Friant.	Deep trough developing to west
		1:26	12:23		1:55	24:54		
02-27-2006	7	17:08	19:16	11	17:10	19:29	Planned aerosol flight starting towards Blodgett with the aerosol aircraft conducting measurements in SFO and OAK area.	Strong frontal band, heavy showers, strong low-level winds
		2:08	14:31		2:19	27:13		
	8	22:14	23:20	12	22:15	23:54		Decreased shower activity as frontal band passes
		1:06	15:37		1:39	28:52		
02-28-2006	9	17:29	20:12	13	17:34	20:30	Measurement of classical orographic clouds over the foothills and the aerosols upwind of the cloud bases.	Strong convection with passage of upper low
		2:43	18:20		2:56	31:48		
	10	22:55	01:45	14	22:54	01:06	Planned aerosol and cloud physics flight measuring convective clouds and aerosols in a mixed boundary layer in the valley and off the coast.	Decreasing shower activity
		2:50	21:10		2:12	34:00		
03-01-2006	11	21:25	00:37	15	21:24	00:23	Planned aerosol and cloud physics flight measuring convective clouds and aerosols over the central valley and the coast.	Post-frontal period as new storm approaches
		3:12	24:22		2:59	36:59		
03-02-2006	12	17:01	18:09	16	17:01	18:55	Planned aerosol and cloud physics flight measuring orographic clouds and aerosols over the foothills and the windward side of the Sierra.	Frontal passage during morning
		1:08	25:30		1:54	38:53		
	13	19:37	20:57	17	19:47	21:00	Same as above to study the evolution of the front.	Post-frontal cloudiness
		1:20	26:50		1:13	40:06		
	14	22:58	00:21	18	22:50	23:55	Same as above to study the evolution and the effects of mixing in the boundary layer.	Post-frontal cloudiness
		1:23	28:13		1:05	41:11		
03-03-2006	15	17:32	19:43	19	17:31	18:43	Planned aerosol and cloud physics flight measuring orographic clouds and aerosols over the foothills and the windward side of the Sierra.	Passage of second cold front in morning
		2:11	30:24		1:12	42:23		
	16	21:35	23:45	20	21:48	23:55	Planned aerosol and cloud physics flight measuring very convective clouds over the foothills of the Sierra.	Vigorous post-frontal convection
		2:10	32:34		2:07	44:30		
03-04-2006								Mostly clear and cool, no suitable clouds
03-05-2006								New front approaching, increasing cloudiness, rain by afternoon and night

**Table 1. (continued)**

03-06-2006	17	17:46	19:28	21	17:40	18:44	Planned aerosol and cloud physics flight measuring orographic clouds and aerosols over the foothills and the windward side of the Sierra.	Frontal passage by sunrise
		1:42	34:16		1:04	45:34		
03-07-2006	18	17:03	19:34	22	17:00	18:30	Planned aerosol and cloud physics flight. Cloud physics aircraft flies to Fresno while the aerosol aircraft flies north.	Passage of sharp upper trough with attendant showers
		2:31	36:47		1:30	47:04		
	19	22:03	23:29	23	22:03	23:56	Planned aerosol and cloud physics flight measuring clouds and aerosols north of Sacramento.	
03-08-2006		1:26	38:13		1:53	48:57		Between upper troughs, increasing high clouds with light rain by evening as new trough digs in
03-09-2006	20	19:28	22:07	24	19:22	23:00	Research flight into orographic clouds in the Sierra foothills to document any N-S differences.	Deep upper trough digging into area with showers and low snow levels
		2:39	40:52		3:38	52:35		
03-10-2006	21	17:07	18:14	25	17:03	20:39	Documentation of the N-S variability of cloud structure and aerosols along the Sierra. Computer fails on Cheyenne and a second flight is attempted.	Very cold, deep upper trough Showers with low snow levels
		1:07	41:59		3:36	56:11		
	22	18:36	20:47					
		2:11	43:10					
03-11-2006	23	17:26	19:43	26	17:21	19:15	Planned research flight from Sacramento to Hangtown and then to the SSE along the foothills.	Very cold, deep upper trough Showers with low snow levels
		2:17	45:27		1:54	58:05		
03-12-2006								Passage of axis of deep cold trough during the day. Very messy weather
03-13-2006	24	18:14	19:55	27	18:06	19:34	Planned aerosol/cloud physics flight for cloud measurements in the foothills and the Sierra crest to measure cap clouds and altocumulus.	Old trough moving away but new trough approaching from west. Overcast middle and high clouds all day.
		1:41	47:08		1:28	59:33		Frontal passage during morning hours
03-14-2006	25	17:49	21:50	28	17:45	20:39	Planned aerosol and cloud physics flight measuring clouds and aerosols in the northern valley and around Mendocino.	showers and thunderstorms in afternoon
		4:01	51:09		2:54	62:27		

**Table 2. HMT-West-2006 Intensive Operating Periods**

<b>Event</b>	<b>Start</b>	<b>End</b>	<b>Blue Canyon Precip (liq. eqv.)</b>	<b>Research Radars</b>		<b>SHS sondes</b>	<b>OAK supplm. sondes</b>
				<b>XPOL</b>	<b>SMARTR</b>		
IOP-1	01DEC05, 00 UTC	02DEC05, 09 UTC	6.98 inches	yes	yes	no	no
IOP-2	18DEC05, 01 UTC	19DEC05, 17 UTC	4.69 inches	yes	yes	no	no
IOP-3	20DEC05, 18 UTC	22DEC05, 12 UTC	4.43 inches	yes	yes	no	no
IOP-4	30DEC05, 12 UTC	01JAN06, 00 UTC	9.58 inches	yes	yes	yes	yes
IOP-5	01JAN06, 21 UTC	03JAN06, 00 UTC	2.20 inches	yes	yes	yes	yes
IOP-6	11JAN06, 00 UTC	11JAN06, 21 UTC	0.57 inches	yes	yes	yes	yes
IOP-7	14JAN06, 03 UTC	15JAN06, 03 UTC	1.05 inches	yes	yes	yes	yes
IOP-8	18JAN06, 00 UTC	19JAN06, 01 UTC	1.32 inches	yes	yes	yes	no
IOP-9	28JAN06, 12 UTC	29JAN06, 09 UTC	1.40 inches	no	no	yes	no
IOP-10	01FEB06, 12 UTC	02FEB06, 20 UTC	2.23 inches	yes	yes	yes	yes
IOP-11	04FEB06, 03 UTC	04FEB06, 21 UTC	0.71 inches	yes	yes	yes	no
IOP-12	27FEB06, 00 UTC	28FEB06, 15 UTC	5.75 inches	yes	yes	yes	yes
IOP-13	02MAR06, 06 UTC	03MAR06, 20 UTC	2.73 inches	yes	no	yes	yes
IOP-14	05MAR06, 09 UTC	07MAR06, 20 UTC	2.85 inches	yes	no	yes	no
Totals		457 IOP hours	46.49 inches	13	11	11	7 IOPs

IOPs captured the main weather events

Daily Precipitation During HMT06  
ALERT/HMT Gauges  
24-Hr Accumulations at 4 a.m. PST (12 UTC)

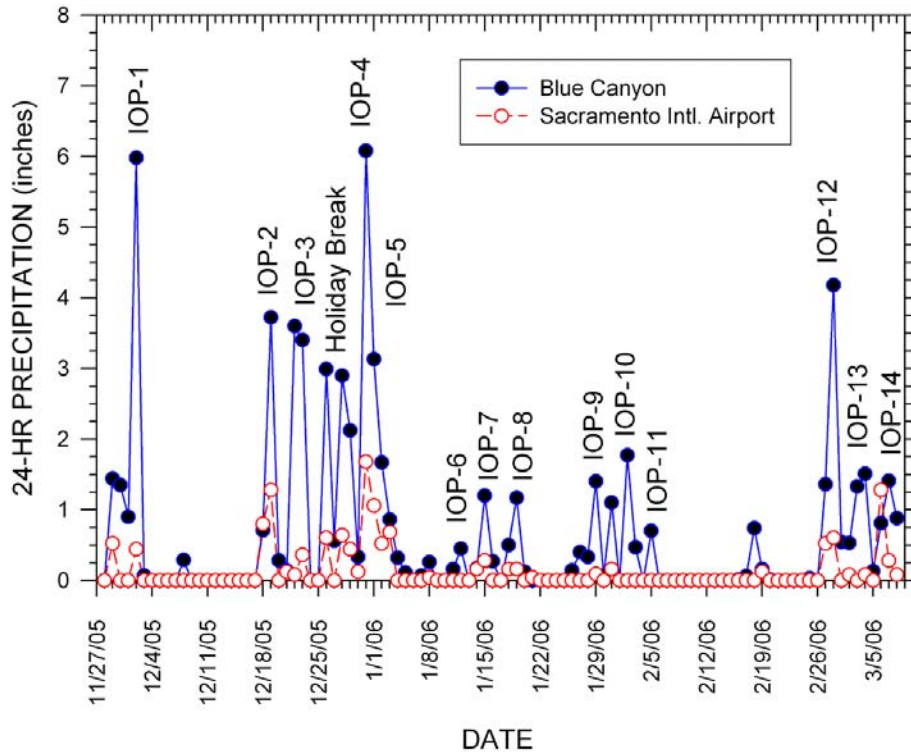


Figure 1. Time plots of the daily precipitation (water equivalent in the case of snow) for Sacramento International Airport and Blue Canyon in the Sierra from November 27, 2005, through March 5, 2006.

## 4.0 Documentation of Weather and Flight Activity on SUPRECIP-2 Priority Case-Study Days

A large body of data was collected during SUPRECIP-2—so much data that it was unreasonable to expect to analyze all of it with the funds and time available. The first step was to prioritize the days and flights for detailed analysis under the contract. Those selected are: the two flights of both research aircraft on February 28 (4 total flights), the flight of both aircraft on March 1 (2 total flights), and the three flights of both aircraft on March 2 (6 total flights). Thus, 12 flights on three flight days were to be subjected to detailed analysis. This section provides the documentation of the weather and flight activity on these days. Comparable documentation for the other flight days of SUPRECIP-2 is given in the SUPRECIP-2 Operational Summary under the contract.

### Aircraft Flight Data: Tuesday, February 28, 2006

#### Weather Situation

A cold front went through our area at about 2130 PST last night with heavy rain and strong winds. The rest of the night had a scattering of showers, but it was partly cloudy by sunrise. The winds veered into the southwest overnight and orographic cloudiness could be seen over the Sierra in the morning satellite images. The morning NWS area forecast discussion, excerpted verbatim each day from the Internet, appears below. Upon considering the weather, the plan of the day was to make a morning flight in order to sample the orographic clouds before widespread convection breaks out later in the day during the passage of the upper trough.

**AREA FORECAST DISCUSSION  
NATIONAL WEATHER SERVICE SACRAMENTO CA  
520 AM PST TUE FEB 28 2006**

**DISCUSSION**

COLD FRONTAL RAIN BAND MOVED ACROSS NORCAL OVERNITE AND REMNANTS OF FRONTAL PCPN CURRENTLY AFFECTING THE EXTREME SERN PORTION OF OUR FORECAST AREA IN SRN TUOLUMNE CO...AND WILL BE MOVING ACROSS YOSEMITE NP THRU 15Z (Figure 2). IN WAKE OF COLD FRONT...DRY SLOT HAS SPREAD OVER NORCAL AS OFFSHORE UPPER LEVEL TROF HAS PUSHED CLOSER TO THE CA COAST AND PUSHED UPPER JET EWD. THIS HAS SHUNTED SUBTROPICAL MOISTURE SE OF OUR FORECAST AREA. BEHIND THE FRONT...SNOW LEVELS BEGINNING TO LOWER...ALTHO PCPN IS ALSO BEGINNING TO WIND DOWN. UPPER LEVEL TROF LOCATED JUST OFF THE CA COAST WILL MOVE ACROSS NORCAL TODAY. CUMULIFORM CLOUDS OFF THE COAST INDICATE A COLD AND UNSTABLE AIR MASS WITH GOES LI'S CLOSE TO -3 IN THE CENTER OF THE UPPER LOW...AND THIS AIR MASS WILL MOVE OVER NORCAL TODAY. 12Z KOAK SOUNDING SHOWS LI OF -4 THIS MORNING (Figure 3). MODEL INSTABILITY PROGS INDICATE CENTRAL VLY WILL BECOME QUITE UNSTABLE THIS AFTN...WITH NAM/GFS MODELS PUTTING CAPE BULLS-EYE OVER SACRAMENTO AREA. SHOWERS/ THUNDERSTORMS OVER NORCAL TODAY LIKELY TO CONTAIN SMALL HAIL OR SLEET. ALTHOUGH OROGRAPHICS FOR THE SIERRA

NEVADA WEAKEN...700 MBS WINDS DECREASE FROM 40-50 KTS TO 15-35 KTS TODAY...SWLY FLOW WILL CONTINUE AHEAD OF THE TROF AND WILL CONTINUE UPSLOPE FLOW OVER SIERNEV. THUS...SHOWERS SHOULD BECOME NUMEROUS AGAIN OVER THE SIERNEV. HOWEVER...QPF WILL BE MUCH LIGHTER WITH AMOUNTS RANGING FROM 3 TO 7 TENTHS OVER THE SIERNEV...AND A COUPLE OF TENTHS IN THE VLY. HOWEVER...WITH CONVECTION...AMOUNTS CAN VARY GREATLY.

THE NEXT ROUND OF PCPN IS EXPECTED OVER NORCAL WED NITE AND INTO THU AS ANOTHER UPPER LOW FROM THE GULF OF AK ROTATES A STRONG VORT LOBE ACROSS THE AREA. THIS LOW IS FORECAST TO TAP A TPW PLUME BETWEEN .70 TO .80 TENTHS OF AN INCH...MUCH WETTER THAN LAST WEEKEND'S STORM... AND WITH COLDER 700 MBS TEMPS FROM -12 TO -14 DEG C...WE EXPECT AN INCREASE IN THE DENDRITIC GROWTH OF ICE CRYSTALS AND PILES OF FINE POWDER FOR THE SIERRA. THIS IS ESPECIALLY SO AS COLDER SHORT WAVES ROTATE AROUND THIS SAME LOW THRU FRI...BRINGING WAVES OF PCPN TO NORCAL. WITH LOW SNOW LEVELS...WE MAY NEED TO ISSUE WINTER STORM WATCH FOR THE MTNS IN NEXT FORECAST PACKAGE.

MAYBE A BRIEF BREAK IN THE WET WX ON SAT...WITH MEDIUM RANGE MODELS FORECASTING STILL ANOTHER UPPER LOW FROM THE GULF OF AK DROPPING SWD AND BRINGING MORE PCPN TO NORCAL.

#### **AVIATION**

UPR TROF OVR NORCAL WITH SCT MVFR AND WDLY SCT IFR CONDS IN SHRA WITH SHSN ABV 035. ISOLD -TSRA OR -TSRAGS PSBL WITH GSTY SFC WINDS. AMS BCMG STBL AFT 03Z WED. MNLY VFR CONDS THRU 00Z THU EXC AREAS IFR CONDS OVR CSTL MTNS AND SHASTA CO IN -RA WITH -SN ABV 025.

There was less radar-echo coverage during the day than was expected. The echo coverage at 2143 Coordinated Universal Time (UTC) is shown in Figure 4. The colorized satellite overpass at 2100 UTC for the Aqua satellite on February 28, 2006 is shown in Figure 5. The methodology that was used to produce this figure is addressed in Appendix D. The satellite images gives a nice view of the Monterey and San Francisco Bay areas. Three areas for which the temperature profiles of effective radius were derived are shown superimposed on the image and the profiles themselves are shown in the insets. Note that the effective radius decreases progressively from the coast (area 1) inland to the central valley (area 3). Figure 6 provides the flight tracks for the two research aircraft (red for Cloud 1 and blue for Cloud 2) on their first flight of the day.

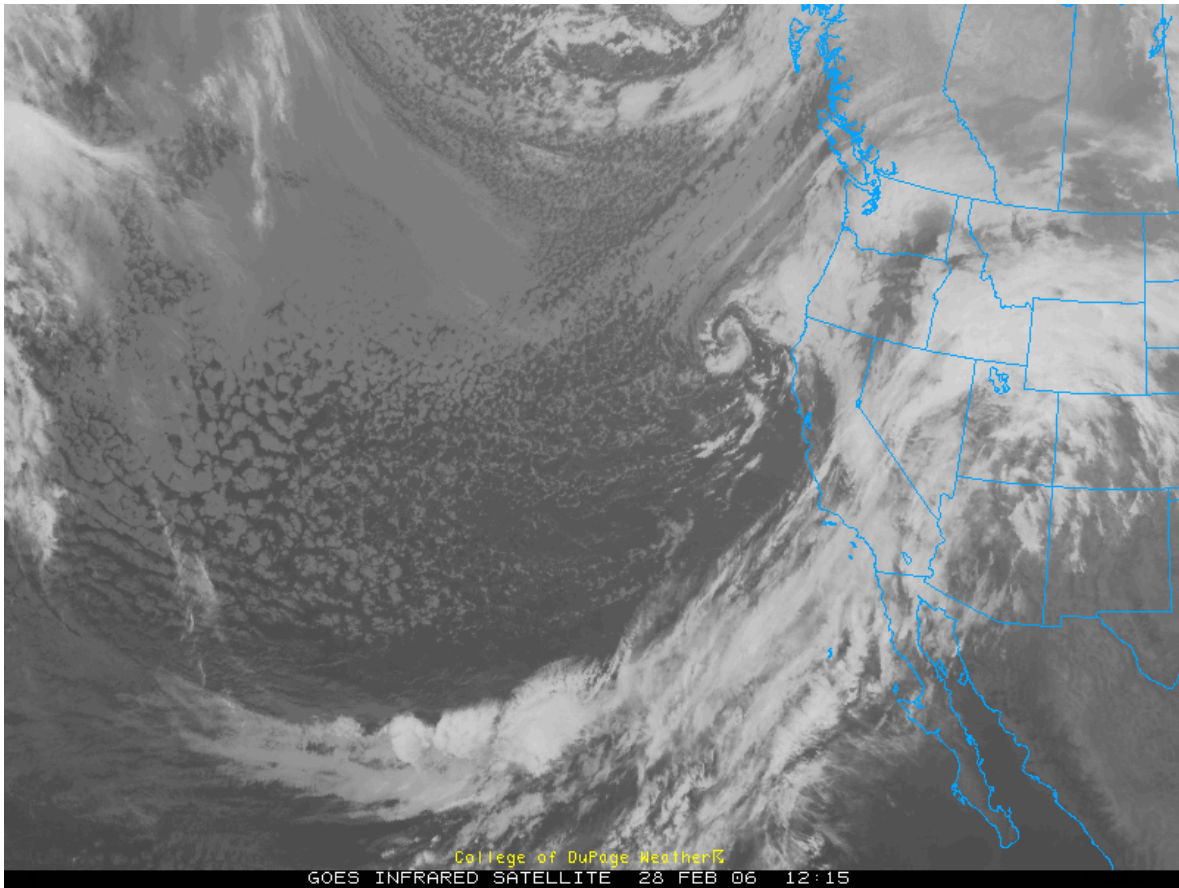


Figure 2. GOES infrared (IR) image at 1215 UTC on February 28, 2006

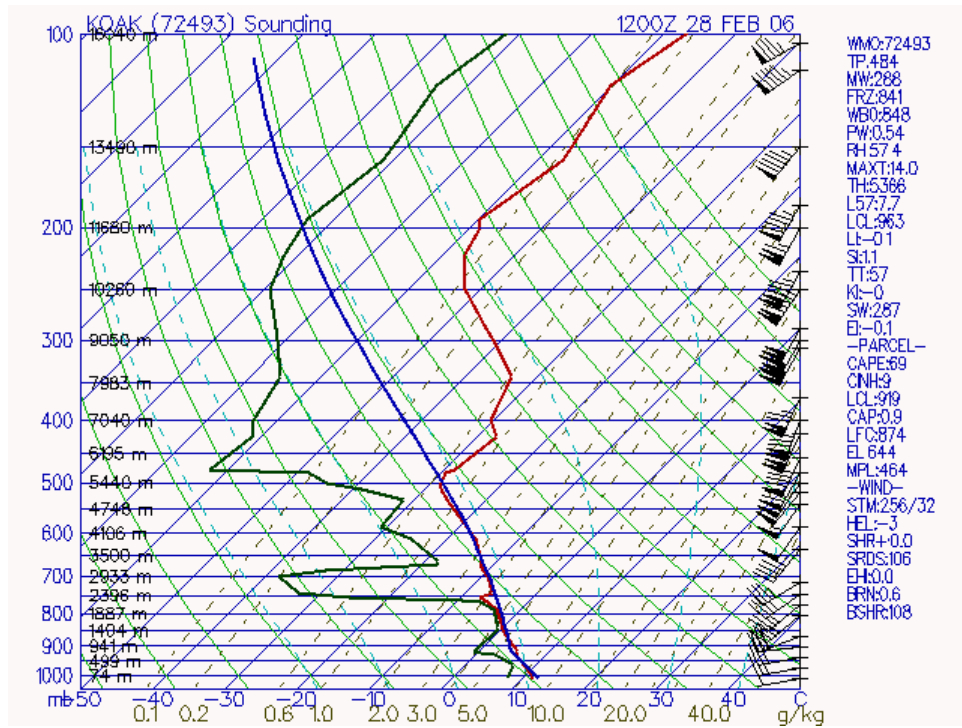


Figure 3. 1200 UTC Oakland sounding on February 28, 2006

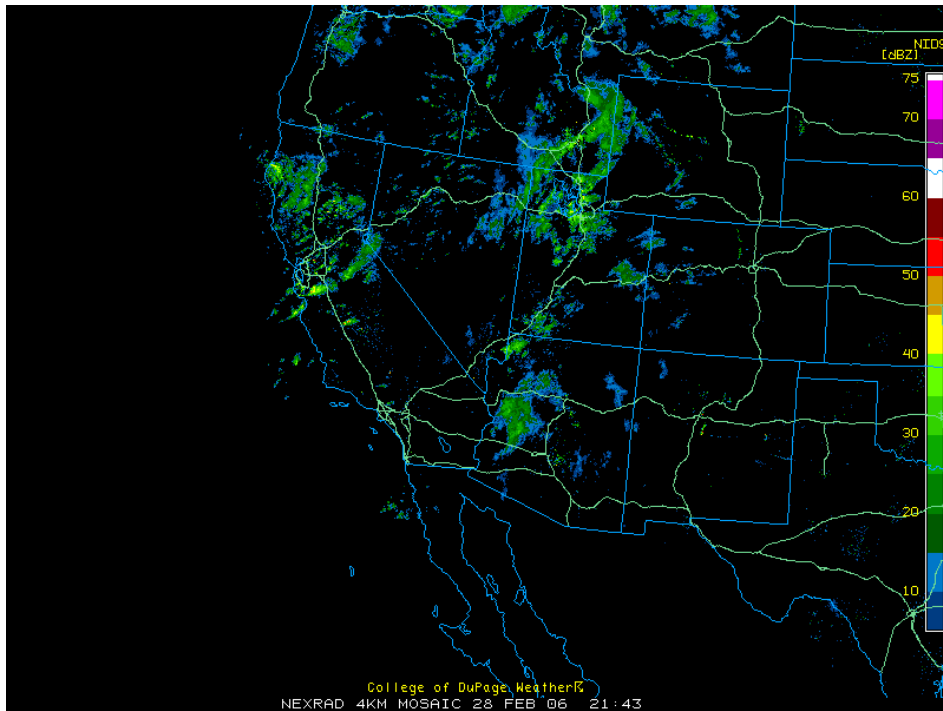


Figure 4. NEXRAD radar composite at 2143 UTC on February 28, 2006

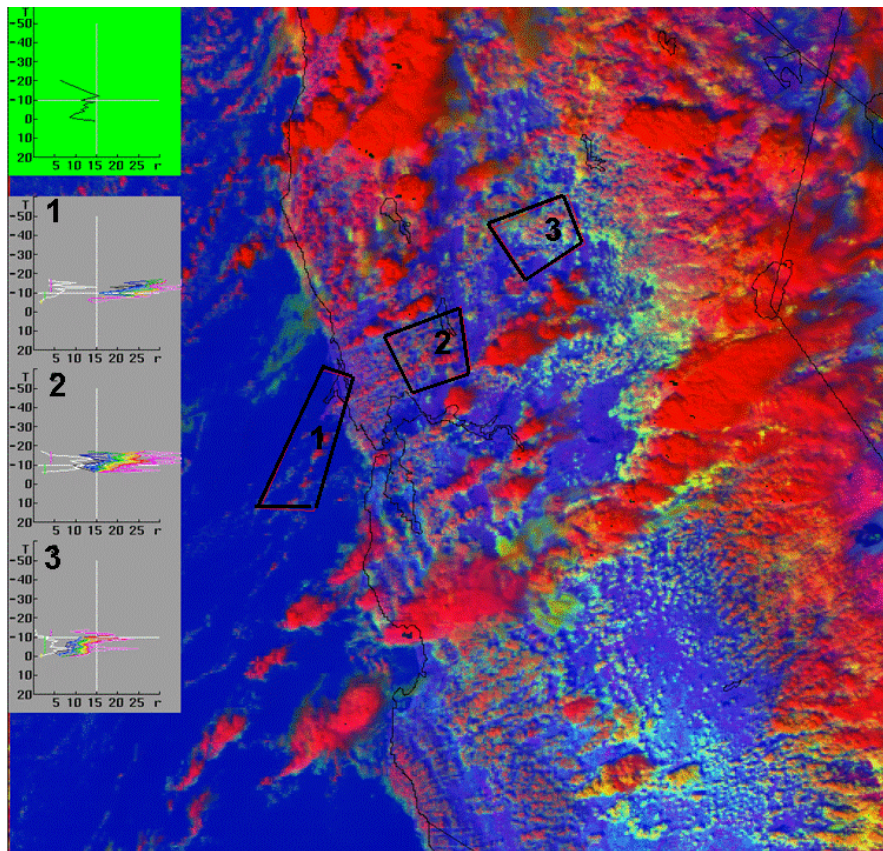


Figure 5. Colorized Aqua satellite image at 2100 UTC on February 28, 2006

## Morning Research Flight on February 28, 2006

**Objectives:** Cold front passed last night, and now we have the perfect orographic clouds to document.

### Crew Cloud 1:

Pilot: Gary Walker

Flight scientist: Daniel Rosenfeld

Instruments operator: Duncan Axisa

### Crew Cloud 2:

Pilots: Brian, Lise

Flight scientist and instrument operator: William Woodley

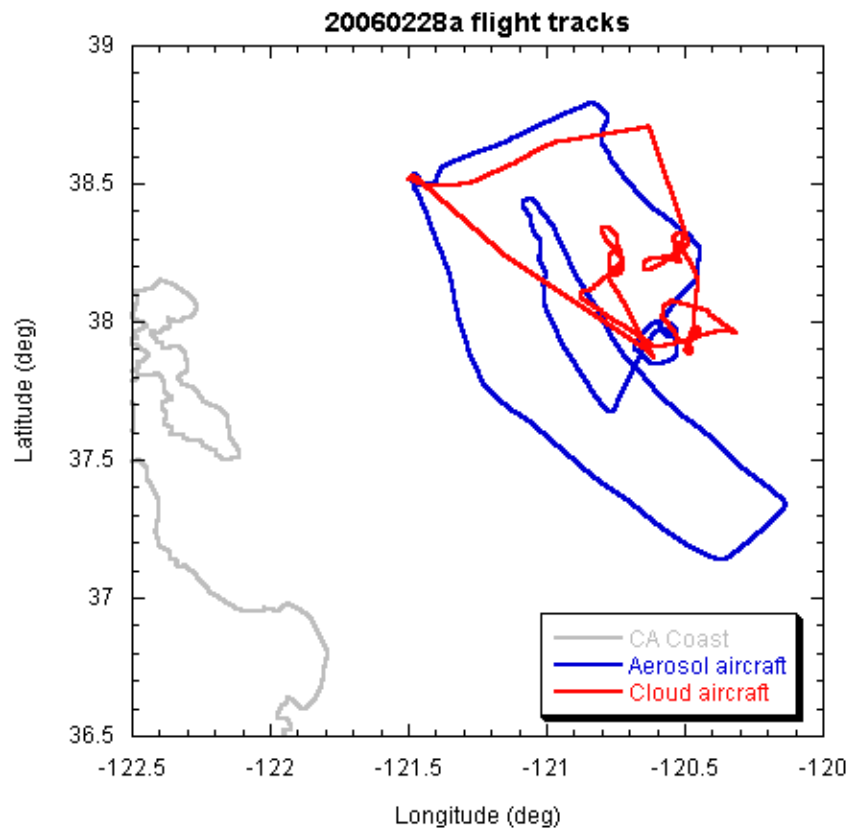


**Figure 6. The flight tracks for the two research aircraft (red for Cloud 1 and blue for Cloud 2) on their first flight on February 28, 2006**

**Synoptic conditions:**

A strong cold front passed by about midnight. Nice orographic clouds along with very cold temperatures aloft,  $-30^{\circ}\text{C}$  at 500 millibars (mb). Cumulonimbus clouds (Cb's) developed over water and propagated inland. A 747 was struck by lightning on approach to SFO. A tornado was reported at 16:00 UTC in Salinas County. The Cb's were moving from the SW at 15 knots, with tops to 28 kilofeet (kft).

The conditions at SAC at 16:53 UTC: 120/5, 10 miles, rain, 3500 broken, 4400 broken, 11/6, 29.99.

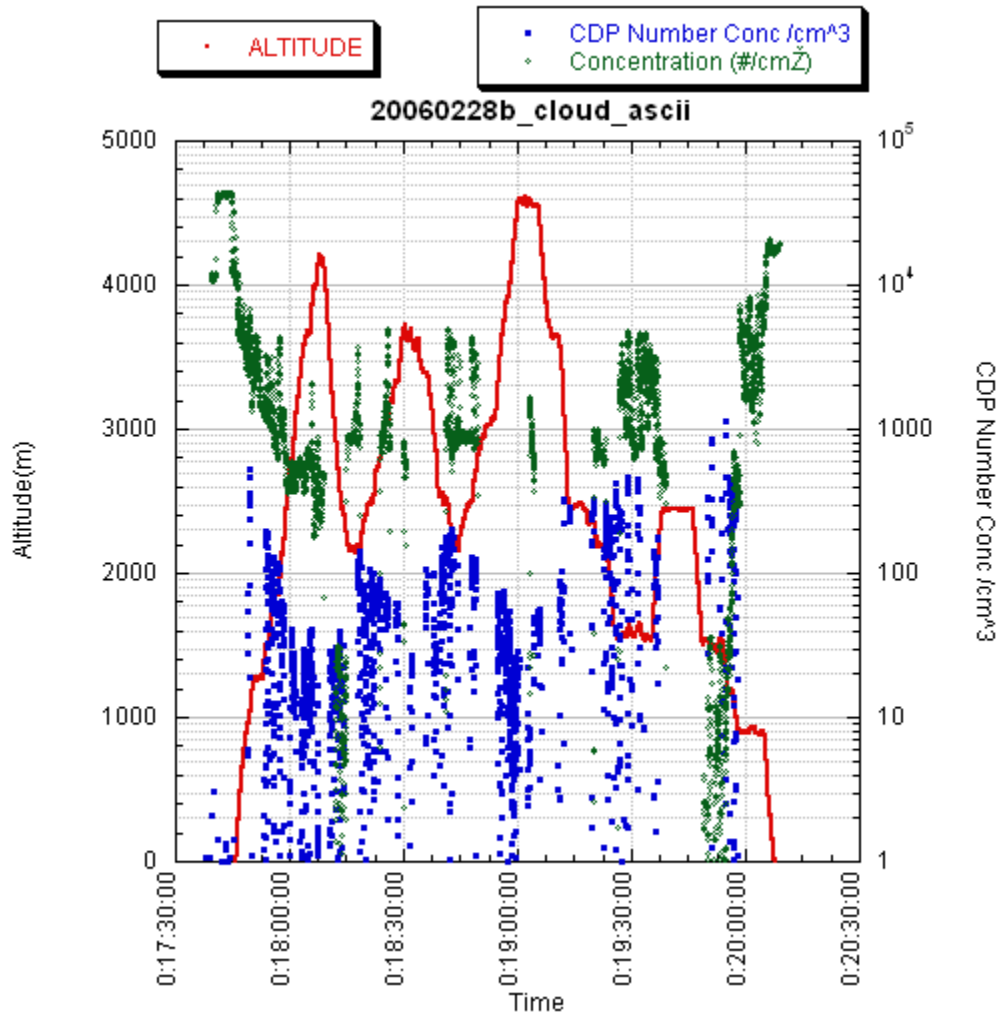


**Figure 7. Plots of cloud drop concentrations (blue), total aerosols (green) and flight altitude of the Cheyenne cloud physics aircraft (Cloud 1) on its first flight on February 28, 2006**

### **Flight report by the flight scientist in Cloud 1 (All times are UTC):**

We took off at 17:45 in rain. A formation flight with Cloud 2 was not possible due to conditions. At 17:39 we ascended through cloud base at 3300' over the valley. The cloud base had  $>500$  CDP drops  $\text{cm}^{-3}$  (See Figure 7 above). Cloud bases had various heights, and we penetrated an elevated cloud base towards Hangtown at 5000' by 17:53. Some lower bases penetrated it from below. The cloud had initially 200 drops in its base, but it dropped when we went higher. When ascending above 8 kft we left the embedded convection and entered the layer clouds that had formed on the western slopes of the hills. The cloud drop concentration decreased to  $< 30$ , and supercooled drizzle appeared.

We turned to a heading of  $150^\circ$  along the ridge and continued climbing up to 12 kft when we were at the top of the layer clouds, which were in part firm and in part fuzzy, having a glaciated appearance at their tops. We still had some glaciation with ice crystals and supercooled or frozen drizzle. Convective heads appeared to grow through these thick layer orographic clouds.

We turned to the SSE while descending through the layer and convective clouds to 7000'. At 18:20 we ascended through a convective cloud back to 12 kft. The cloud had about 120 drops at the low levels, but dropped to less than 70 aloft.

In the mean time Cloud 2 found an area of elevated CN concentrations some 100 km to the SSE of Hangtown, over Lake Melones. We flew to that location and profiled convective clouds downward. We circled in the convective clouds at 7 kft and found up to 200 CDP drops  $\text{cm}^{-3}$ . We continued SE climbing through convective clouds that were imbedded in the layer clouds, with some strong updraft at 18:55. This was a long ascent in heavy icing conditions in clouds that were quite maritime,  $< 70$  CDP drops  $\text{cm}^{-3}$ . We continued in these conditions eastward almost to the ridge line at an altitude of 14 kft, where we topped the orographic clouds. The clouds had only a few tens of drops  $\text{cm}^{-3}$  and drizzle.

At that time (19:05) we descended westward to a new location in the valley where Cloud 2 had identified an aerosol plume. We circumvented a Cb to our left and penetrated its flank while descending. That cloud had 200-300 drops  $\text{cm}^{-3}$ . We continued NW and monitored the clouds in the area that Cloud 2 called us as having  $> 400$  drops  $\text{cm}^{-3}$ . There was some visible haze below cloud base (19:26).

Cloud-2 called us to a more southerly location with similar aerosols, but at about 19:40 the left generator of the airplane quit, and we had to return to base. On the way back at 19:50 we crossed a gust front of a thunderstorm, which shot the cloud drop concentrations to  $> 1000$   $\text{cm}^{-3}$ .

We landed at 20:08.

### **Impressions**

After a stormy night with cold frontal passage and very strong winds there were still large concentrations of aerosols near the surface in the morning, which do not mix vertically very well into the orographic clouds. Convection that develops from the elevated air mass over the

foothills is still not very contaminated. The convective elements that start to develop during late morning bring more aerosols into the clouds and over the mountains.

**Report by the flight scientist (Woodley) in Cloud 2 for its first flight on February 28, 2006:**

I was in Cloud 2 as of 1730Z. There was a sprinkling of rain from convective showers in the vicinity. While sitting in the aircraft I learned that a commercial aircraft had been hit by lightning and that a tornado had been reported over Salinas County.

Just prior to takeoff at 1748Z the CPC reading was 12,000 p/cc. It was very dark to the W and SW as a shower approached the airport. I took picture 1 of this shower area during the takeoff roll. After takeoff the CPC reading was 7,000 p/cc while flying at 1,500 ft. Initial cloud base was 3,000 ft where the CPC values ranged between 4,000 and 5,000 p/cc then variable to 2,500/cc and the CCN were only 200/cc at 0.8% super saturation. Cloud 1 was flying around Hangtown at 1758Z.

Cloud 2 got as close as it could to Hangtown and then turned S beginning at 1802Z. The CPC counts were 2,000/cc. The Sierra was covered by showers. Blue sky could be seen through small breaks in the overcast overhead. We were at 3,500 at cloud base at 1806Z and in a shower at 1809Z. At 1817Z we were at cloud base at 4,000 ft where the CPC readings were about 1,000/cc.

The CPC counts did not change much until we approached New Melones Lake where the CPC counts jumped to 20,000/cc. This was a big surprise, so we orbited the area for a time. I took picture 2 of Tulloch Lake at 1837Z during the orbit. A small grass or trash fire could be seen nearby. The CPC counts were high and variable and not related to the fire in the area since the counts were just as high upwind of the fire as they were downwind. At 1842Z the CPC counts were 15,000/cc and variable.

Because there were some growing cumuli in the area, I called Cloud 1 and suggested that they consider coming to these clouds for sampling since the CPC counts were high right up to cloud base. It was not long before they were in the area. Meanwhile, we took a heading across the valley toward San Francisco to see how long the CPC counts would remain high. The plan was to "track" this plume, first by flying N to determine its northern extent and then S to determine its southern extent.

We turned N in Cloud 2 at 1847Z. I took picture 3 at 1848Z of clouds over the polluted area that we had just left. The CPC counts were still quite elevated at 1854Z as we flew at the 3,000 ft cloud base just to the south of Linden VOR. The counts were still quite elevated on the N side of Stockton. These aerosols went right up to and likely were ingested by the convective clouds in the area.

The CPC counts had dropped to 2,000 to 3,000 at 1904Z but they were still variable. Because heavy showers blocked our path ahead, we turned back S at 1905Z. I took picture 4 at 1920Z of the old cloud area that we had monitored originally that had developed into a small Cb complex. My camera batteries were weak and my backup batteries were weak as well.

The CPC counts went back to near 20,000/cc at 1923Z as we flew S. They increased to 25,000/cc at 1926Z when we were flying at 3,500 ft. The CPC counts had decreased by 1939Z and we appeared to be nearing the south edge of the pollution plume. The origin of the extensive pollutants was unknown.

Cloud 2 turned W at 1940Z and there was some rapid changes in aircraft altitude around 1944Z as our aircraft was maneuvered to avoid another aircraft. The counts appeared to be affected briefly by these maneuvers. We then flew N and parallel to HWY 99 and about 8 miles to its W. There were strong showers in the area. The CPC counts were elevated again just SW of Modesto, but they dropped dramatically to 1,000/cc and then further to only 600/cc as we passed through the shower area. I interpreted these readings as evidence of atmospheric cleansing by the strong line of showers that had passed through the region. The counts were also quite low over Stockton where they had been so high during yesterday's second flight.

Despite the high CPC counts during the flight the visibility was never very bad. I managed to take picture #5 at 2014Z looking to the NE at the northern extent of the cloud line in the Sierra. This was the same line through which we had passed earlier. The CPC counts stayed fairly low after we passed Stockton, but they increased again as we descended toward the Sacramento Executive airport where we landed at 2026Z.

Impressions: I was surprised and gratified by the flight. Seeing such high CPC counts right up to cloud base provides evidence that the clouds ingest the pollutants under unstable conditions. The very low counts documented in areas just traversed by showers were likely evidence of atmospheric cleansing by heavy precipitation. I can't think of a better reason for the suddenly decreased counts. The CPC counts of today should be plotted and analyzed in an attempt to infer the origin of the pollutants. I am assuming now that they were generated locally in the valley.

### **Research flight on the afternoon of February 28, 2006**

**Objectives:** This afternoon there are surface southerly winds, so no north-south gradient is expected over the Central Valley. The focus will be on contrasting the convective and orographic clouds over the Sierra foothills, the coastal range and over the ocean. The flight tracks for the research aircraft on this flight are presented in Figure 8. The aerosol measurements by the Cloud 2 aircraft are provided in Figure 9.

#### **Crew Cloud 1:**

Pilot: Gary Walker

Flight scientist: Daniel Rosenfeld

Instruments operator: Duncan Axisa

#### **Crew Cloud 2:**

Pilots: Brian, Lise

Flight scientist and instrument operator: William Woodley

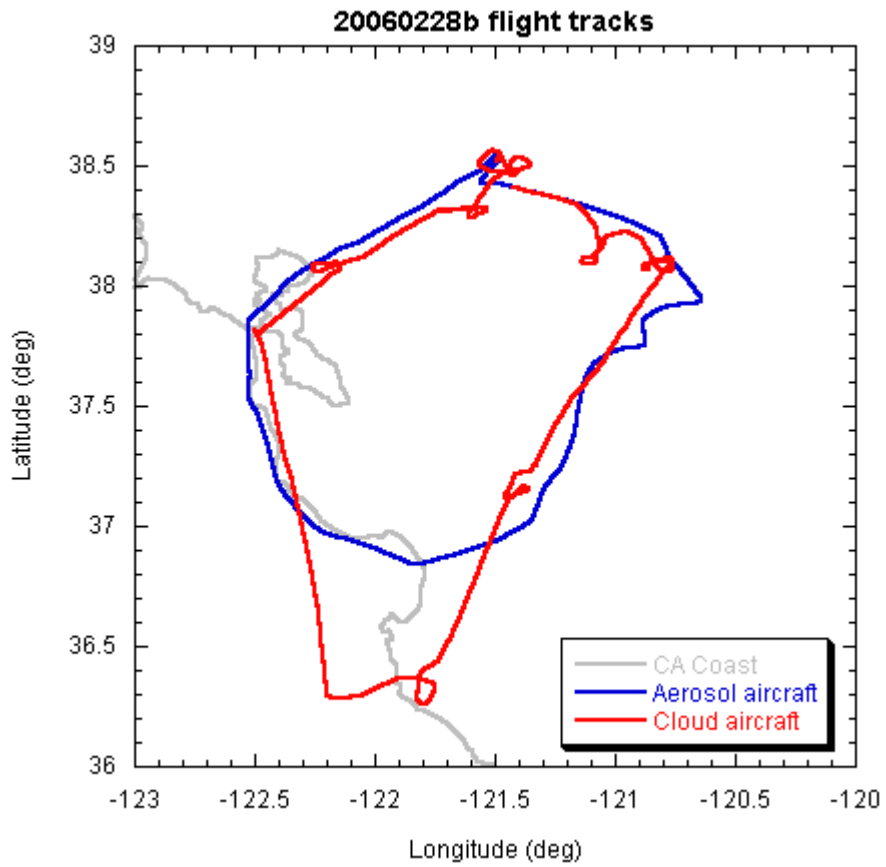


**Figure 8.** The flight tracks for the two research aircraft (red for Cloud 1 and blue for Cloud 2) on their second flight on the afternoon of February 28, 2006

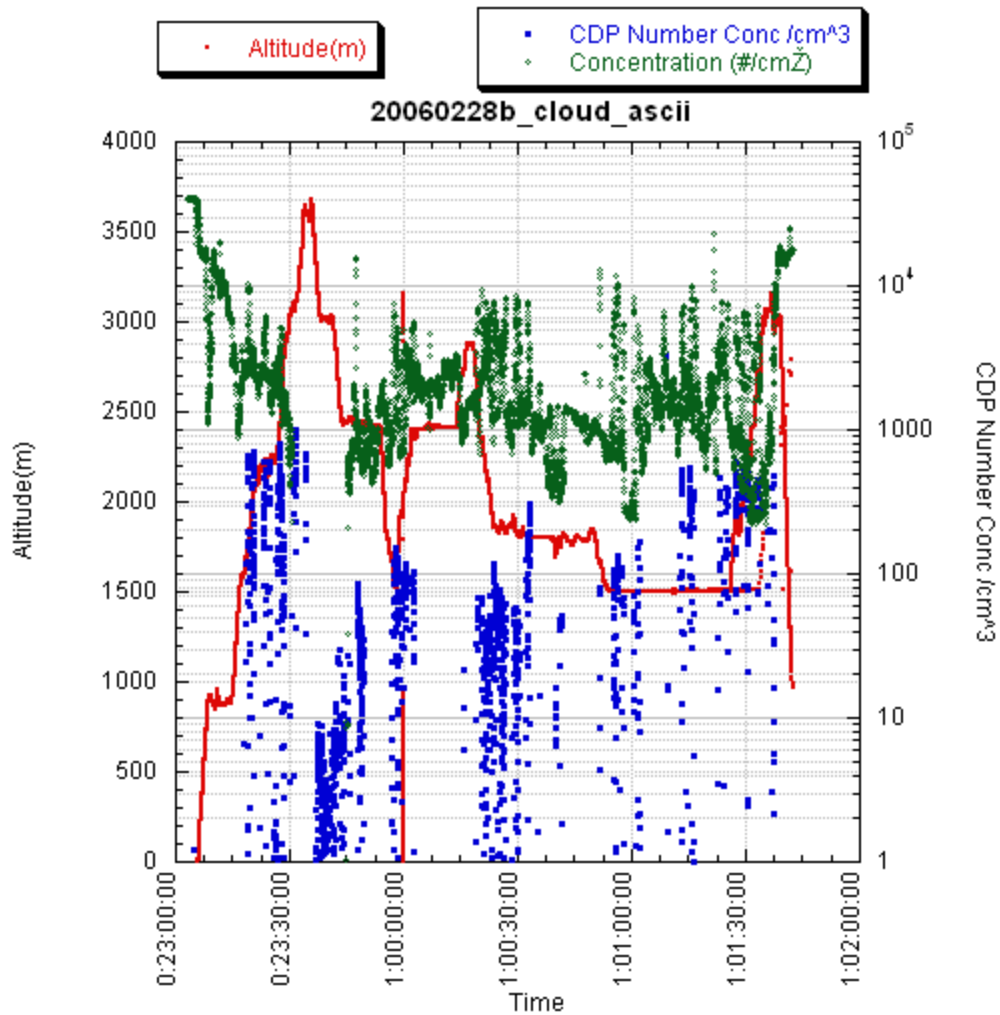


**Figure 9. Plots of cloud drop concentrations (blue), total aerosols (green) and flight altitude of the Cheyenne cloud physics aircraft (Cloud 1) from its second flight on February 28, 2006**

**Synoptic conditions:**

We are in post frontal flow, but the winds are still SW due to a low off the coast of Northern California

Conditions on takeoff: 118/12 1 miles, 4400 scattered, 5000 broken, 14/6, 3005.

**Flight report for Cloud 1:**

We took off at 23:05 and joined with Cloud 2 at 15:09 and broke off at 15:14.

Cloud base was penetrated near the foothills to the east of Sacramento at 23:18 (500 feet above base) with 700-800 CDP drops  $\text{cm}^{-3}$ . We initially encountered rain and moved to a rain free area, but were restricted by the ATC. We flew farther east through the rain cloud and found good towers there that we sampled in cross section up to 12 kft. They had peak CDP of 1000, and no visible hydrometeors on the windshield. We lost the CIP for the penetrations at 10 and 12 kft.

We continued to the SW to Salinas at 10 and then 8 kft, flying through old low-level glaciated cloud remnants. The CIP came back on line at 23:40.

At 23:47 we went through a cloud with an elevated base at 8 kft.

At 23:54 we measured a cloud cluster forming over the hills to the NE of Salinas at 8 kft. The clouds had slightly more than 100 CDP drops  $\text{cm}^{-3}$ . Nearby old clouds seemed to be glaciating at or slightly above our level.

We continued to the hills to the east of Big Sur, where cloud tops reached just under 10 kft. They had CDP mostly  $< 80$  droplets  $\text{cm}^{-3}$ , and contained significant drizzle and rain below cloud tops. We made a vertical profile from 10 to 6 kft, which was the lowest that we could get.

We crossed the coast over the ocean and flew around a shallow Cb to our right with glaciated top at about 12 kft. We flew through the flanks at 6 kft at 00:25. CDP concentrations were  $< 100 \text{ cm}^{-3}$ , but occasionally exceeded that, with one cloud reaching a peak value of 300 at 00:34. There was some haze visible over the ocean.

We continued over the ocean to the north at 6 kft. On the way we passed through a very thin layer cloud with 40-50 drops  $\text{cm}^{-3}$ . We passed over San Francisco airport and the Golden Gate at 6 kft. Clouds over the Golden Gate had 100 to 200 drops  $\text{cm}^{-3}$ . A cloud to the NE of SFO exceeded 500  $\text{cm}^{-3}$  at 5 kft. Similar hard looking clouds developed over Sacramento. We documented them with a vertical cross section between 5 and 10 kft. Their bases were at about 4 kft.

We dived to landing from 10 kft over the airport at 01:41.

## **Impressions**

The greater mixing in the afternoon lowered the low level CN but enhanced the mid tropospheric CN and continentality of the clouds. The orographic clouds had become mostly convective in nature by the afternoon and the enhanced aerosols suppressed the warm rain and early glaciation over the Central Valley and the Sierra. Over the coastal range the clouds readily produced drizzle and warm rain. Isolated vigorous clouds over the ocean had about 1/3 of the drops of equally vigorous clouds over land.

## **Report by the flight scientist (Woodley) in Cloud 2 for its second flight on February 28, 2006:**

I was back in Cloud 2 by 2245Z and I took my first picture with Duncan Axisa's camera at 2258Z of a nice short line of developing cumuli. We were on the taxiway at the time and the CPC counts were enormous, due probably to the presence of Cloud 1 running its engines upwind. Cloud 2 took off at 2304Z. Immediately after takeoff the CPC counts dropped to

28,000 cm<sup>-3</sup>. Cloud base was at 3,200 ft where the CPC readings were 17,000 cm<sup>-3</sup>. Cloud 1 was already flying.

I took picture 2 at 2311Z looking down a cloud line that culminated in a heavy shower. By 2313Z the CPC counts had decreased to < 5,000 cm<sup>-3</sup>. Photo 3 was taken at 2321Z of a shower and rainbow. Cloud 2 turned to the S at New Hogan Reservoir. Picture 4 was taken at 2323Z of a hard cloud base where the CPC readings were ~6,000 cm<sup>-3</sup>. We turned W at 2328Z. The CPC counts were variable and low, generally between 2,000 and 1,000 cm<sup>-3</sup>. Cloud 2 was now in the region of the morning high counts. We were at 3,000 ft and the CPC counts were < 1,000 cm<sup>-3</sup>.

At 2351Z we climbed briefly to 5,000 ft in order to pass over some low clouds that blocked our way to the Salinas Valley and ultimately San Francisco. At 2358Z I took picture #5 of the Salinas Valley with the Pacific evident in the distance. We were back to 3,000 ft from 5,000 ft. Picture 6 was taken looking N over the Coast Range. We were over Frazier Park at 0000Z and on the Pacific shore at 0008Z and heading W over the Pacific in flight to the south of Santa Cruz. The CPC counts were only about 800 cm<sup>-3</sup>. Picture 7 was taken looking back at the shoreline at 0008Z. The CCN counts were only around 50 to 100 cm<sup>-3</sup>, which was quite low.

Photo 8 was taken at 0013Z looking down at Santa Cruz and #9 was taken at 0015Z looking at the orographic clouds that shrouded the higher terrain NW and N of Santa Cruz. The CPC counts were on the order of 600 cm<sup>-3</sup>. I took picture 10 of my pilot Kevin McLaughlin at his request at 0017Z. Picture 11 was taken at 0023Z looking to the ESE to the high terrain N of Santa Cruz that was covered by orographic clouds. We were at 2,000 ft at 0024Z

Cloud 2 had descended to 1,500 ft as of 0031Z upon the request of Air Traffic Control. Pictures 12 and 13 were taken at 0036Z of the Golden Gate Bridge. Picture 14 at 0037Z was of Sausalito with the Golden Gate in the background. The CPC counts had decreased to only 200 cm<sup>-3</sup> over the North Bay, but both the CPC and CCN increased on its eastern end. We were flying at 3,000 ft as of 0046Z. The counts were later very high as we descended toward Sacramento Executive Airport where we landed at 0100Z.

### **Impressions**

Where did all of the aerosols go? I was blown away by the decreased CPC counts over areas where we had observed very high counts at cloud base during the morning flight. I am guessing that vertical mixing was responsible since it had not rained much along the morning flight track.. The air was quite clean over the water upwind of the populated areas.

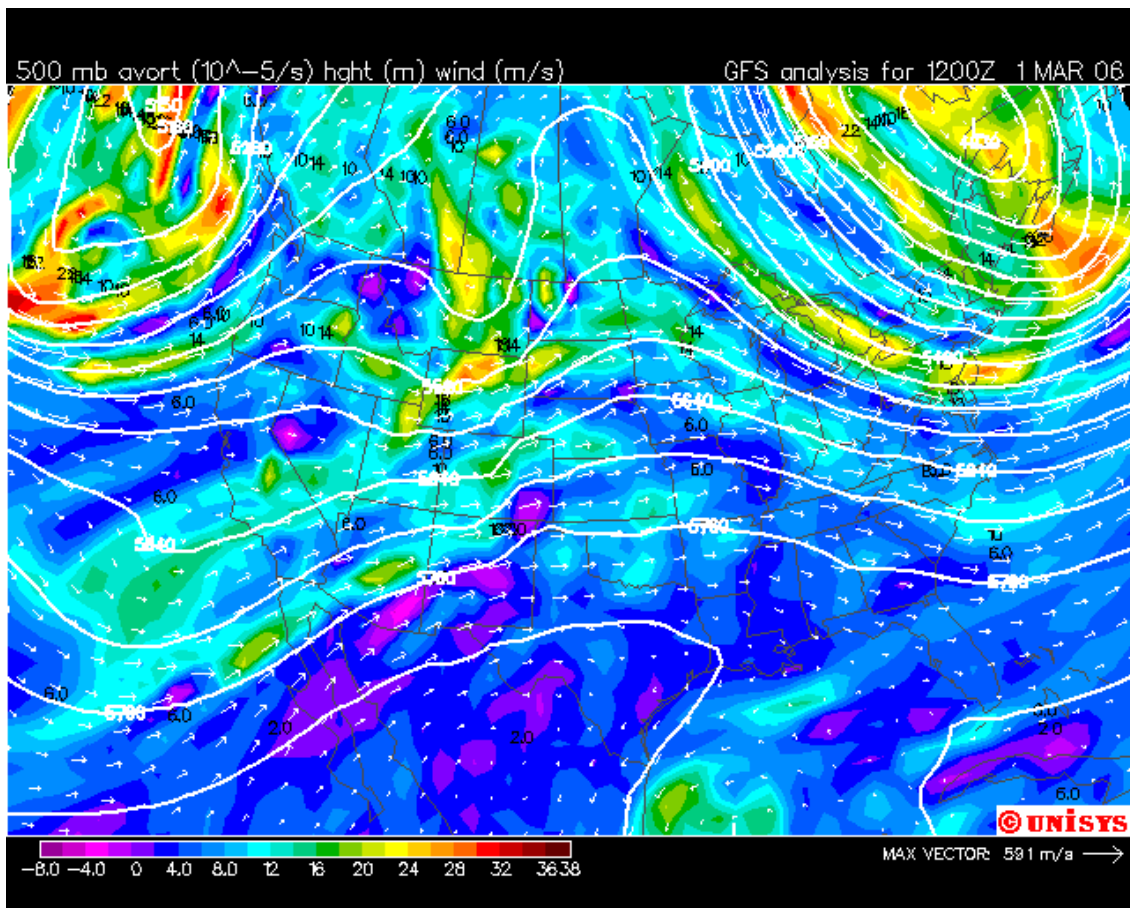
## **Aircraft Flight Data: Wednesday, March 1, 2006**

### **Weather Situation**

The weather was cool, clear, calm and hazy in Sacramento this morning. The visible satellite image revealed what appeared to be orographic cloudiness over the northern Sierra and northern Coast Range in the wake of yesterday's trough that had passed east of the area (Figure 10). A new trough and front was moving southeast from the Gulf of Alaska toward Northern

California (Figure 11). Some of the cloudiness in extreme northwest California was at the leading edge of this next storm. It should bring us rain tonight and a frontal passage tomorrow morning. There was little precipitation over California during most of the day, since the sounding was dry and stable (Figure 12). Plots of the Blodgett aerosol measurements, showing an increase throughout the day, are shown in Figure 13. Mean aerosol plots as provided by Dr. Jim Hudson of the Desert Research Institute (DRI) are given in the main report.

The plan of the day for the research aircraft was to change the oil on the Cessna 340 (Cloud 2) during the morning and then possibly fly thereafter. Two flights were conducted during the day to measure aerosols and the structures of convective clouds over the central valley and the coast.



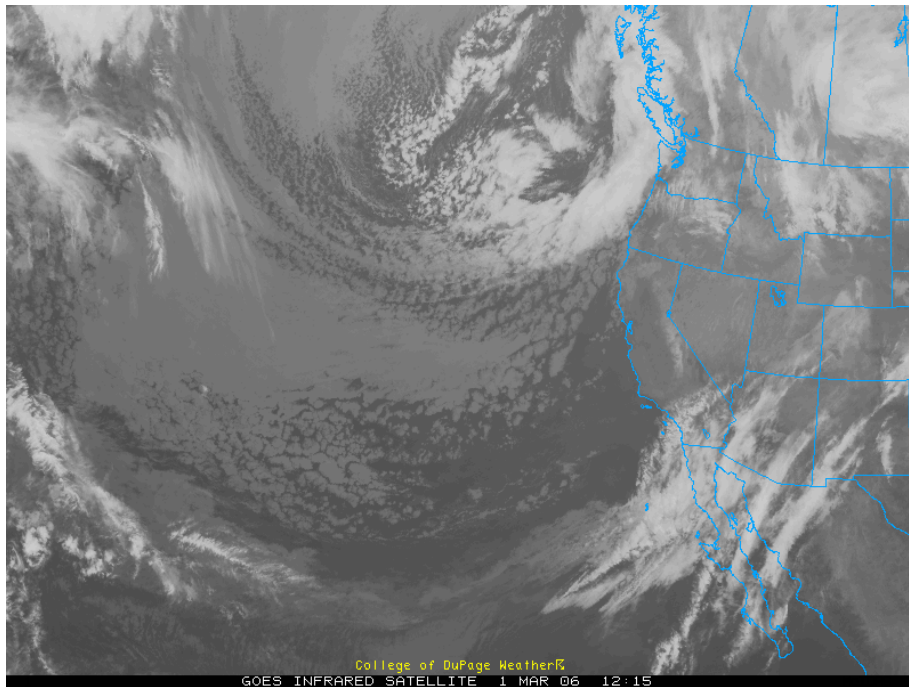


Figure 11. GOES IR image at 1215 UTC on March 1, 2006

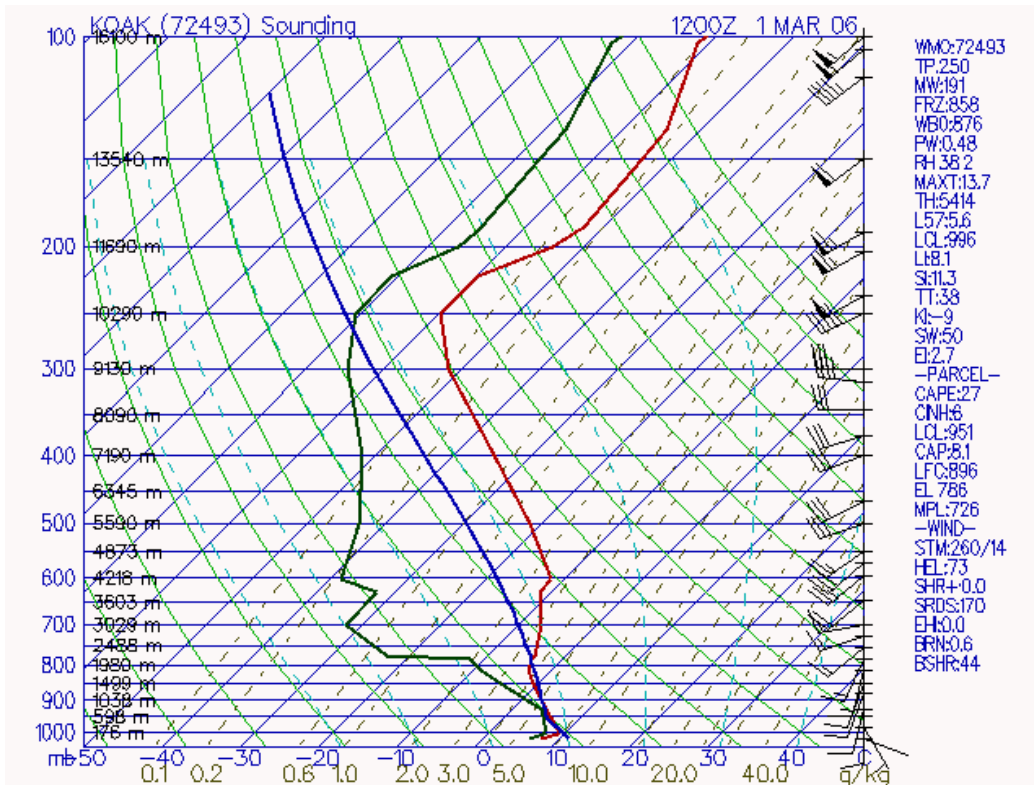
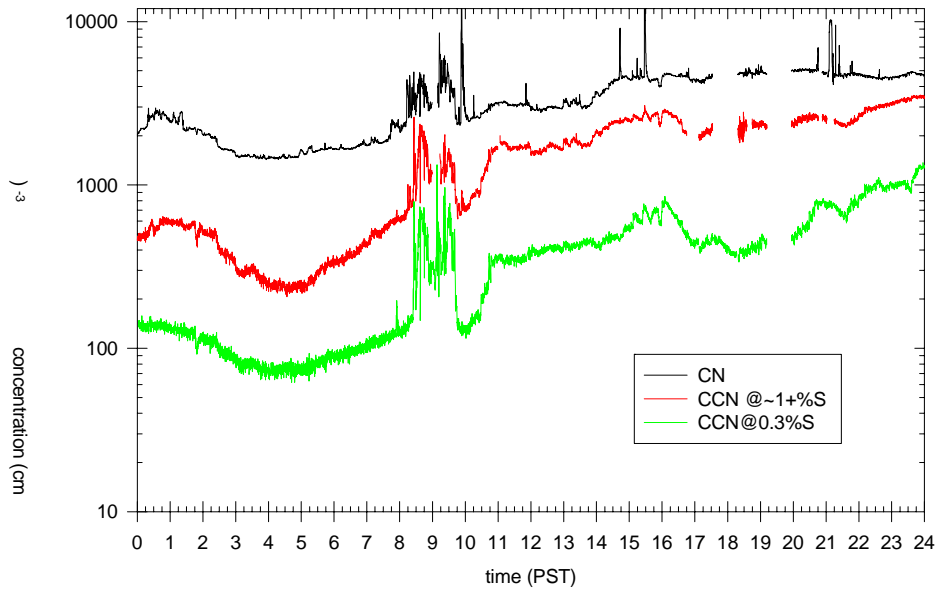


Figure 12. The atmospheric sounding made at Oakland, California, at 1200Z on March 1, 2006

March 1, 2006, Blodgett, CA



**Figure 13. Plots of the aerosol measurements at the Blodgett Research Station on March 1, 2006**

**Research Flights on March 1, 2006**

**Objectives:** Document the Sierra to ocean east to west gradient of clouds in moderate SW flow ahead of the regenerated new cold front that is approaching during the day. The southerly component will not allow good documentation of north-south gradient of cloud properties. The flight tracks for the research aircraft on this flight are presented in Figure 14. The aerosol measurements by the Cloud 2 aircraft are provided in Figure 15.

**Crew Cloud 1:**

Pilot: Gary Walker

Flight scientist: Daniel Rosenfeld

Instruments operator: Duncan Axisa

**Crew Cloud 2:**

Pilot: Kevin Laughlin

Flight scientist and instrument operator: William Woodley

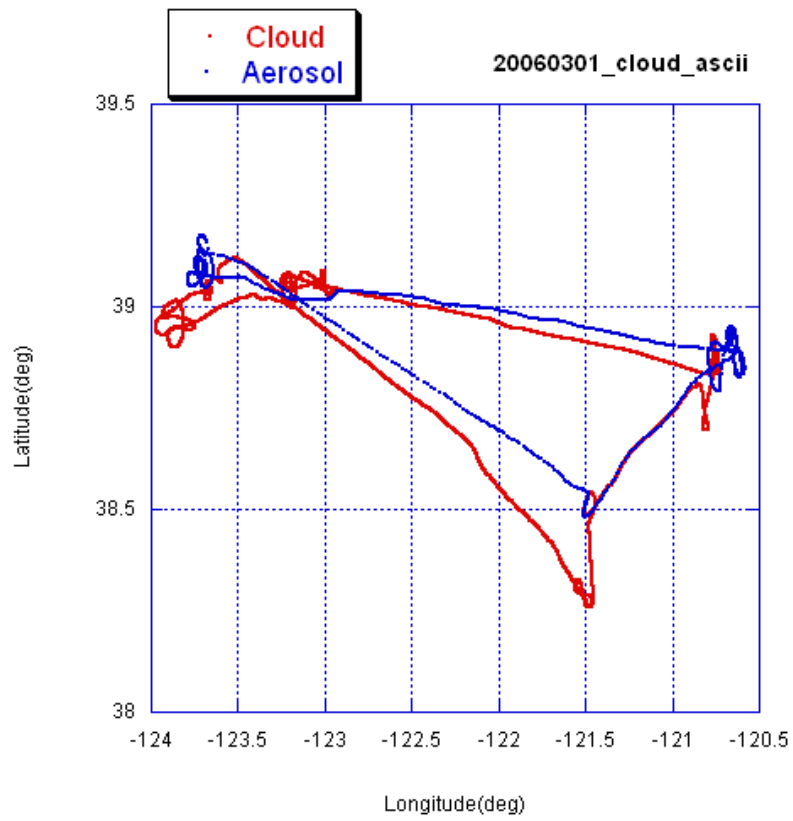


**Figure 14. The flight tracks for the two research aircraft (red for Cloud 1 and blue for Cloud 2) for their flights on March 1, 2006**

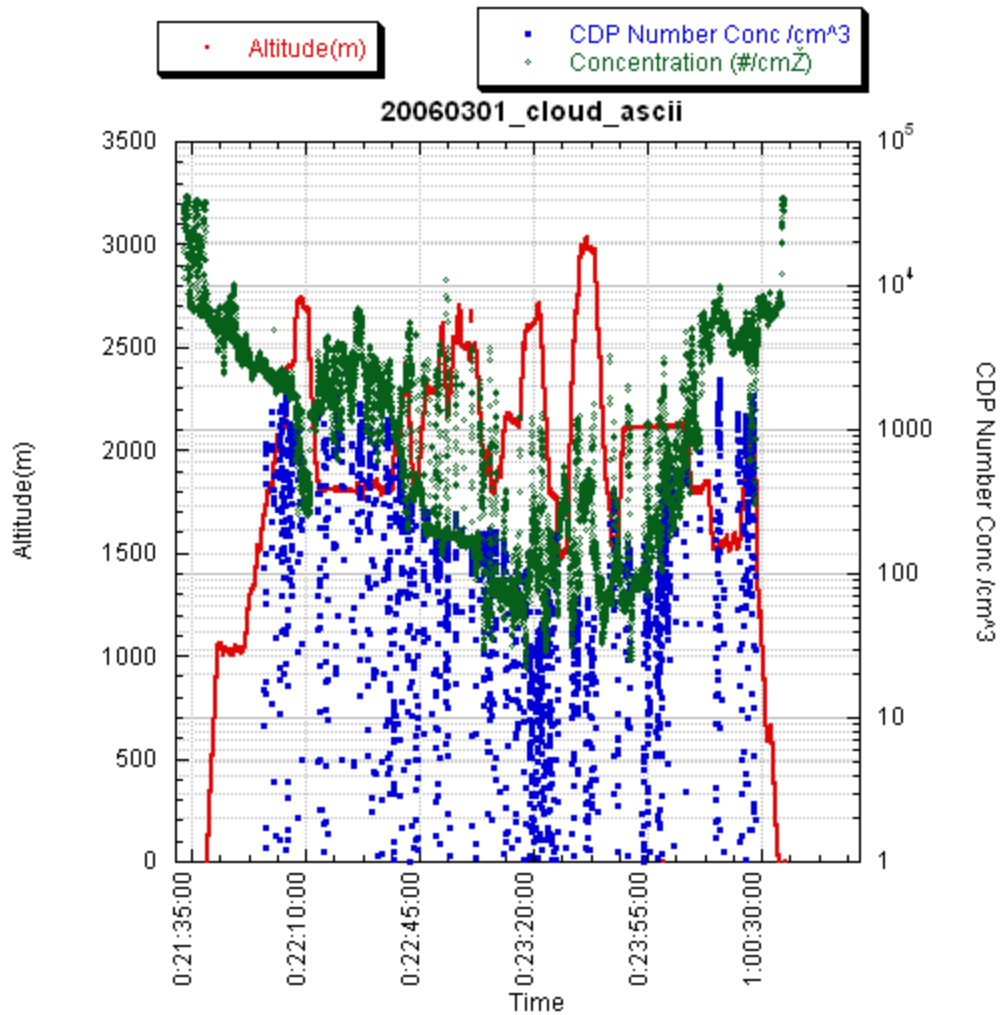


**Figure 15. Plots of cloud drop concentrations (blue), total aerosols (green) and flight altitude of the Cheyenne cloud physics aircraft on March 1, 2006**

**Synoptic conditions:** We are in post frontal flow, but the winds are still SW due to the approaching new front.

**Conditions on takeoff:** 170/7, 10 miles, broken 4000, broken 5000, 14/6 1018 mb.

**Flight report for Cloud 1:**

We took off in early afternoon (21:39) when a field of fair weather convective clouds was well developed. We flew in formation with Cloud 2 to Hangtown, and then broke off and started our measurements. Cloud base was at 5600' (21:57) with 800 CDP drops. We ascended through the convective clouds over Hangtown and Blodgett up to their tops at 8900'. The clouds had peak concentrations of 1100–1800 CDP drops  $\text{cm}^{-3}$ . CCN was in the same range, and CN was 3000–4000  $\text{cm}^{-3}$ .

We descended to 6000' and continued through the fair weather cumulus westward towards Mendocino. Cloud and CN properties remained the same all the way to the west edge of the Central Valley (122W). Aerosols and cloud droplets started to decrease there.

We used an altitude block of 6–8 kft and documented the clouds from 6 kft to tops at 8 kft as we progressed westward. At Mendocino the droplet concentrations decreased to about 350  $\text{cm}^{-3}$ . We measured clouds over the coastal range with heights up to 8500', and drops up to 300  $\text{cm}^{-3}$ . The clouds developed some needles.

We continued westward over the ocean. The water had abundant white caps and the air appeared quite hazy, probably from the sea spray, because the maximum CN and CCN values at an altitude of 4,500 ft were about 200 and 150 particles  $\text{cm}^{-3}$ , respectively. An elevated base of layer clouds was over the ocean, apparently associated with the approaching front. The air just below its base was quite pristine: CN= $\sim$ 80 and  $\sim$ 60 CCN  $\text{cm}^{-3}$ . The cloud drop concentration was  $\sim$ 50 and peaked at 80  $\text{cm}^{-3}$ . The clouds produced virga. Cloud 2 identified it as a virga of drizzle. Above the cloud tops at 10 kft the CCN concentration increased to 100-120  $\text{cm}^{-3}$  and CN to 200  $\text{cm}^{-3}$  (locally up to 500  $\text{cm}^{-3}$ ).

We circled above the ocean down to 6 kft and back through cloud base to cloud top at 10 kft. At 23:36 we penetrated a separate thin layer just above the cloud tops. That layer had the same drop concentration of 60-80 drops  $\text{cm}^{-3}$ .

We headed back to the coast line and measured at 5 kft (23:45) a cloud that was forming by the mountains just east of the coast line with a base of about 500' below us. That cloud had more than 400 drops  $\text{cm}^{-3}$ . This cloud already was the same as the cloud mass at Mendocino and to the west. There were a few boundary layer low clouds over the ocean but they were too low for us to reach.

We then returned towards Sacramento at 7 kft through clouds, documenting the increase in cloud droplet concentrations and aerosols in reverse order on our way from Sacramento.

A hard looking cloud line with tops of up to about 8 kft had a NE-SW orientation to the SW of Sacramento. We crossed the base of this line at 5 kft (00:16) and encountered up to 2200 CDP drops  $\text{cm}^{-3}$ . We could not get the Travis controller to allow us to backtrack for measurements, so we continued flying ESE towards another similar looking line. We crossed the base of that line at 00:24 and found up to 1200 CDP drops  $\text{cm}^{-3}$ . We made repeated penetrations at 6 and 7 kft (cloud top) where up to 1800 drops  $\text{cm}^{-3}$  were measured. This brought us nearly overhead the airport, where we landed finally at 00:35.

On descent to Sacramento Cloud2 measured at 6 kft a large increase of CCN to  $\sim$  2000  $\text{cm}^{-3}$ , but they were only 1000  $\text{cm}^{-3}$  at the ground. The CN increased at the same time to about 10,000  $\text{cm}^{-3}$  and remained that high on the ground.

## **Impressions**

Clean air that came from the ocean in SSW flow created moderate maritime clouds over the coastal range. The elevated bases there ingested elevated aerosols that came over the ocean

above the MBL, but were still by far cleaner than the clouds in the Central Valley and over the Sierra. Clouds in the wake of SFO appear to be extremely polluted.

We have documented the continentalization of clouds moving from the ocean inland with a clear maximum downwind of SFO. It is a replication of and addition to yesterday's findings.

### **Report by the flight scientist (Woodley) in Cloud 2 for its flight on March 1, 2006:**

We started engines in Cloud 2 at 2125Z. Picture 1 was taken on the ramp at 2133Z looking at Cloud 1 running up nearby. The cloud particle counts (CPC) values on the ground were near 6,500 particles  $\text{cm}^{-3}$ . Cloud 2 took off at 2138Z and the CPC counts increased briefly after takeoff, reaching 15,000  $\text{cm}^{-3}$  at one point. The CCN were around 2,000  $\text{cm}^{-3}$ . Picture 2 was taken at 2143Z while Cloud 1 flew alongside us on the right as we headed toward Blodgett. The CPC counts were highly variable at this time. The estimated cloud base was 4,200 ft. At 2152Z we were at 4,000 ft. The CPC value was 3,700  $\text{cm}^{-3}$ . Picture 3 was taken at 2153Z.

Cloud 2 arrived over Blodgett at 2153Z flying at 5,500 ft. The CPC and CCN values were 2,700 and 700  $\text{cm}^{-3}$ , respectively. The cloud bases had risen as we flew toward the mountains, reaching 6,500 ft as we orbited around Blodgett. Picture 4 was taken at 2201Z looking at the cloud bases in the region. During the orbit around Blodgett we extended one leg to try to intercept some smoke from a ground fire, but the CPC counts did not change all that much as we flew by.

Cloud 2 began its ascent above the clouds at Blodgett at 2211Z. Picture 5 was taken at 2215Z from 10,000 ft looking at the tops of the clouds around Blodgett. The CPC counts were only in the 300  $\text{cm}^{-3}$  range, which was a big drop from the values we had measured below cloud. At 2218Z Cloud 2 was at 10,500 ft.

Cloud 2 left the Blodgett area at 2224Z and took a heading toward Mendocino VOR to the WSW. We began our descent below the clouds at 2226Z and the CPC counts increased again, reaching 1,800  $\text{cm}^{-3}$  at 8,000 ft, 3,000  $\text{cm}^{-3}$  at 6,000 ft and nearly 10,000  $\text{cm}^{-3}$  at 2233Z at an altitude of 5,000 ft. The CPC counts increased further to 11,000  $\text{cm}^{-3}$  at 2235Z. The cloud bases became lower as we flew to the west down to a minimum of about 3,500 ft. The cloud bases increased somewhat we encountered the higher terrain of the Coast Range. The CPC counts decreased as we flew to the west.

Picture 6 was taken at 2258Z as we flew on the north side of Indian Valley. The aircraft was over Clear Lake at 2305Z when picture #7 was taken. The CPC counts were 1,000 and the CCN about 200  $\text{cm}^{-3}$  while we flew at 4,200 ft. As we neared the west side of the coast range we encountered some drizzle below the clouds at 2318Z. The CCN were only about 50  $\text{cm}^{-3}$ . By 2320Z we had crossed the shoreline flying at 4,500 ft, and the CPC counts were only 170  $\text{cm}^{-3}$ , which represented a huge drop from the higher values farther to the east. No doubt the cloud microstructure was correspondingly different.

By 2323Z we began a climb to above the clouds, noting a frizzy cloud mass with drizzle virga to our immediate west. Cloud 1 was in the area working that cloud. At 2325Z our CPC counts were only  $80 \text{ cm}^{-3}$ . Picture 8 was at 2326Z of the drizzling cloud. The CPC counts had decreased to an amazing  $7 \text{ cm}^{-3}$  at 7,000 ft, but they increased as we continued our climb, reaching  $440 \text{ cm}^{-3}$  at 8,000 ft. Picture 9 was taken at 2330Z of the tops of the drizzling cloud mass. High layer clouds could be seen farther SW-NW as the leading edge of the cloud band associated with the approaching front. At 10,000 ft the CPC and CCN readings were  $200 \text{ cm}^{-3}$  and  $100 \text{ cm}^{-3}$ , respectively.

One of the engines of Cloud 2 was running a little rough at 2338Z, prompting a return toward Sacramento. At 2340Z at 10,000 ft the CCN and CPC counts were about equal at 150 to  $200 \text{ cm}^{-3}$ . Thus, over the day the CPC counts showed more variation than the CCN. At very low aerosol readings the CPC and CCN are not much different.

Cloud 2 began its descent from 10,500 ft at 2357Z. By this time the engines were running more smoothly. Even so, there still may have been problems that would have to be checked out on the ground. The CPC counts at 8,000 ft, 6,000 ft and the cloud base of 5,300 ft were 250, 4000, and about  $6,000 \text{ cm}^{-3}$ , respectively.

During the return to Sacramento I discovered that I had not turned on the Rosemount and telemetry systems during the initial part of the flight. This was a dumb, stupid, unacceptable mistake on my part that resulted from my not using the checklist. We would have to try to recover the lost data from the new Garmen GPS system that had been purchased for our use on Cloud 2.

The CPC counts were elevated to about  $12,000 \text{ cm}^{-3}$ . Cloud 2 landed at 0017Z. The CPC counts were on the order of  $8,000 \text{ cm}^{-3}$  on the ground. After landing and after a major effort on everyone's part it was discovered that the navigation data for Cloud 2 could be recovered by downloading the information from the new Garmen GPS.

### **Impressions**

The flights today were very useful in documenting the CPC and CCN aerosols and the cloud microstructure associated with changes in the aerosols. The clouds over the Sierra had a continental structure while those over the Pacific were highly maritime. Thus, aerosols appear to make the pivotal difference.

## **Thursday, March 2, 2006**

### **Weather Situation**

The frontal band of clouds and showers moved into the Sacramento area over night bringing light rain to our area. The backside of the rain showers was nearing Sacramento at 1120 UTC (Figure 16). Documentation of the frontal band in the GOES IR imagery over most of March 2,

2006 is provided in Figures 17 to 19. Note that the front moved steadily forward over half of the day, but it had weakened and stalled to the southeast of Sacramento during the latter half of the day. The Oakland 1200 UTC sounding is shown in Figure 20. The balloon apparently went up through the frontal surface as seen by the frontal inversion. The winds are light near at the lowest levels, but they reach 60 kts from the southwest at 700 mb. A more detailed discussion of the weather situation is given in the Sacramento NWS area forecast discussion below.

**AREA FORECAST DISCUSSION  
NATIONAL WEATHER SERVICE SACRAMENTO CA  
430 AM PST THU MAR 2 2006**

**DISCUSSION**

COLD LOW PRESSURE SYSTEM IN THE EASTERN PACIFIC PIVOTING A COLD FRONT INTO THE SIERRA CASCADE RANGE THIS MORNING. PRECIPITATION WITH THIS FRONT WEST OF THE SIERRA AND NORTH OF SACRAMENTO WAS LIMITED BUT OROGRAPHICS HELPING TO SQUEEZE OUT SOME ADDITIONAL PRECIPITATION AS THE FRONT MOVES INTO THE SIERRA. PRECIP AMOUNTS OVER THE SIERRA HAVE RANGED FROM A FEW TO SEVERAL TENTHS OF AN INCH. COLD AIRMASS BRINGING LOW SNOW LEVELS. BASED ON RAW DATA WOULD ESTIMATE THAT SNOW LEVELS THIS MORNING ARE SOMEWHERE AROUND 2500 TO 3000 FEET ACROSS THE CWA. AIRMASS CONTINUES TO COOL HOWEVER SO SHOULD SEE EVEN LOWER SNOW LEVELS LATER TODAY. SHOWERS BEHIND TODAYS FRONTAL BAND SHOULD BE FOLLOWED BY A PERIOD OF HEAVIER PRECIPITATION TONIGHT AS A SHORTWAVE NOW DROPPING DOWN THE BACK SIDE OF THE COLD LOW PIVOTS THROUGH THE NORTHERN HALF OF THE STATE. LATEST GFS INDICATED THAT MODERATE DYNAMICS WILL CONTINUE OVER THE SIERRA THROUGH AT LEAST 00Z SATURDAY SO EXTENDED THE WINTER STORM WARNING FOR WEST SLOPE OF THE SIERRA ZONES THROUGH 6 PM FRIDAY. SNOW LEVELS AND SNOW AMOUNTS AT ELEVATIONS BELOW 3000 FEET SHOULD WARRANT CURRENT SNOW ADVISORY BUT LOOK AT SURFACE PRESSURE GRADIENTS THROUGH FRIDAY INDICATE THAT LOW LEVEL WINDS WILL NOT BE ALL THAT STRONG. THEREFORE...DROPPED THE WINTER WEATHER ADVISORY AND EXCHANGED IT FOR A SNOW ADVISORY FOR THE LOWER ELEVATION SNOWFALL. A FAIRLY STRONG GRADIENT STILL EXISTS AT THE UPPER LEVELS THIS AFTERNOON AND TONIGHT AS THE DISTURBANCE PIVOTS THROUGH. ETA SURFACE CAPE THIS AFTERNOON THROUGHOUT THE SACRAMENTO AND SAN JOAQUIN VALLEYS RANGING ANYWHERE FROM AROUND 200 J/KG TO NEARLY 500 IN THE NORTHERN SACRAMENTO VALLEY SO HAD NO PROBLEM LEAVING IN THUNDERSTORM CHANCES FOR THE LOWER ELEVATIONS TODAY IN UNSTABLE AIRMASS AND LIKELY AT LEAST SOME BREAKS IN CLOUD COVER THIS AFTERNOON. SIMILAR CONDITIONS EXPECTED ON FRIDAY ALTHOUGH NOT QUITE AS UNSTABLE BEHIND DISTURBANCE MOVING THROUGH NORTH STATE TONIGHT.

LOOKS LIKE ONLY A BRIEF BREAK ON SATURDAY BEFORE ANOTHER STRONG AND COLD LOW PRESSURE SYSTEM DROPS OUT OF THE GULF OF ALASKA AND ONTO THE NORTH COAST ON SUNDAY AFTERNOON. SNOW LEVELS WILL LIKELY START OUT FAIRLY HIGH AHEAD OF THE LOW THEN DROP ON MONDAY AS THE COLD FRONT MOVES INTO THE SIERRA. AGAIN...ANY BREAK BEHIND THIS SYSTEM WILL BE BRIEF WITH EXTENDED GFS BRINGING YET ANOTHER STRONG LOW PRESSURE SYSTEM INTO NORTHERN CALIFORNIA AROUND MID WEEK.  
SMITH

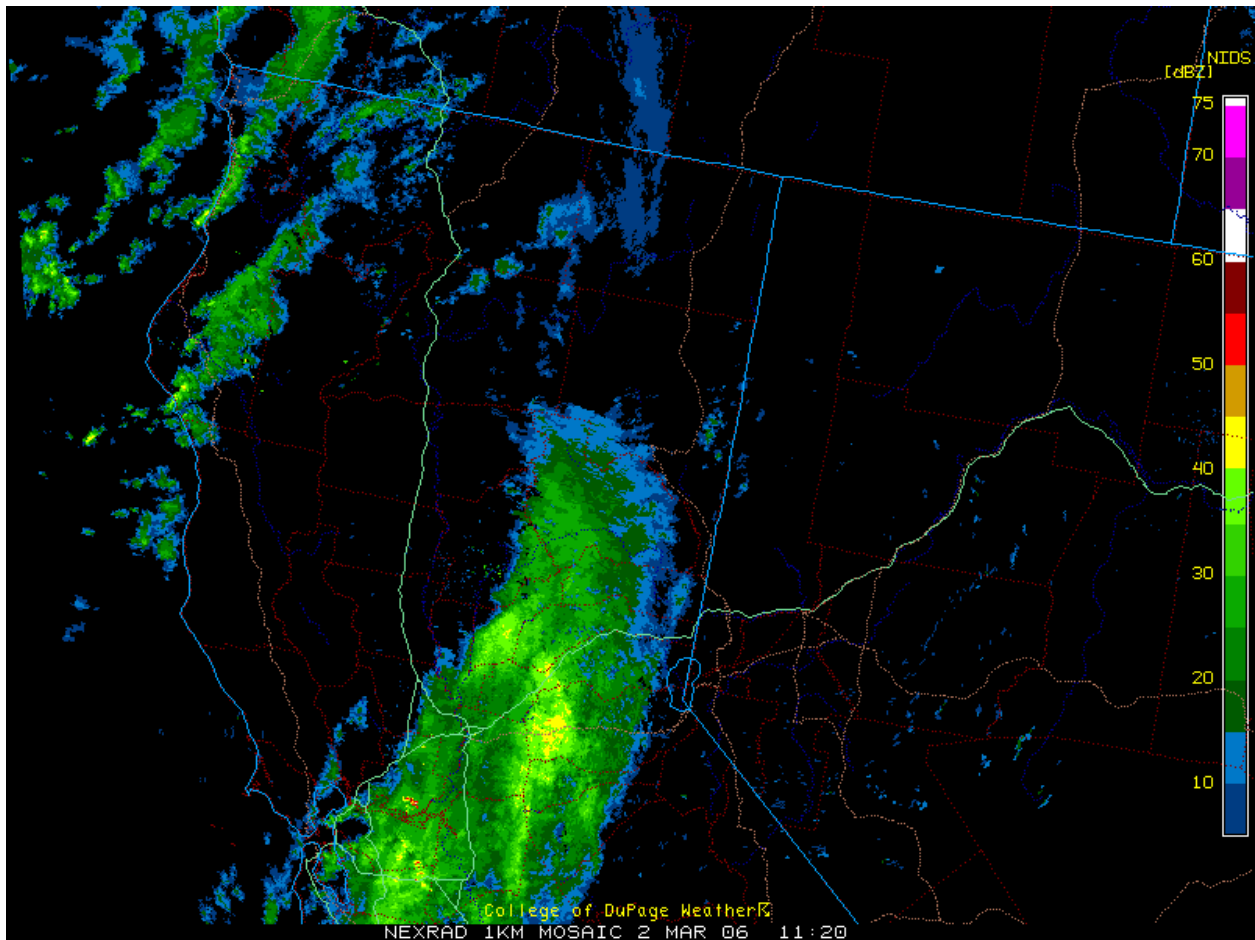


**Figure 16. NEXRAD radar mosaic at 1120 UTC on March 2, 2006**

By sunrise the west half of the sky from Sacramento had only scattered clouds while the east half had overcast skies and showers as the frontal band moved east. Each of the two project aircraft had three flights today for a total of six flights. The first two flights documented the frontal conditions and the last four documented the post-frontal conditions. The time plots of the CN and CCN aerosols at Blodgett are given in Figure 21.

The colorized Aqua satellite image at 2050 UTC on March 2, 2006 is reproduced in Figure 22. Three areas are superimposed on the image. The first is in the central valley, the second is in the Sierra foothills and the third is east of the Sierra crest. The effective radius values are largest over the upwind Sierra slope, indicating precipitation.

The morning front had dissipated to the southeast of Sacramento by late afternoon and a new disturbance was organizing into a second frontal band was organizing to the west and northwest of the Northern California coast. This front was poised to traverse Northern California during the night and morning hours as had its frontal predecessor. The center of the parent upper low could be seen farther to the west of the new frontal band (Figure 17).

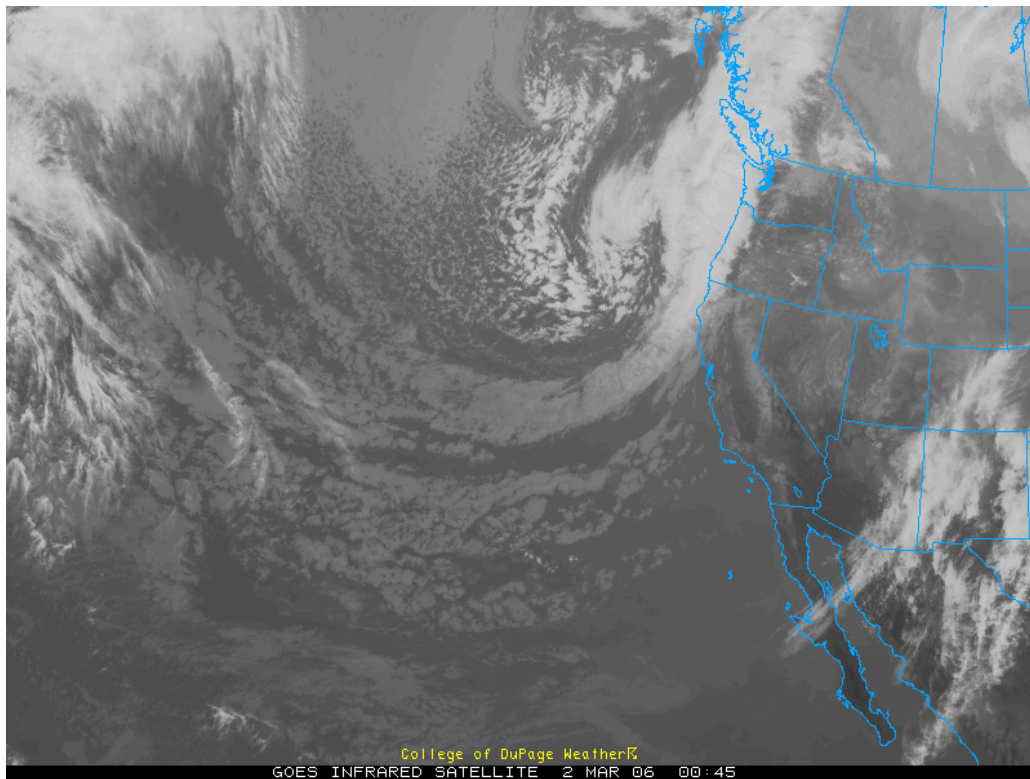


**Figure 17. GOES infrared image at 0045 UTC on March 2, 2006**

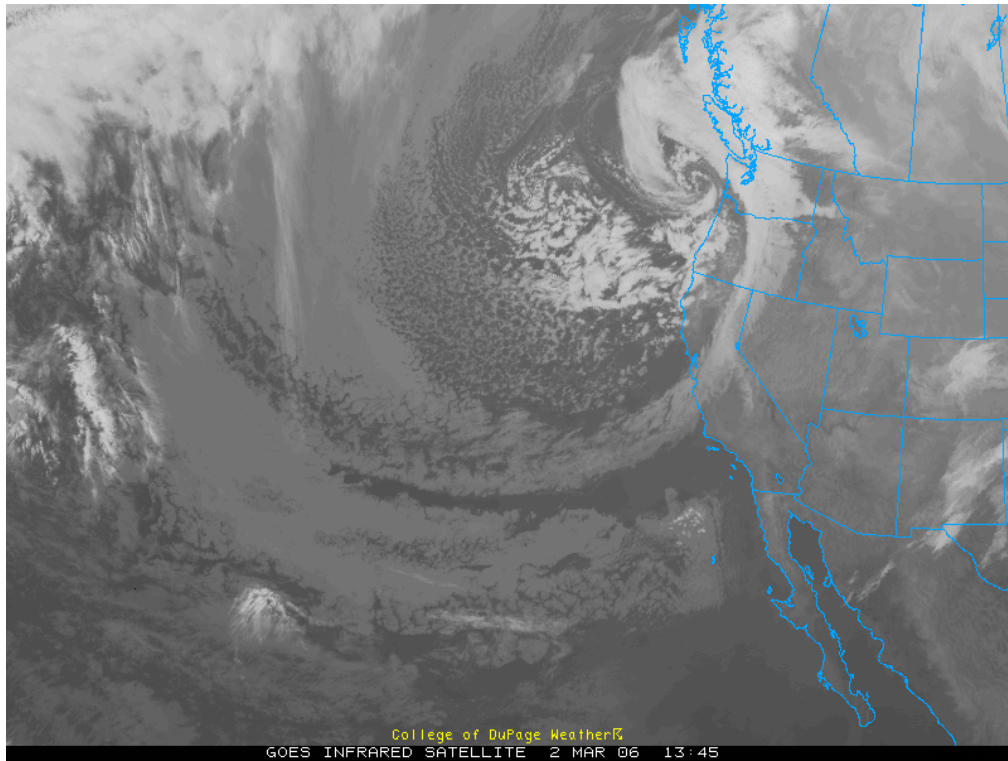


**Figure 18. GOES infrared image at 1345 UTC on March 2, 2006**

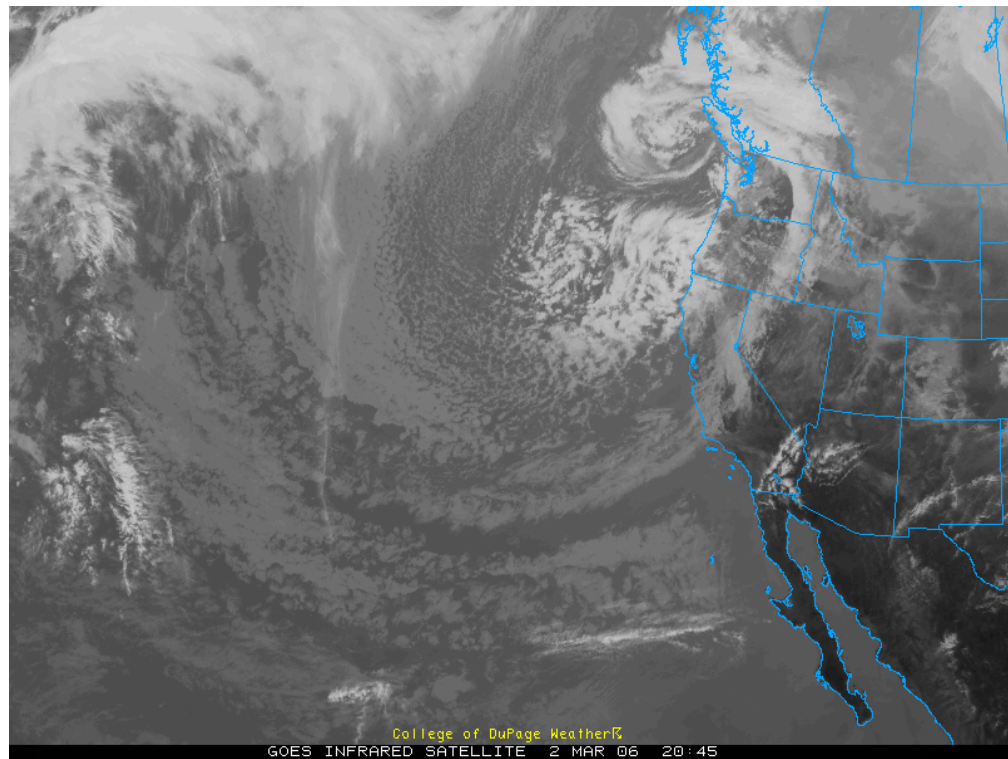


**Figure 19. GOES infrared image at 2045 UTC on March 2, 2006**

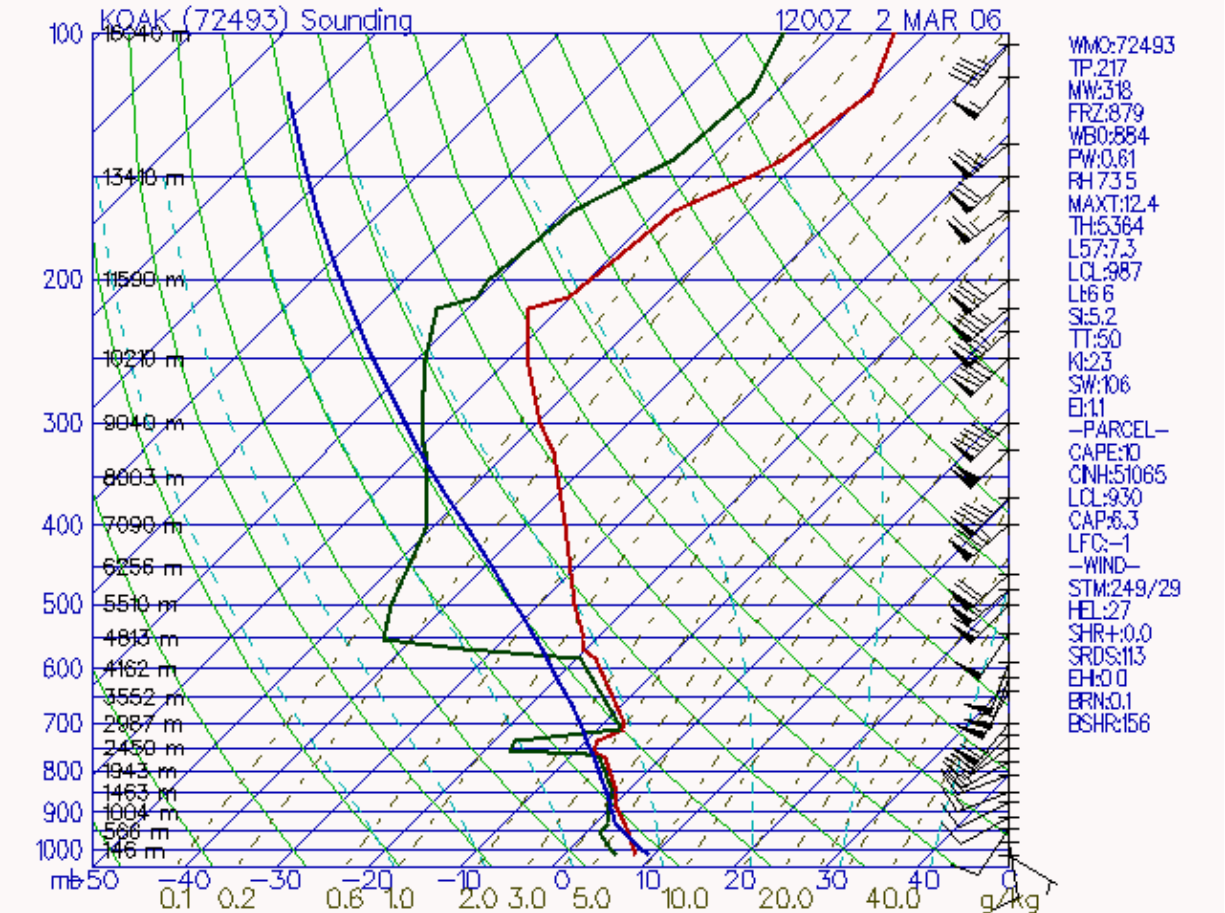


Figure 20. The Oakland 1200 UTC sounding on March 2, 2006

March 2, 2006, Blodgett, CA

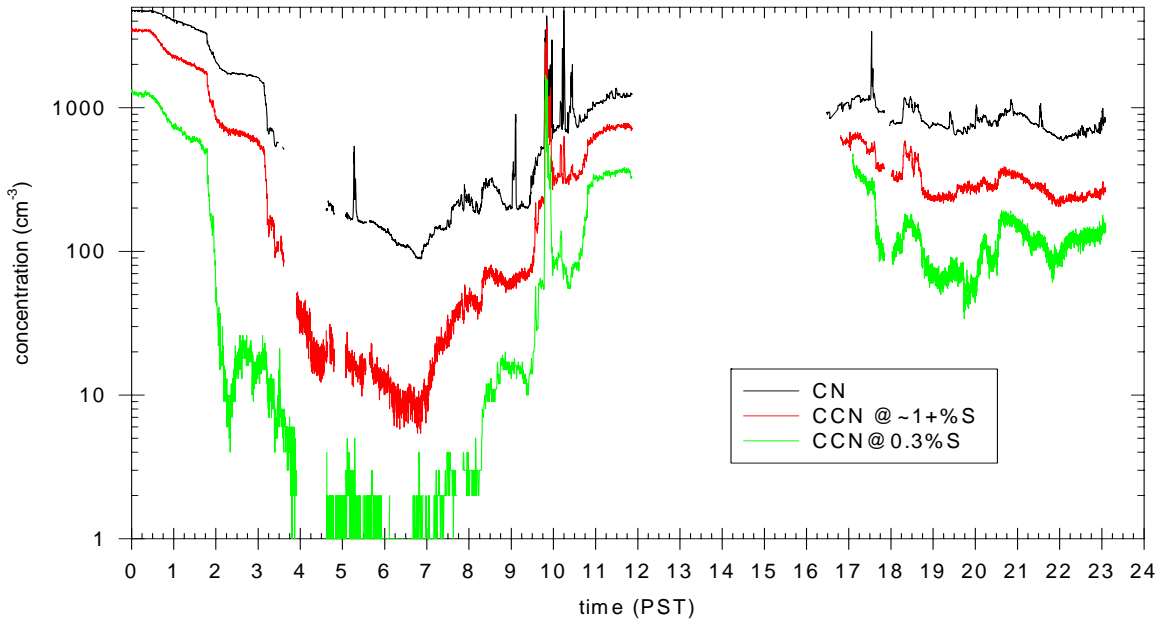


Figure 21. CN and CCN times plots at the Blodgett aerosol site on March 2, 2006

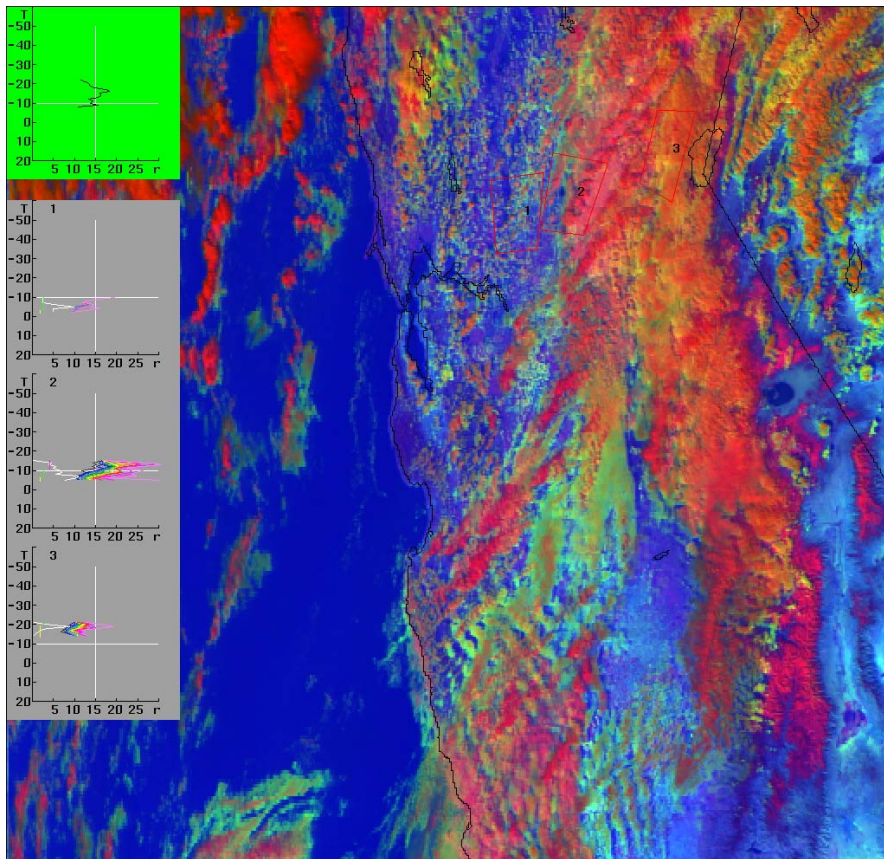


Figure 22. The colorized Aqua satellite image at 2050 UTC on March 2, 2006

## **Triple Research Flights on March 2, 2006**

### **Objectives:**

A weakening cold front causes orographic clouds with embedded convection. The front is nearly stationary with SSW flow also behind it due to trough deepening and another shot of cold air to its NW.

Today we will document the time evolution of the aerosols and cloud properties from Sacramento to the ridge line of the Sierra to the NE, i.e., Blodgett and Squaw Valley.

### **Crew Cloud 1:**

Pilot: Gary Walker

Flight scientist: Daniel Rosenfeld

Instruments operator: Duncan Axisa

### **Crew Cloud 2:**

Pilots: Kevin Laughlin

Flight scientist and instrument operator: William Woodley

The flight tracks of Cloud 1 and Cloud 2 for the first flight of the day are given in Figure 23.

### **Flight 1 of Cloud 1:**

SAC at 16:53 130/5 10 miles, few 3500, broken 7000, 8/6, 30.09

We took off at 17:12, and went through the lower broken cloud base at about 1000', with  $CDP > 500 \text{ cm}^{-3}$ . A second base at 4000' (17:16) had about 15 drops  $\text{cm}^{-3}$ . We flew to the NE and penetrated a yet higher base at 5500' (17:19) with 130 drops  $\text{cm}^{-3}$ . It had some needles.

We continued ascending through almost solid cloud with light icing (17:21) and 100–150 drops  $\text{cm}^{-3}$ . We emerged at the top of slightly convective layer at 10000' (17:23) and soon entered a solid layer through which we climbed over the steepest slopes of the Sierra. We collected some icing, and had about 150 drops  $\text{cm}^{-3}$ , which was almost the same concentration as the CN (200–300  $\text{cm}^{-3}$ ).

We emerged above cloud tops over the crest of the Sierra at just above 16 kft (17:36) at  $-17^\circ\text{C}$ , and saw a flat top of water clouds with no glaciation at all. We made a  $360^\circ$  turn for a panoramic photo, and descended back to the SW at the lowest safety altitude through the orographic clouds, adding some more ice load to the airplane. The clouds had 80–120 drops  $\text{cm}^{-3}$ , small graupel and drizzle. At 6000' (17:52) we encountered an imbedded convective element that had high LWC, much icing and 250 drops  $\text{cm}^{-3}$ . We continued descending through the clouds that formed in the BL of the valley that had 200–800 drops  $\text{cm}^{-3}$  (18:02). We flew at the formation level at 1800' (18:06) and landed at SAC at 18:08.

### **Report by the flight scientist (Woodley) in Cloud 2 for its first flight on March 2, 2006:**

I was in the Cessna 340 (Cloud 2) at 1700Z and the engines were started at 1703Z. I took picture 1 at 1710Z looking to the S along the western edge of the cloud band that had passed and was progressing to the E. At 1712Z the CPC readings were enormous at  $10^5$  to  $10^6$  particles  $\text{cm}^{-3}$ . Take off of Cloud 2 took place at 1714Z when the CPC readings were  $20,000 \text{ cm}^{-3}$ . The bases of the scud clouds were at 1,000 ft, so there was no thought of flying toward Blodgett. The CPC had dropped to  $3,000 \text{ cm}^{-3}$  as we flew to the S and W of the airport to make aerosol measurements.

Our initial measurements were made beginning at 1719Z while flying at 1,000ft. The CPC measurements made at 1,000 ft between 1719 and 1725Z ranged between 700 and  $11,000 \text{ cm}^{-3}$ . I found this variability rather amazing. We were at 1,500 ft between 1728 and 1732Z and the CPC values ranged between 600 and  $3,000 \text{ cm}^{-3}$ . Between 1732 and 1737Z at 2,000 ft the CPC values ranged between 470 and  $5,000 \text{ cm}^{-3}$ . I took picture 2 at 1735Z. Cloud 2 was at 2,500 ft between 1741 and 1747Z where the CPC values ranged from 400 to  $2,500 \text{ cm}^{-3}$ . The temperature at 2,500 ft was  $4.6^\circ\text{C}$ . I took picture 3 at 1746Z looking to the E toward the cloud band. From 1750 to 1756Z Cloud 2 was at 3,000 ft making CPC measurements ranging between 140 to  $1,100 \text{ cm}^{-3}$ .

Cloud 2 was flying at 4,000 ft between 1759 and 1804Z where the counts ranged from 200 to  $420 \text{ cm}^{-3}$ . At 5,000 ft from 1807 to 1813Z the values ranged from 350 to  $3,000 \text{ cm}^{-3}$  while the CCN were in the 50 to  $100 \text{ cm}^{-3}$  range. Picture 4 was taken at 5,000 ft looking to the W at a mushy Cb that was located by radar as being near Pt. Reyes. Cloud 2 had to climb next to 7,500 ft for measurements between 1818 and 1819 of  $1,800 \text{ cm}^{-3}$ . It was at 8,000 ft between 1820 and 1825Z for CPC observations ranging from 600 to  $2,000 \text{ cm}^{-3}$ . Picture 5 was made at 1823Z looking to the W at a slowly building cumulus cloud field. The next flight level was 10,000 ft between 1828 and 1834Z where the CPC values ranged between 250 and  $400 \text{ cm}^{-3}$ . Picture 6 was taken of a cumulus cloud with pileus at 1833Z and #7 was taken at 1834Z looking to the W at the growing cloud field.

We began our descent back to Sacramento Executive Airport at 1836Z. Cloud base was now at 1,800 ft. Landing took place at 1849Z. The CPC counts were  $20,000+$   $\text{cm}^{-3}$  just before landing.

### **Impressions**

We made slow deliberate measurements of the aerosols from the surface to 10,000 ft this morning. The counts were large near the surface and dropped off with height. It is hoped that these measurements will be useful in interpreting the observations made by Cloud 1.

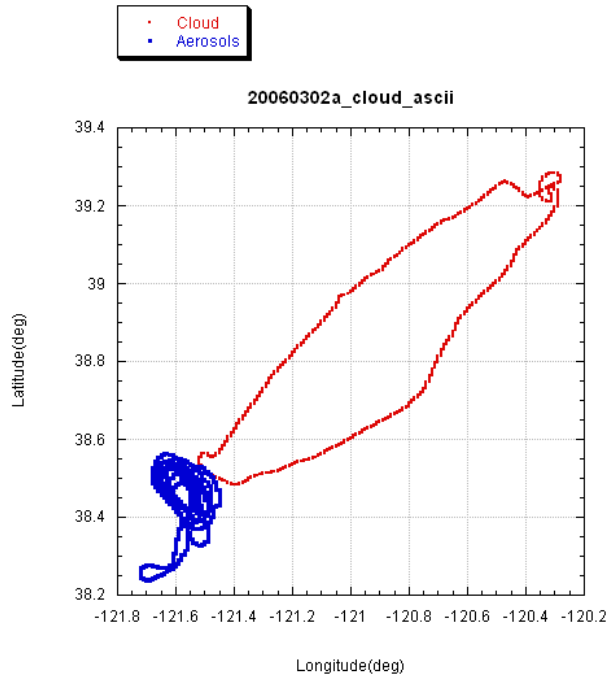


**Figure 23. Plots of the flight tracks of Cloud 1 (red) and Cloud 2 (blue) for the first flight of the day on March 2, 2006**

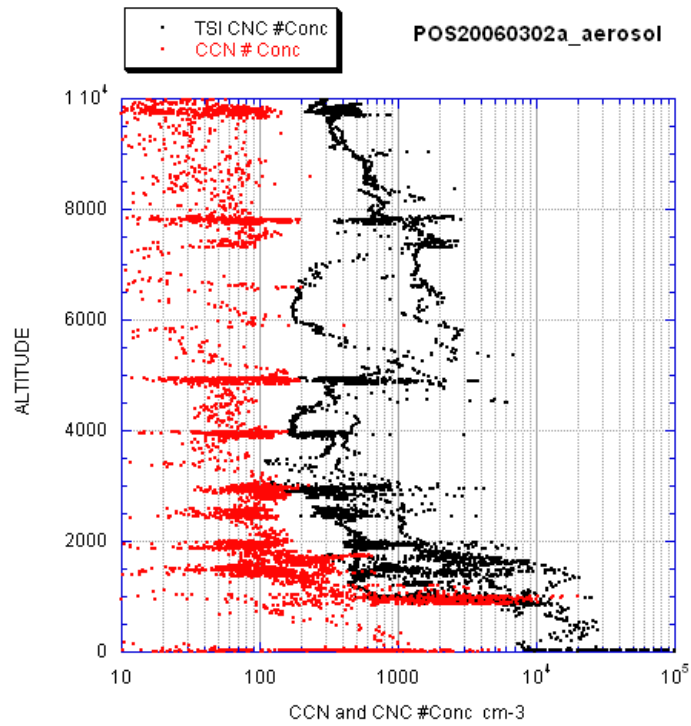


**Figure 24. Plots of the total CNC (black) and CCN (red) aerosol concentrations vs. height (ft) as measured by instrumentation on the first flight of the aerosol (Cloud 2) aircraft on March 2, 2006**

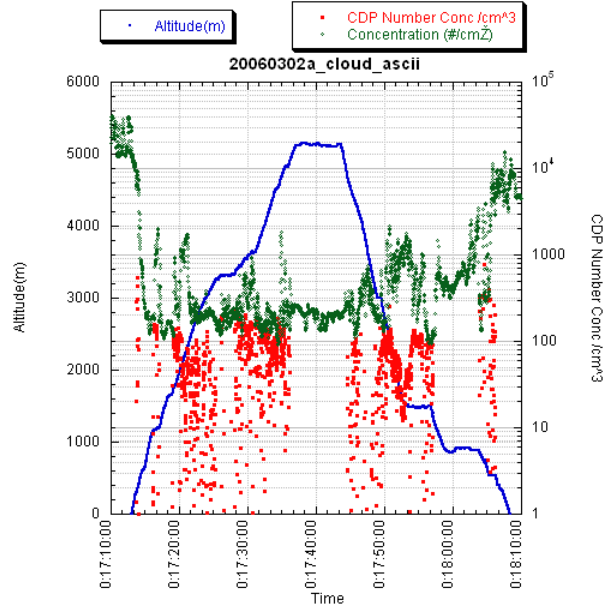


**Figure 25. Plots of the cloud particle concentrations (red), total aerosol concentrations (green) vs. altitude (blue in m) as measured by the Cloud 1 cloud physics aircraft on its first flight of the day on March 2, 2006.**

### The Second Paired Flights of the Research Aircraft on March 2, 2006

Both research aircraft flew a second time beginning in the late morning on March 2, 2006. The flight tracks for both aircraft are given in Figure 26, and plots of aerosol and droplet measurements as a function of time for the aerosol and cloud physics aircraft are provided in Figures 27 and 28, respectively.

#### Flight 2 of the cloud physics aircraft (Cloud 1):

By late morning convection had developed in Sacramento, and the frontal activity was not evident any longer.

SAC weather: 160/6, 10 miles, scattered 2000, overcast 3100, 11/6, 30.08

We took off at 19:47, and went through the lower broken cloud base at 2000' (21:50), with CDP 200-300  $\text{cm}^{-3}$ . We kept climbing to the NE through rising convective elements at the foothills. We passed (12:06) through 12 kft at the top of convection near Blodgett with peak CDP of 80-100 drops  $\text{cm}^{-3}$ . We continued climbing to the crest through solid layer clouds with peak CDP of 80  $\text{cm}^{-3}$ . We emerged through the cloud tops at 15500' (20:13). There was no visible glaciation in the clouds. Some tops with soft convective appearance reached 16 kft where the temperature was  $-20^{\circ}\text{C}$ .

We ascended to 17 kft for panoramic photography (20:18) and then descended to 13 kft (20:23) circling in place over Squaw Valley. We continued descending to the SW at the lowest safety altitude. Peak drop concentrations were 80-150  $\text{cm}^{-3}$ .

Continued descent through deep layer and embedded (with convective-like tops) (20:37) and convective clouds (20:41) had drop concentration contrast between 80 and 300  $\text{cm}^{-3}$ . The BL clouds near Sacramento had a peak concentration of 1000 drops  $\text{cm}^{-3}$  at 2300' (20:47).

We landed at 20:52. Once we were on the ground we took a picture of a cap of ice that remained on the nose of the aircraft.

### **Report by the flight scientist (Woodley) in Cloud 2 for its second flight on March 2, 2006:**

I was back in Cloud 2 at 1950Z and I took a picture of Kevin at 1953Z as a marker to separate flights 1 and 2 today. The CPC counts were only 4,900  $\text{cm}^{-3}$  as we sat under a broken cumulus cloud field. Takeoff on Runway 120° took place at 1959Z. The plan was to find a location in the Sacramento area that would permit aerosol measurements in VFR flight to 10,000 ft. In essence we were to repeat the earlier morning measurements to see how much change had occurred.

The CPC values were up to 11,000 particles  $\text{cm}^{-3}$  at 2000Z. Cloud base was found at 2,500 ft where the CPC values were on the order of 10,000  $\text{cm}^{-3}$ . Picture 2 was taken at 2007Z of the cloud bases while flying over old McClellan Air Force Base. Although there was a lot of cloudiness, it was fairly open for a slow VFR climb in this location. The CPC reading was about 1,200  $\text{cm}^{-3}$  at 3,500 ft at 2012Z. Cloud 2 was at 4,500 ft between 2014 and 2018Z where the CPC readings ranged between up to 1,200  $\text{cm}^{-3}$ . Between 2019 and 2021Z the CPC values were from 400 to 700  $\text{cm}^{-3}$  and the CCN values were on the order of 100  $\text{cm}^{-3}$ . Even so, the CPC readings had climbed up to 3,000  $\text{cm}^{-3}$  at 7,000 ft at 2026Z. Picture 3 was taken at 2028Z of clouds below the aircraft, leaning to the N.

At 7,500 ft at 2029Z the CPC values ranged up to 1,500  $\text{cm}^{-3}$ . At 8,500 ft the values were on the order of 1,000  $\text{cm}^{-3}$  at 2033Z. At 9,500 ft at 2037Z the CPC readings were in the range of 250 to 600  $\text{cm}^{-3}$ . Picture 4 was taken at 2040Z of the cloud field looking to the W, and photo 5 was taken at 2042Z looking to the E over the cloud field leading into the Sierra. The clouds looked to be orographic with convective protuberances. At 10,000 ft the representative CPC value was 300  $\text{cm}^{-3}$  between 2044 and 2045Z.

Cloud 2 began its descent to the airport at 2046Z. I took pictures 6 and 7 at 2054Z of downtown Sacramento as we approached Runway 12. Landing was at 2057Z. We had been in the air for a total of 58 minutes.

### **Impressions**

There had not been too much change in the aerosol readings since the earlier flight. This documentation will be useful to the analyses, especially in interpreting the microphysical measurements of Cloud 1.

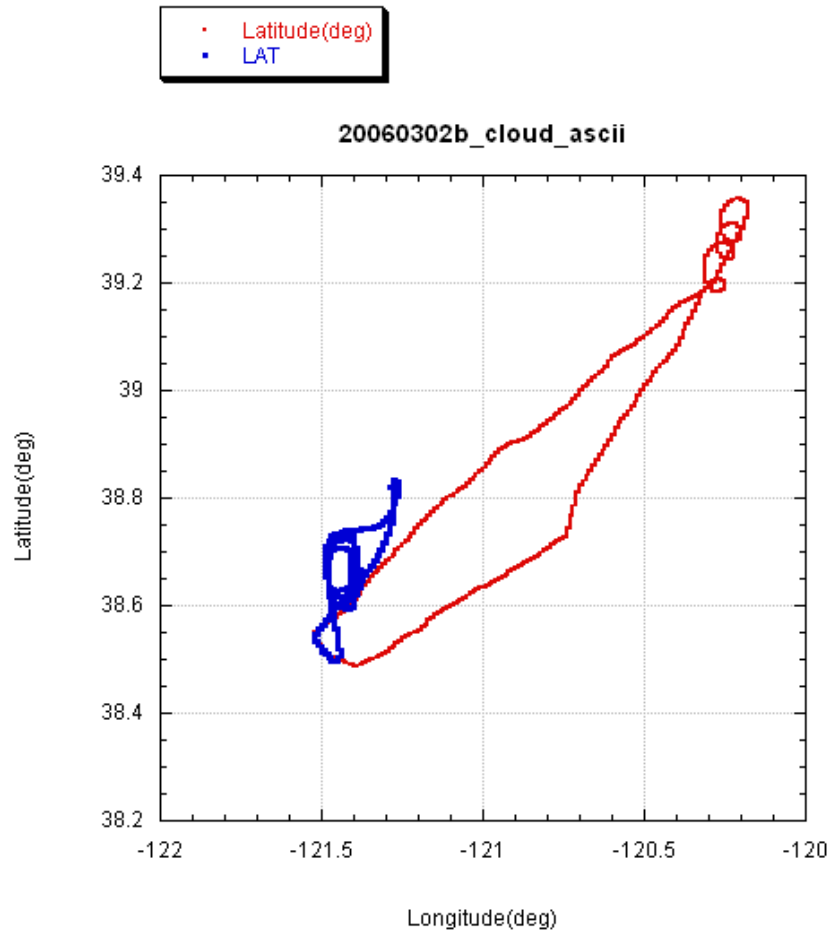


**Figure 26. Plots of the flight tracks of Cloud 1 (red) and Cloud 2 (blue) for the second flight of the day on March 2, 2006**

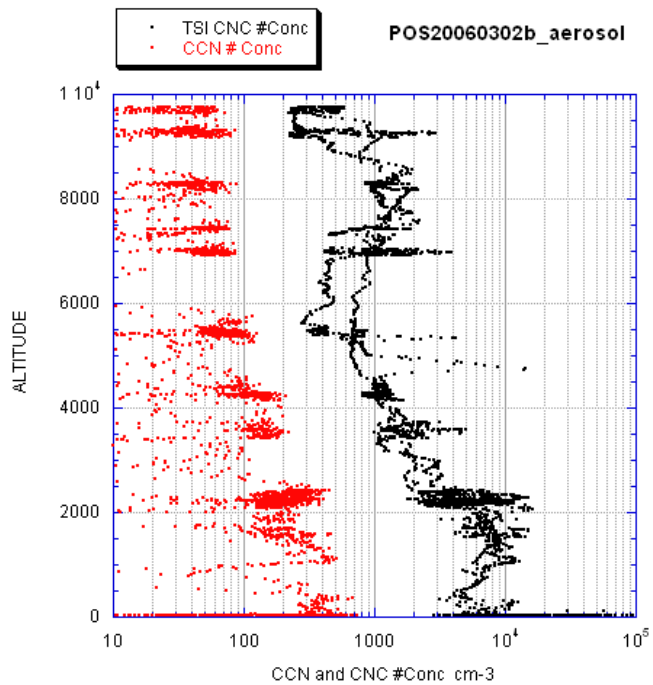


Figure 27. Plots of the total CNC (black) and CCN (red) aerosol concentrations vs. height (ft) as measured by instrumentation on the aerosol (Cloud 2) aircraft on its second flight on March 2, 2006

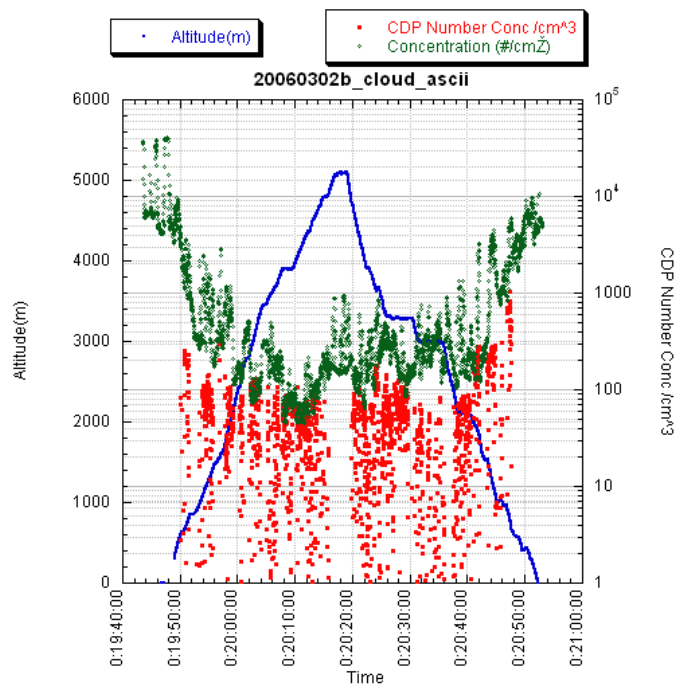


Figure 28. Plots of the cloud particle concentrations (red), total aerosol concentrations (green) vs. altitude (blue in m) as measured by the Cloud 1 cloud physics aircraft on its second flight of the day on March 2, 2006

## The Third Flight of the Cloud Physics Aircraft (Cloud 1)

Both research aircraft flew a third time beginning in the afternoon on March 2, 2006. The flight tracks for both aircraft are given in Figure 29, and plots of aerosol and droplet measurements as a function of time for the cloud physics and aerosol aircraft are provided in Figures 30 and 31, respectively. In the afternoon there were non-precipitating convective clouds with some more development seen to the east towards the mountains.

SAC 120/9 10 miles, few 3600, scattered 4700, scattered 6000, 12/4, 29.98

We took off at 15:08, and went through cloud base at 3500' (15:11), with  $CDP > 600 \text{ cm}^{-3}$ . The computer froze while going through 4000' flying to a buildup of convection several miles to the SW of Hangtown. We circled in the clear air until the computer was reset and back up again (23:25) and then penetrated the clouds about 500' above their bases. We started ascending through this cloud cluster, which appeared to be precipitating to the north. It had  $> 700$  drops  $\text{cm}^{-3}$  at heights up to 7000', and then decreased gradually to 200 drops  $\text{cm}^{-3}$  at the convective cloud top at 11800' which was at  $-12^\circ\text{C}$  (23:34). Old cloud tops at 12 kft were glaciated. The growing clouds were not glaciated.

We continued NE to the orographic layer clouds (23:44) at 13000' and climbed through them. Drop concentration was about  $80 \text{ cm}^{-3}$ . The top of the orographic layer over the crest was 15000 (23:49). It was not as solid as in the previous flights, and some mountain tops could be seen occasionally in the clouds. A veil of ice crystals/snow was seen evaporating downwind of the crest over Nevada. We ascended to 16 kft and took a panoramic photograph (23:50), and then returned to the SW at the lowest safely altitude. Most of the clouds were below our level of 13 kft, and some clouds that grew higher produced glaciated sections. At the western slopes and the foothills there were still harder convective tops through which we descended and found progressively more drops when going lower and into the valley (from 200 to 1000 drops  $\text{cm}^{-3}$ ). Cloud base was at 4000'. We landed at 00:17.

## Impressions

The impressions from the three flights of each aircraft combined are:

1. The aerosols over the valley are concentrated in the BL in the morning, and disperse to 8000' by the mid afternoon via the convective clouds.
2. The elevated aerosol levels aloft in the morning could be a result of convective mixing upwind in SW California.
3. The orographic clouds at the mid-level ingest aerosols in three ways:
  - a. By direct convection from the cloud base. This works at the lower foothills. This mechanism is not operative at the higher elevations where the terrain rises above the top of the BL of the valley, which is 5000' at most.
  - b. Indirectly by detrainment of the aerosols from the valley and foothills convection, and then incorporation in the orographic cap cloud at lower concentrations.
  - c. Indirectly by a longer range transport of elevated aerosol layers.

4. The clouds have sufficiently large drops to develop ice multiplication, but not large enough to form significant drizzle and warm rain.
5. The cap orographic clouds produce some ice precipitation, but the fact that they are not glaciated at the crest means that much cloud water passes the ridge and evaporates instead of being precipitated.
6. The area that appears to be affected most is the lower foothills, just to the east of the elevation contour of 3000' to 5000', which is the range of the top of the valley BL. This is in agreement with the rain gauge analyses of Givati (Givati and Rosenfeld, 2004 ).

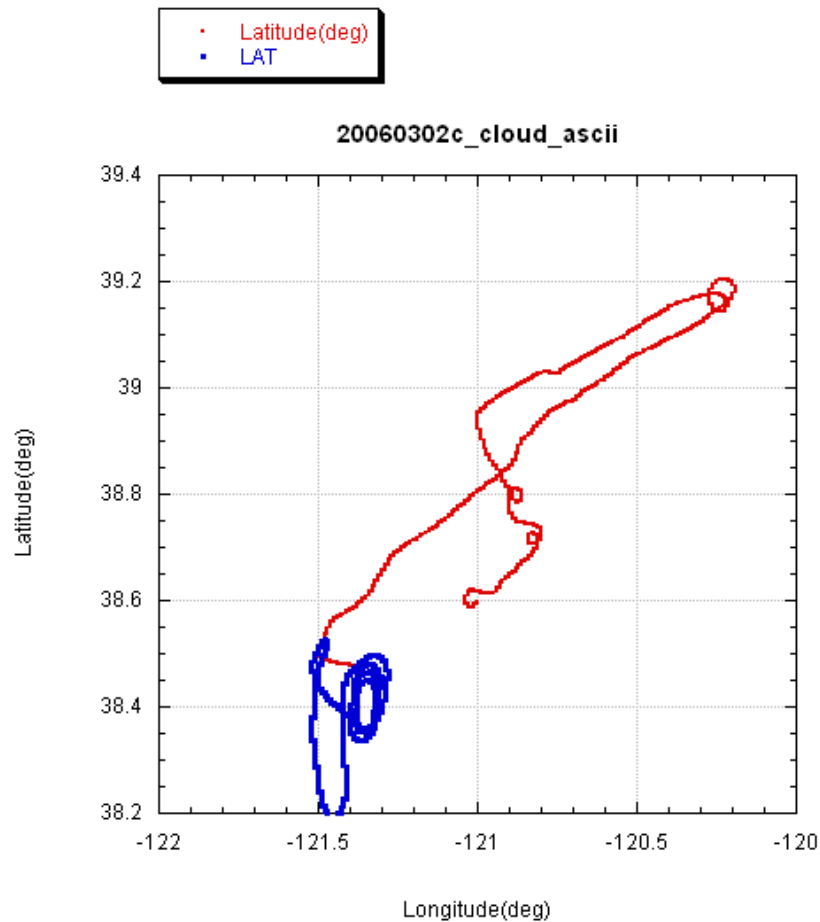


**Figure 29. Plots of the flight tracks of Cloud 1 (red) and Cloud 2 (blue) for the third flight of the day on March 2, 2006**

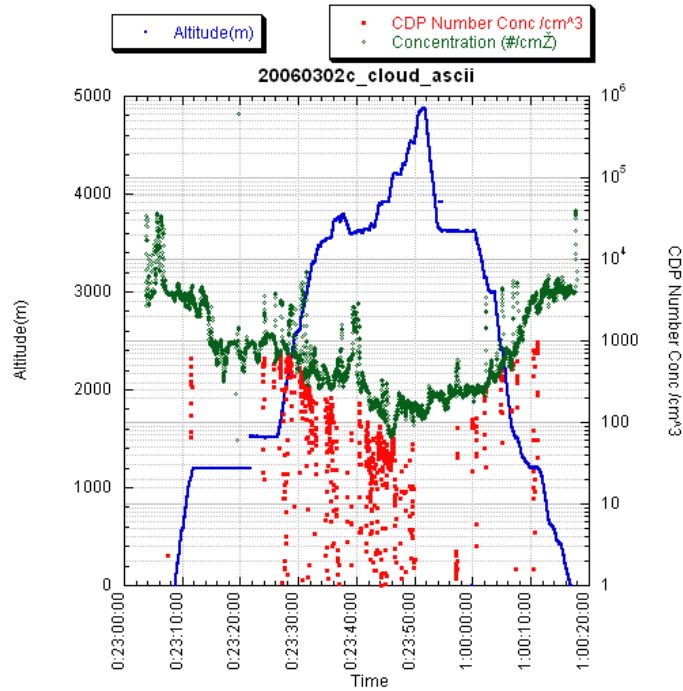


Figure 30. Plots of the cloud particle concentrations (red), total aerosol concentrations (green) vs. altitude (blue in m) as measured by the Cloud 1 cloud physics aircraft on its third flight of the day on March 2, 2006

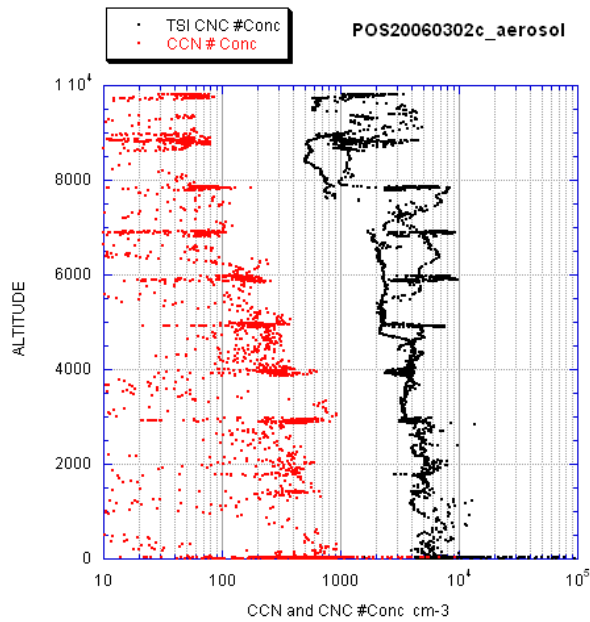


Figure 31. Plots of the total CNC (black) and CCN (red) aerosol concentrations vs. height (ft) as measured by instrumentation on the aerosol (Cloud 2) aircraft on its third flight on March 2, 2006



## 5.0 References

- Albrecht, B. S., 1989: Aerosols, cloud microphysics and fractional cloudiness, *Science* 245, 1227.
- Alpert, P. and H. Shafir, 1991: On the role of the wind vector interaction with high-resolution topography in orographic rainfall modeling. *Quart. J. R. Meteor. Soc.*, 117, 421–426.
- Andreae M. O., D. Rosenfeld, P. Artaxo, A. A. Costa, G. P. Frank, K. M. Longo, and M. A. F. Silva-Dias, 2004: Smoking rain clouds over the Amazon. *Science*, 303, 1337–1342.
- Borys, R. D., D. H. Lowenthal, and D. L. Mitchel, The relationship among cloud physics, chemistry and precipitation rate in cold mountain clouds, *Atmos. Environ.*, 34, 2593–2602, 2000.
- Borys, R. D., D. H. Lowenthal, S. A. Cohn, and W. O. J. Brown, Mountaintop and radar measurements of anthropogenic aerosol effects on snow growth and snow rate, *Geophys. Res. Lett.*, 30(10), 1538, doi:10.1029/2002GL016855, 2003.
- Coakley, J. A., Bernstein, R. L., and Durkee, P. A., 1987: Effect of ship-track effluents on cloud reflectivity: *Science*, 237, 1020–1022, 1987.
- Gagin, A., and J. Neumann, 1974: Rain stimulation and cloud physics in Israel. *Weather and Climate Modification*, W. N. Hess, Ed., John Wiley and Sons, 454–494.
- Gagin, A., and J. Neumann, 1981: The second Israeli randomized cloud seeding experiment: Evaluation of the results. *J. Appl. Meteor.*, 20, 1301–1321.
- Givati, A., and D. Rosenfeld, 2004: Quantifying precipitation suppression due to air pollution. *Journal of Applied Meteorology*, 43, 1038–1056.
- Givati, A., and D. Rosenfeld, 2005: Separation between Cloud Seeding and Air Pollution Effects. *Journal of Applied Meteorology*, 44, 1298–1314.
- Dusek, U., G. P. Frank, L. Hildebrandt, J. Curtius, J. Schneider, S. Walter, D. Chand, F. Drewnick, S. Hings, D. Jung, S. Borrmann, and M. O. Andreae, 2006: Size matters more than chemistry for cloud nucleating ability of aerosol particles: *Science*, 312, 1375–1378.
- Griffith, D. A., M. E. Solak, and D. P. Yorty, 2005: Is air pollution impacting winter orographic precipitation in Utah? *Weather modification association. J. Wea. Modif.*, 37, 14–20.
- Gunn, R., and B. B. Phillips, 1957: An experimental investigation of the effect of air pollution on the initiation of rain. *J. Meteor.*, 14, 272–280.
- Hallett J., and S. C. Mossopp, 1974: Production of secondary ice particles during the riming process. *Nature*, 249, 26–28.
- Jirak, I. L., and W. R. Cotton, 2006: Effect of air pollution on precipitation along the Front Range of the Rocky Mountains. *J. Appl. Meteor.*, 45, 236–245.

- Khain, A. P., D. Rosenfeld, and A. Pokrovsky, 2001: Simulation of deep convective clouds with sustained supercooled liquid water down to  $-37.5$  C using a spectral microphysics model. *Geophysical Research Letters*, 3887–3890.
- Khain, A., D. Rosenfeld, and A. Pokrovsky, 2005: Aerosol impact on the dynamics and microphysics of convective clouds. *The Quarterly Journal of the Royal Meteorological Society*, 131, 1–25.
- Kirchstetter, T. W., J. Aguiar, S. Tonse, D. Fairley, and T. Novakov, 2007: Black carbon concentrations and diesel vehicle emission factors derived from coefficient of haze measurements in California: 1967–2003. *Atmospheric Environment*, 42, 480–491.
- Koren, I., Y. J. Kaufman, L. A. Remer, and J. V. Martins, 2004: Measurement of the effect of Amazon smoke on inhibition of cloud formation: *Science*, 303, 1342–1345.
- Kovetz, A., and B. Olund, 1969: The effect of coalescence and condensation on rain formation in a cloud of finite vertical extent. *J. Atmos. Sci.*, 26, 1060–1065
- Lowenthal, D. H., B. Zielinska, J. C. Chow, J. G. Watson, M. Gautam, D. H. Ferguson, G. R. Neuroth, K. D. Stevens, 1994 : Characterization of heavy-duty diesel vehicle emissions. *Atmos. Environ.*, 28 , 731–743.
- Lynn B., A. Khain, D. Rosenfeld, W. L. Woodley, 2007: Effects of aerosols on precipitation from orographic clouds, *J. Geophys. Res.* , In press.
- Mantua, N. J., S. R. Hare, Y. Zhang, J. M. Wallace, and R. C. Francis, 1997: A Pacific interdecadal climate oscillation with impacts on salmon production. *Bull. Amer. Meteor. Soc.*, 78, 1069–1079.
- Maricq, M. M., R. E. Chase, D. H. Podsiadlik, and R. Vogt, 1999: “Vehicle Exhaust Particle Size Distributions: A Comparison of Tailpipe and Dilution Tunnel Measurements,” SAE Paper No. 1999-01-1461, Society of Automotive Engineers, Warrendale, Penn.
- Mossop, S. C., and J. Hallett, 1974: Ice crystal concentration in cumulus clouds: Influence of the drop spectrum. *Science*, 186(4164):632–634.
- Pierson, W. R., and W. W. Brachaczek, 1983 : Particulate Matter Associated with Vehicles on the Road II. *Aerosol Sci. Technol.* 2, 1–40.
- Phillips, V. T. J., T. W. Choulaton, A. M. Blyth, and J. Latham, The influence of aerosol concentrations on the glaciation and precipitation of a cumulus cloud, *Q. J. Roy. Meteor. Soc.*, 128 (581), 951–971, 2002.
- Ramanathan, V., P. Crutzen, J. Kiehl, and D. Rosenfeld, 2001: Aerosols, Climate, and the Hydrological Cycle, *Science*, 294, 2119–2124.
- Ramanathan, V., C. Chung, D. Kim, T. Bettge, L. Buja, J. T. Kiehl, W. M. Washington, and Q. Fu, 2005: D. R. Sikka, and M. Wild, Atmospheric Brown Clouds: Impacts on South Asian Climate and Hydrological Cycle, *Proc. Nation. Acad. Sci.*, 102 (15), 5326–5333.

- Rosenfeld, D., and I. M. Lensky, 1998: Satellite-based insights into precipitation formation processes in continental and maritime convective clouds. *The Bulletin of American Meteorological Society*, 79, 2457–2476.
- Rosenfeld, D., 1999: TRMM Observed First Direct Evidence of Smoke from Forest Fires Inhibiting Rainfall. *Geophysical Research Letters*. 26, (20), 3105–3108.
- Rosenfeld, D., 2000: Suppression of Rain and Snow by Urban and Industrial Air Pollution. *Science*, 287 (5459), 1793–1796.
- Rosenfeld, D., R. Lahav, A. P. Khain, and M. Pinsky, 2002: The role of sea-spray in cleansing air pollution over ocean via cloud processes. “Research Article” in *Science*, 297, 1667–1670.
- Rosenfeld, D., and W. L. Woodley, 2003: Closing the 50-year circle: From cloud seeding to space and back to climate change through precipitation physics. Chapter 6 of "Cloud Systems, Hurricanes, and the Tropical Rainfall Measuring Mission (TRMM)" edited by Drs. Wei-Kuo Tao and Robert Adler, 234 pp., p. 59–80, *Meteorological Monographs* 51, AMS.
- Rosenfeld, D., and A. Givati, 2006: Evidence of orographic precipitation suppression by air pollution induced aerosols in the western U.S. *J. Applied Meteorology and Climatology*, 45, 893–911.
- Rosenfeld, D., I. M. Lensky, J. Peterson, A. Gingis, 2006: Potential impacts of air pollution aerosols on precipitation in Australia. *Clean Air and Environmental Quality*, 40, No.2. 43–49, May 2006.
- Rosenfeld D., 2006a: Aerosol-Cloud Interactions Control of Earth Radiation and Latent Heat Release. *Space Science Reviews*. In press, DOI: 10.1007/s11214-006-9053-6, 2006a.
- Rosenfeld, D., 2006b: Aerosols Suppressing Precipitation in the Sierra Nevada: Results of the 2006 Winter Field Campaign. Presented at the Third Climate Change Research Conference, California Energy Commission, Sacramento, California, 13–15 September 2006. Presentation available at:  
  
[www.climatechange.ca.gov/events/2006\\_conference/presentations/2006-09-14/2006-09-14\\_ROSENFELD.PDF](http://www.climatechange.ca.gov/events/2006_conference/presentations/2006-09-14/2006-09-14_ROSENFELD.PDF)
- Rosenfeld, D., Jin Dai, Xing Yu, Xiaohong Xu, Xing Yang, Chuan Li Du, and Zhanyu Yao, 2007a: Suppression of precipitation by air pollution at Mountain Hua, Shaanxi, China. Submitted.
- Rudich, Y., O. Khersonsky, and D. Rosenfeld, Treating clouds with a grain of salt, *Geophys. Res. Lett.*, 29, 2060, doi:10.1029/2002GL016055, 2002.
- Rudich Y., A. Sagi, D. Rosenfeld, 2003: Influence of the Kuwait oil fires plume (1991) on the microphysical development of clouds. *J. Geophys. Res.*, 108, D15, 4478, doi:10.1029/2003JD003472.

- Segal Y., A. Khain, M. Pinsky, and D. Rosenfeld, 2004: Effects of hygroscopic seeding on raindrop formation as seen from simulations using a 2000-bin spectral cloud parcel model. *Atmospheric Research* 71, 3–34.
- Squires, P., 1958: The microstructure and colloidal stability of warm clouds. I. The relation between structure and stability, *Tellus*, 10, 256–271.
- Stanhill, G., and S. Cohen, 2001, Global dimming: A review of the evidence for a widespread and significant reduction in global radiation with discussion of its probable causes and possible agricultural consequences, *Agric. For. Meteorol.*, 107, 255– 278.
- Takemoto, B. K., B. E. Croes, S. M. Brown, N. Motallebi, F. D. Westerdahl, H. G. Margolis, B. T. Cahill, M. D. Mueller, J. R. Holmes, 1995: Acidic deposition in California: Findings from a program of monitoring and effects research. *Water, Air & Soil Pollution*, 85, 261–272.
- Teller, A., and Z. Levin, The effects of aerosols on precipitation and dimensions of subtropical clouds; a sensitivity study using a numerical cloud model, *Atmos. Chem. and Phys.*, 6, 67–80, 2006.
- TRMM, 1997: TRMM (Tropical Rainfall Measuring Mission) was launched on 28 November 1997 as a cooperative project of the National Aeronautics and Space Administration (NASA), and the National Space Development Agency of Japan (NASDA). The TRMM are available at [http://daac.gsfc.nasa.gov/CAMPAIGN\\_DOCS/hydrology/hd\\_trmm\\_intro.html](http://daac.gsfc.nasa.gov/CAMPAIGN_DOCS/hydrology/hd_trmm_intro.html).
- Van Den Heever S. C., G. G. Carrió, W. R. Cotton, P. J. Demott, A. J. Prenni, 2006: Impacts of Nucleating Aerosol on Florida Storms. Part I: Mesoscale Simulations. *J. Atmos. Sci.* 63, 1752–1775.
- Warner, J., 1968: A reduction in rainfall associated with smoke from sugar cane fires - an inadvertent weather modification? *J. Appl. Meteor.*, 7, 247 (1968).
- Weingartner, E., H. Burtscher, and U. Baltensperger, 1997: Hygroscopic properties of carbon and diesel soot particles. *Atmos. Environ.*, 31, 2311–2327.
- Williams, D. J., J. W. Milne, S. M. Quigley, and D. B. Roberts, 1989: Particulate-emissions from in-use motor vehicles. *Atmos. Environ.*, 23, 2647–2661.
- Woodley Weather Consultants, and D. Rosenfeld: 2005. The Use of a Cloud Physics Aircraft for the Mapping of Pollution Aerosols Detrimental to Winter Orographic Precipitation over the California Sierra Nevada. California Energy Commission, PIER Energy-Related Environmental Research. CEC-500-2005-205.
- Woodley, W. L., D. Rosenfeld, A. Khain, B. Lynn, and A. Givati: 2006: Physical/Statistical and Modeling Documentation of the Effects of Urban and Industrial Air Pollution in California on Precipitation and Stream Flows in Mountainous Terrain Downwind. California Energy Commission, PIER Energy-Related Environmental Research. CEC-500-2007-019.

Zhang, Y., J. M. Wallace, D. S. Battisti, 1997: ENSO-like interdecadal variability: 1900–93. *J. Climate*, 10, 1004–1020.



## **Appendix C**

### **The SOAR Research Aircraft During SUPRECIP-2**



## APPENDIX C

### The SOAR Research Aircraft during SUPRECIP-2

#### 1.0 Specifications of the Soar Cheyenne II Cloud Physics Aircraft During Suprecip-2

The SOAR Cheyenne II research aircraft (Figure 1) is an airborne platform for atmospheric research consisting of instrumentation that has the capability of measuring in situ microphysical properties of clouds and their thermodynamic environment, documenting the composition of clouds and diagnosing the physical processes within them. This aircraft has been especially modified and equipped for atmospheric research together with the crew and infrastructure needed to support its use. The SOAR Cheyenne II research aircraft, entirely dedicated to atmospheric research, is a versatile flying laboratory offering several scientific configurations: basic meteorological instrumentation, turbulent flux equipment, microphysics sensors, and in-situ chemistry instruments. Many instruments on the Cheyenne II are provided, maintained, and operated by the SOAR (Seeding Operations & Atmospheric Research) Group.



Figure 1. The SOAR Cheyenne II cloud physics aircraft

## **1.1 The Cloud Droplet Probe (CDP: 2 $\mu$ m to 50 $\mu$ m)**

During SUPRECIP-2, the Cheyenne II research aircraft will be mainly equipped to conduct cloud physics measurements to document the microphysical properties of orographic clouds in the Sierra-Nevada. The instrumentation platform is composed of the Droplet Measurement Technologies (DMT) Cloud Droplet Probe (CDP) and the Cloud Imaging Probe (CIP), and the Particle Measuring Systems Forward Scattering Spectrometer Probe (FSSP). In addition, an Aircraft-Integrated Meteorological Measurement System (AIMMS-20) collects data relevant to the thermodynamic and environmental surroundings of the aircraft.

The Cloud Droplet Probe (CDP) is a new forward light-scattering spectrometer that can measure cloud particles in the range of 2  $\mu$ m to 50  $\mu$ m. The instrument counts and sizes individual droplets as they traverse a laser beam. Droplets that hit the laser beam within the sample volume scatter light and the forward scattered light is collected onto an optical beam splitter and then onto a pair of photo detectors, the sizing detector and the qualifying detector. The CDP accepts and sizes only particles that pass through a uniform power region of the laser beam since the scattered light is focused through an optical mask that defines the depth of field (DOF). Different voltage pulses from the sizing detector are compared with the voltage pulses from the qualifying detector, and a digital flag is raised if the masked detector's output exceeds that of the signal to be sized, hence rejecting the particle (DOF rejected). The DOF qualified photon pulse is then converted, amplified and digitized into a sizing bin. The range of the CDP is fixed and the output is distributed in 30 size channels. The CDP is mounted external to the aircraft below the right wing and adjacent to the Cloud Imaging Probe (CIP).

## **1.2 The Forward Scatter Spectrometer Probe (FSSP)**

The Forward Scattering Spectrometer Probe (FSSP SPP-100) is similar in operation to the CDP and is also used to collect size distributions of airborne particulates ranging from 2 - 47 $\mu$ m. For ease of service and compatibility the probe mounts in the 7-inch OD cylinder as a plug-in assembly with two internal connectors at 90° to each other allowing the probe light tubes to be oriented either perpendicular or parallel to the mounting pad. The FSSP is mounted below the left wing.

## **1.3 The Cloud Imaging Probe (CIP: 25 $\mu$ m to 1.55 mm)**

The DMT Cloud Imaging Probe (CIP) is very similar in technical operation to the 2D-OAP developed by PMS. A linear array of laser beams is focused on a sampling area where the particles' shadows are optically magnified to provide the imaging data. Whenever a detector diode is shadowed by a passing particle, the on-board digital electronics begin storing diode information at the true airspeed (TAS) frequency. The TAS is determined using an on-board pitot tube mounted just adjacent to the sampling area, providing accurate airspeed at the instrument itself. On the SOAR aircraft, the AIMMS-20 provides more accurate TAS data, so the TAS clock is provided from the AIMMS-20 air data probe. The CIP incorporates a 64-element photo-diode array and has a 25-  $\mu$ m size resolution. The data output is distributed in 62 channels making the minimum detectable particle size at 12.5  $\mu$ m and the largest particle at 1562.5  $\mu$ m. Particles that shadow the two end diodes (1 and 64) are end rejected.

The CIP incorporates a Liquid Water Content (LWC) detector. The LWC is a hot-wire sensor. The sensor head of the LWC holds a hot wire element. The temperature of the wire is maintained constant at 125°C. The more liquid water present in the immediate environment, the greater the number of cloud droplets impinging on the heated sensor element that is exposed to the airflow outside the aircraft. This causes a cooling effect that increases the power needed to maintain the sensor temperature constant. The additional power needed to react to the drop in the temperature is a function of the liquid water content and the true airspeed.

#### **1.4 Aircraft Integrated Meteorological Measurement System (AIMMS-20)**

Aircraft Integrated Meteorological Measurement System (AIMMS-20) gives up-to-the-second real-time three-dimensional wind conditions evaluated using the Kalman Filter Digital Signal Processing (DSP) technique. Wind Vector Software provides a real-time display of the horizontal wind component. The AIMMS-20AQ consists of four components: an Air Data Probe (ADP), a carrier-phase Geostationary Positioning Satellite (GPS) measurement module, an Inertial Measurement Unit (IMU) and Central Processing Module (CPM). The ADP is mounted below the lower wing surface while the other three modules are located in the cockpit. The system gives position and velocity information from the GPS with six-axis inertial rates from the IMU's three rate gyros and accelerometers and aerodynamically corrected 3D aircraft-relative flow vector data from the ADP. The CPM then processes this sensor data at 20 times per second, combines the differential GPS carrier-phase data with the inertial data to determine accurate aircraft attitude, and then combines these data with the raw air-motion data to precisely determine the wind solution to better than 0.5m/s accuracy. In addition, the AIMMS-20AQ also measures the flow direction, true heading, barometric pressure, altitude, temperature and relative humidity. This makes the AIMMS-20AQ a suitable instrument to measure research grade atmospheric soundings close in time and space to the intended cloud studies. The AIMMS-20AQ is also suitable for cloud draft measurements, since the ADP on the SOAR aircraft is a de-iced version.

#### **1.5 TSI Model 3010 Condensation Particle Counter (CPC)**

The Model 3010 Condensation Particle Counter (CPC) is a compact, rugged instrument that detects airborne particles down to 10 nanometers in diameter. Due to a high signal-to-noise ratio that limits false background counts to nearly zero, it detects these small particles with remarkable accuracy. The Model 3010 CPC samples and counts sub  $\mu\text{m}$  particles on a continuous basis, enlarging them to a size that can be detected easily. It offers an upper concentration limit of 10,000 particles per cubic centimeter and responds quickly to concentration changes, showing accurate readings in a matter of seconds. The 3010 is mounted inside the cabin of the aircraft and the instrument samples the environmental aerosol through an inlet affixed to the aircraft fuselage.

## 2.0 Specifications of the SOAR Cessna 340 II Aerosol Aircraft During SUPRECIP-2

The Cessna 340 aircraft (Figure 2) was equipped specifically for SUPRECIP-2. This aircraft carries aerosol-measuring equipment for sampling airborne aerosols and cloud condensation nuclei (CCN). The Cessna 340 can fly at airspeeds as slow as 60 m/s, yet carry a sizeable load of instruments. The 340 is able to carry the DMT CCN counter, the TSI Model 3022A, the DMT Liquid Water Content (LWC) probe and the Rosemount temperature probe (Figure 3). To sample aerosols accurately, the Cessna 340 has been modified to sample aerosols isokinetically. This is achieved by slowing the sampled air down using a double diffuser type inlet. In addition, the 340 is capable of measuring the GPS position, altitude and groundspeed, and transmit these data to the Cheyenne. These data are processed in real time in the Cheyenne research aircraft and become useful when both research aircraft need to coordinate flight profiles for accurate plume tracking and stacked downwind cloud measurements.



Figure 2. The Cessna 340 II aerosol research aircraft

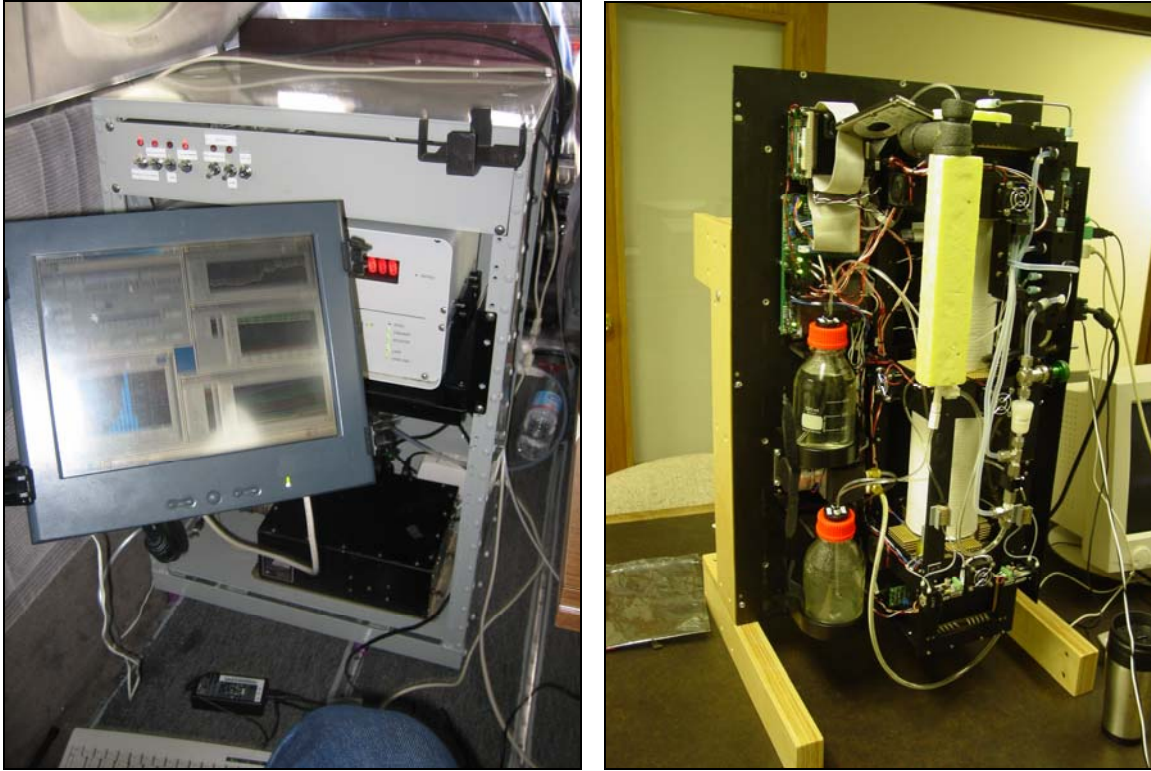


**Figure 3. The TSI CPC and the DMT CCN counter display in the cabin – the CCN counter on the bench during testing**

## 2.1 The Brechtel Inlet

The Brechtel inlet is a twin-diffuser cone assembly design with  $\frac{3}{4}$ " outside diameter (OD) inlet tubing (Figure 4). The two-diffuser cone assembly is designed with NACA air foil contours on the outer tip surfaces and elliptical contours on the inner tip surfaces of each cone. The first, smaller diffuser is approximately 1.5" long and tapers from a 0.2" OD at its tip to a 0.5" OD at its end, while the second, larger diffuser is approximately 3" long and tapers from a 0.25" to a 1" OD. The system was developed for improved particle sampling efficiency and for control of flow rates to maintain isokinetic flow conditions at the inlet-cone tip. The new inlet employs a two-stage diffuser cone assembly, which was designed to test the concept of removing the turbulent boundary layer within the first-stage diffuser by passively pumping the turbulence away at the end of the first cone. Another motivation for using a two-stage diffuser assembly was to avoid the large diffuser cone half angles of single-cone designs, because large half angles or expansion ratios may cause flow separation and hence particle losses in the diffuser due to turbulence.

When sampling aerosols using aircraft, it is also important to monitor flow conditions downstream of the inlet, where large particles will have sufficient inertia to impact on the inner diameter of the tubing leading to the individual instrument inlets. Calculations indicate losses on the order of ~7% of 1  $\mu\text{m}$  particles occur in each 90 degree  $\frac{1}{4}$ " bend at 28 lpm (drop loss of up to 2.2% for 0.5  $\mu\text{m}$  particles). The latter should not be too serious of a loss for pollution aerosols having a peak in sub  $\mu\text{m}$  mass but would result in underestimates of dust aerosols

aspirated into the aircraft. In the Cessna 340, it is important that a constant volumetric flow of 28 lpm (for 94 m/s air speed) be maintained through the main inlet sample line so that isokinetic sampling conditions are maintained at the tip of the diffuser.

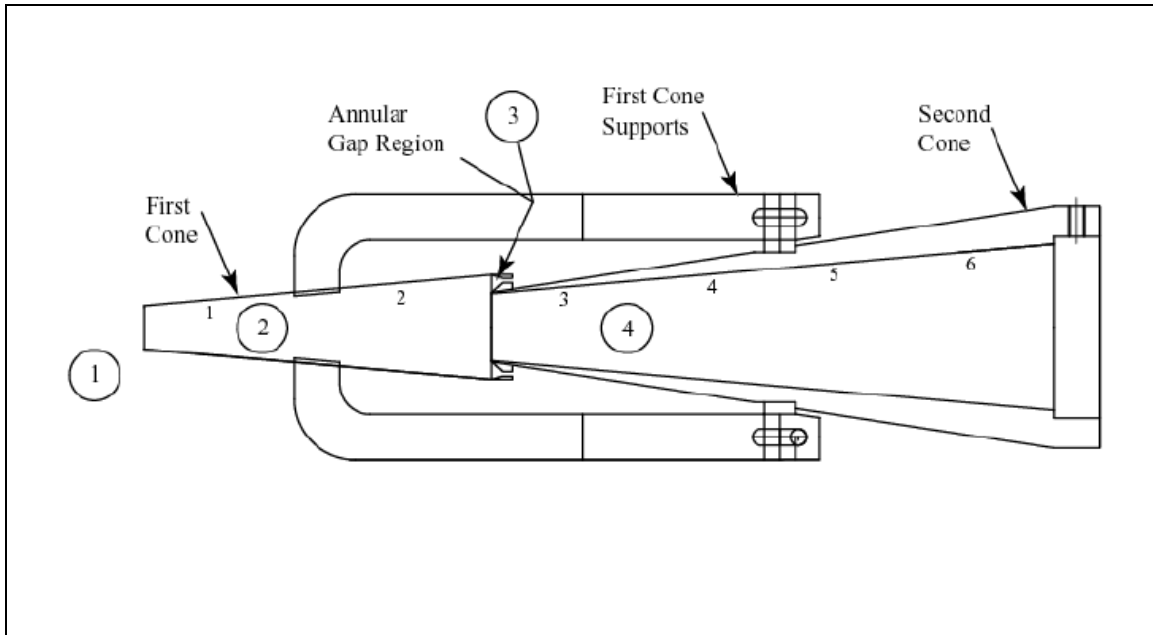


Figure 4. Brechtel dual cone diffuser inlet design on the SOAR Cessna 340 research aircraft

## 2.2 The DMT Cloud Condensation Nuclei (CCN) Counter

The DMT Cloud Condensation Nuclei (CCN) (Figure 3) counter samples aerosols from outside the aircraft to measure their capability to act as cloud condensation nuclei (CCN). An air sample is introduced in the CCN chamber via a 0.25-inch diameter inlet on top of the aircraft fuselage and non-conductive tubing that is plumbed from the CCN instrument to the aircraft fuselage. The air enters the top center of the vertical cylindrical column and is surrounded by an aerosol-free humidified uniform supersaturation flow environment. As the air sample flows down through the chamber, CCN activate in response to the exposed supersaturation and grow to droplets. An optical particle counter at the base or outlet of the chamber detects all particles with diameters larger than  $0.5\mu\text{m}$ . The heart of the instrument is the 50 cm long cylindrical column which provides the environment to activate and grow aerosol particles. The column is mounted vertically with the ambient aerosol entering at the top, and the increase in supersaturation takes place down the column.

The unit operates at a single supersaturation at a time. The supersaturation depends on the temperature difference between the top and bottom of the column as well as the flow rate in the column. The supersaturation can be varied between 0.1 % and 1.2 %. The column has three temperature control zones for rapid shifting between supersaturations. The data output is distributed in 20 bins of resolution over the sizing range of  $0.75\mu\text{m}$  to  $10\mu\text{m}$ . The particle sizing data are updated at 1-second intervals. At a sample flow rate of 60 vccm, 6000 particles per cubic centimeter can be counted with a maximum of a 10 % coincidence. The CCN counter is

mostly operated at supersaturation steps of 0.1, 0.4, 0.8 and 1.0 %. Particles that exit the base of the column and are in bin 1 through bin 20 comprise the measured CCN concentration.

### 2.3 The TSI Model 3022A

The Model 3022A Condensation Particle Counter (CPC) measures the number concentration of sub  $\mu\text{m}$  airborne particles larger than or equal to 7 nanometers ( $7 \times 10^{-9}$  m) in diameter. The particles are detected and counted by a simple optical detector after a supersaturated vapor condenses onto the particles, causing them to grow into larger droplets. The range of detection is wide, from less than .007 particles/cm<sup>3</sup> to  $9.99 \times 10^6$  particles/cm<sup>3</sup>. Its unique advantage is that it detects these small particles over a wide range of concentrations. Using both single-count and photometric detection modes, the Model 3022A provides highly accurate measurements, even in concentrations up to  $10^7$  particles per cubic centimeter.

## 3. The Use of The TSI Aerosol Instruments in the Cessna 340 and the Cheyenne

The TSI Model Condensation Particle Counters (CPCs) are industry standard instruments that have been used for airborne and ground based measurements of aerosol particles. The Cheyenne is equipped with the model 3010 and the Cessna 340 is equipped with the model 3022A. Since the Cheyenne will be flying mostly above the boundary layer, a concentration of aerosols up to 10,000 particles/cc. The model 3022A is capable of a 10,000,000 particles/cc (see Table 1), so this instrument is installed in the Cessna 340, which will be flying mostly within the boundary layer. An inter-comparison flight between the two aircraft will be conducted to compare the two instruments above the boundary layer and within the boundary layer.

**Table 1. TSI condensation particle counter model features**

Feature	TSI Model	
	3010	3022A
Minimum particle size (50% efficiency, nm)	10	7
Aerosol flow rate (cm <sup>3</sup> /min)	1000	300
Upper concentration limit (particles/cm <sup>3</sup> )	$10^3$	$10^6$
Lower concentration sensitivity (particles/cm <sup>3</sup> )	0	0
False background counts (particles/cm <sup>3</sup> )	<0.00001	<0.01
Response time (sec for 95% response)	<5	<13

## 4. Additional Instrumentation in the Cheyenne

Table 2 summarizes the parameters and measuring devices used on the SOAR Cheyenne II.

### 4.1 The TSI Model 3091 Fast Mobility Particle Sizer (FMPS)

The TSI Model 3091 Fast Mobility Particle Sizer (FMPS) spectrometer measures sub  $\mu\text{m}$  aerosol particles in the range from 5.6 to 560 nanometers in diameter. Due to its unique design, the FMPS spectrometer is capable of making particle size distribution measurements with one-second resolution, enabling you to visualize particle size distributions and events in real time. The FMPS spectrometer is ideally suited for measuring the dynamic behavior of sub  $\mu\text{m}$  particles over a wide range of applications, including particle formation and growth studies.

**Table 2. Summary of parameters and measuring devices used on the SOAR Cheyenne II**

VARIABLE	INSTRUMENT	RANGE	ACCURACY	RESOLUTION	FREQUENCY
Air temperature (reverse flow)	0.038" DIA. Bead Thermistor	-30°C to +50°C	0.05°C/0.3°C incl DHC	0.01°C	< 1 s TC
Relative humidity (reverse flow)	Thermoset Polymer RH Sensor	0 to 100% RH	2% RH	0.1% RH	5 s TC @ 20°C
Barometric pressure	MEMS Pressure Sensor	0 to 110000 Pa	100 Pa	10 Pa	20 Hz
u wind component (+ North)	Extended Kalman Filter (EKF)		0.50 m/s @ 75 m/s TAS	0.01 m/s	5 Hz
v wind component (+ East)	Extended Kalman Filter (EKF)		0.50 m/s @ 75 m/s TAS	0.01 m/s	5 Hz
w wind component (+ Down)	Extended Kalman Filter (EKF)		0.50 m/s @ 75 m/s TAS	0.01 m/s	5 Hz
Position (Latitude/Longitude)	WAAS DGPS		2 m (2 $\sigma$ )	< 1 m	5 Hz
Altitude	WAAS DGPS	-300 to 18000 m	5 m (2 $\sigma$ )	< 1 m	5 Hz
Geometric Altitude	King KRA 405 Radar Altimeter	0 to 2000 ft	3% < 500 ft 5% > 500 ft	0.48 ft (0.15 m)	
Roll Attitude ( $\phi$ )	MEMS IMU/GPS/EKF	-60 to +60°	0.1°	0.01°	5 Hz
Pitch Attitude ( $\theta$ )	MEMS IMU/GPS/EKF	-60 to +60°	0.2°	0.01°	5 Hz
Yaw Attitude ( $\psi$ )/ Heading	MEMS IMU/GPS/EKF	0 to 360°	0.1°	0.01°	5 Hz
Angle of attack ( $\alpha$ )	MEMS Pressure Sensor	-15 to +15°	0.03° @ 150 m/s	0.001° @ 150 m/s	20 Hz
Side-slip ( $\beta$ )	MEMS Pressure Sensor	-15 to +15°	0.03° @ 150 m/s	0.001° @ 150 m/s	20 Hz
True Air Speed	MEMS Pressure Sensor	0 to 150 m/s	0.1 m/s	0.01 m/s	20 Hz
Video record	Sony DCR-DVD 201				
Logging, telemetry & event markers	ESD DTS (GPS)				1 Hz
Cloud droplet spectra	DMT CDP	2 to 50 $\mu$ m		1 to 2 $\mu$ m, 30 bins	1 Hz
Cloud particle spectra	DMT CIP	25 to 1550 $\mu$ m		25 $\mu$ m, 62 bins	1 Hz
Cloud particle image	DMT CIP	25 to 1550 $\mu$ m		25 $\mu$ m	
Liquid water content	DMT LWC-100	0 to 3 g/m <sup>3</sup>	0.05 g/m <sup>3</sup>	0.01 g/m <sup>3</sup>	1 Hz
	CDP calculated	> 3 g/m <sup>3</sup>			1 Hz
Aerosol spectrometer	PMS PCASP SPP-200	0.1 to 3 $\mu$ m		0.02 $\mu$ m, 30 bins	1 Hz
Aerosol properties	TAMU DMA/TDMA	See text			1 Hz
CCN	DMT CCN counter	0.5 to 10 $\mu$ m 0.1 to 1.2 % SS	see text	0.5 $\mu$ m, 20 bins	1 Hz

This instrument is a new instrument and has not been flown on any aircraft for an extensive period. The University of North Dakota Citation aircraft flew the instrument for a short flight. SOAR has requested to carry the instrument in the Cheyenne for a period of one week to evaluate this instrument for potential future use in aerosol measurements.

## 5. Data Acquisition and Quality Control (Both Aircraft)

### 5.1 The Aircraft Data Acquisition System

The main aircraft data acquisition system is a software called DAQFactory. DAQFactory provides all the tools needed to acquire data, log it, display it, graph it, and analyze it. DAQFactory includes an advanced serial driver that can be easily setup to communicate with most serial devices.

The features of the DAQFactory system are the following:

- data acquisition from different instrument inputs at 1Hz. The DAQFactory system logs data from the CIP, CDP, AIMMS-20 and the PCASP.
- continuous data logging to an ASCII file for each instrument. During the data logging process, one data file is created for each instrument per hour.
- user definable screens for different measurement objectives during the research flight.

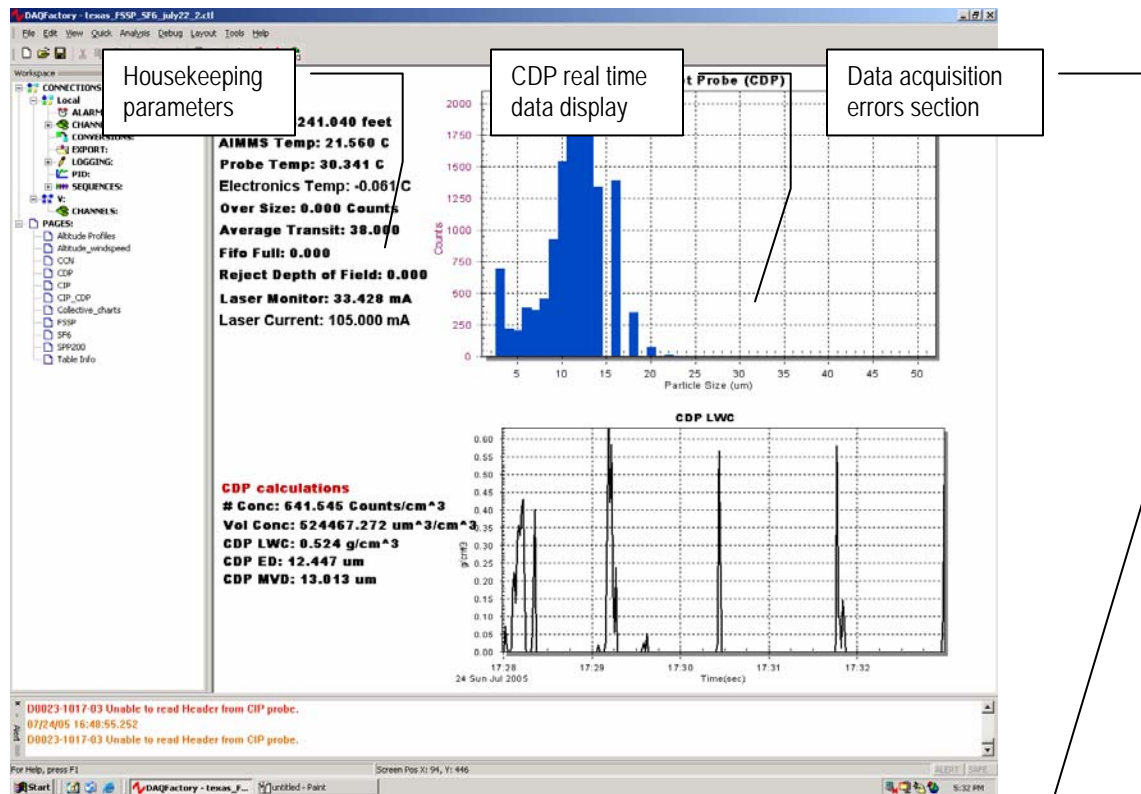


Figure 5. DAQFactory screen shot in-flight during a cloud penetration

Figure 5 shows the DAQFactory screen shot during a cloud penetration. The data are displayed in real time as shown. The housekeeping parameters are data that are specific to the operation of the instrument. If the housekeeping parameters fall within known unreliable values, the instrument operator can diagnose the operation of the instrument. With this feature, the instrument operator can maintain a certain level of quality assurance in real time operation of the instruments.

## 5.2 Post Processing of the Data and Quality Control

The post processing of the aircraft data is performed using LabVIEW. National Instruments LabVIEW delivers a powerful graphical development environment for signal acquisition, measurement analysis, and data presentation. After each flight, the research meteorologist collects the DAQFactory data from each instrument and processes this data using LabVIEW. The LabVIEW software checks for errors in each data file, synchronizes all the data from all the instruments, performs calculations, and creates data files for further analysis.

Figure 6 shows a screenshot from the CCN counter playback software. Using this software, the research meteorologist plays all the data for each instrument for all the flight or for portions of the flight. Quality control of the data can be assured during the playback after each flight.

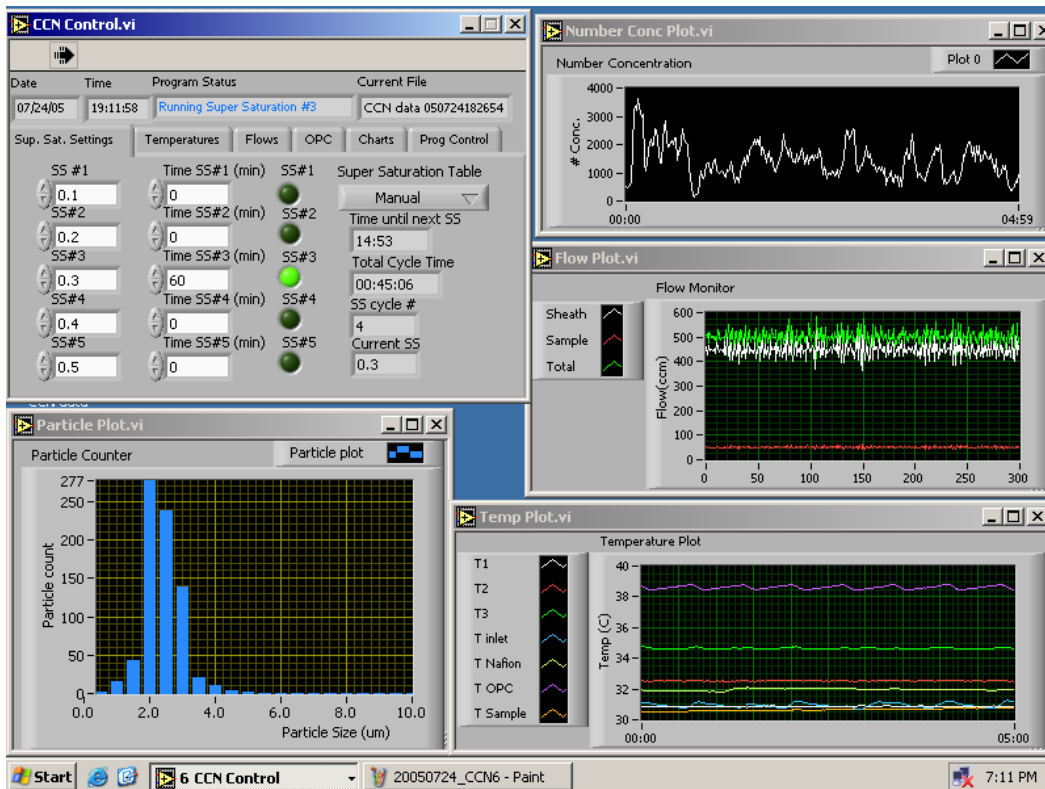


Figure 6. LabVIEW playback software

## **6. The DMT CCN Counter**

The DMT CCN counter samples aerosols from outside the aircraft to measure their capability to act as cloud condensation nuclei. The air sample enters the top center of the 50 cm long vertical cylindrical column and as the air sample flows down through the chamber, CCN activate in response to the exposed supersaturation and grow to droplets. An optical particle counter at the base or outlet of the chamber detects all particles with diameters larger than 0.5 $\mu\text{m}$ . The unit operates at a single supersaturation. The supersaturation can be varied between 0.1% and 1.2%. Approximately 30 seconds are required for a shift from one supersaturation to another, although operation in the field shows that shifting from a high supersaturation (1.0%) to a low supersaturation (0.1%) may take more than a minute since the column's three temperature controllers are more efficient at warming than at cooling. The data output is distributed in 20 bins of resolution over the sizing range of 0.75  $\mu\text{m}$  to 10  $\mu\text{m}$ . At a sample flow rate of 60 vccm, 6000 particles per cubic centimeter can be counted with a maximum of a 10% coincidence. The CCN counter is mostly operated at supersaturation steps of 0.1, 0.25, 0.5 and 1.0%. Particles that exit the base of the column and are in bin 1 through bin 20 comprise the measured CCN concentration.

## **7.0 Upgrades Installed on the Standard Package of the Soar Cheyenne Specifically for the SUPRECIP Program**

### **7.1 Terrain Awareness and Warning System (TAWS)**

The SUPRECIP program brings challenges to the field measurement program that needed special attention. One of these challenges was measurement of cloud microphysical properties using the SOAR Cheyenne research aircraft in the proximity of mountainous terrain. The addition of Terrain Awareness and Warning System (TAWS) on the SOAR Cheyenne enables the SOAR crew to interpret terrain features when flying in low visibility or in clouds. This is achieved by the installation of the TAWS enabled Garmin GNS 530 to graphically display the surrounding terrain and obstacles in bright yellow and red, relative to the aircraft's current altitude (Figure 7). Yellow is used to depict conflicts 1,000 to 100 vertical feet below the aircraft. Red is used to depict conflicts 100 vertical feet below the aircraft's current altitude and above. Working in tandem with the aircraft's audio system, the TAWS-certified GNS 530 provides audible cautions and warnings to alert the pilot of a possible terrain and obstacle conflict. Audible and graphical alerts include forward-looking terrain avoidance, imminent terrain impact, premature descent during approach, altitude loss after takeoff, 500-foot callout and excessive rate of descent.

The GNS 530 is an integrated system with IFR oceanic-approved GPS, VHF navigation with instrument landing system, and VHF communication with 8.33-kHz channel spacing. Its five-inch (diagonal) color TFT display features an electronic map with a built-in database of cities, highways, rivers, lakes and coastlines, as well as a complete TAWS database. The TAWS data include:

- Terrain Database: 30 arc-second resolution coverage of the world (75 N-60 S).
- Obstacle Database: Consists of all obstacles higher than 200' within the USA.
- Airport Terrain Database: 9 arc-second resolution in 12 nm by 12 nm coverage around every USA airport.

## 7.2 Traffic Collision Avoidance System (TCAS)

Another challenge in SUPRECIP is flying in conditions when other aircraft are maneuvering in close proximity. Traffic Collision Avoidance System (TCAS) consists of a radio transmitter and receiver, directional antennas, computer and cockpit display. It sends out signals, called interrogations. When another airplane's transponder receives an interrogation, it transmits a reply. The TCAS computer uses the time between interrogation and reply to calculate distance. It uses information from the directional antennas to determine direction. If the other aircraft has a transponder that provides altitude data, TCAS displays its relative altitude and whether it is climbing or descending. For example, if the other airplane is 1,400 feet below the interrogating airplane and climbing, "14" and an arrow pointing upward will appear above the aircraft's symbol.

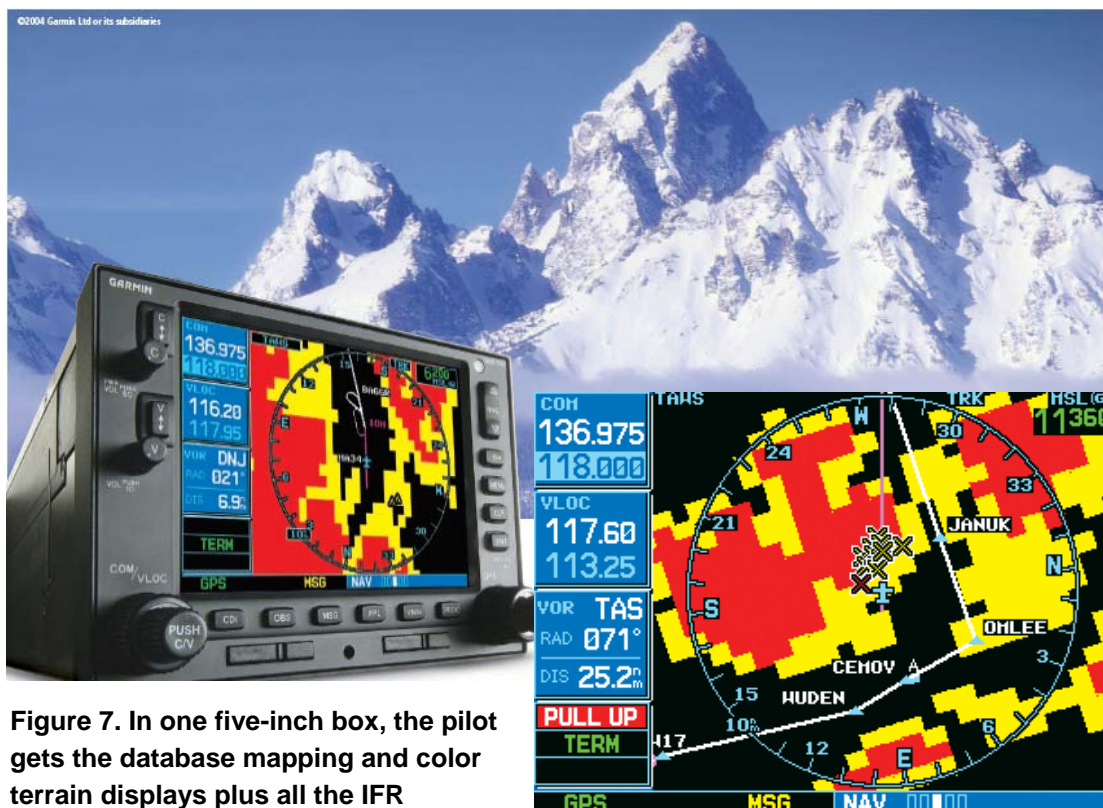
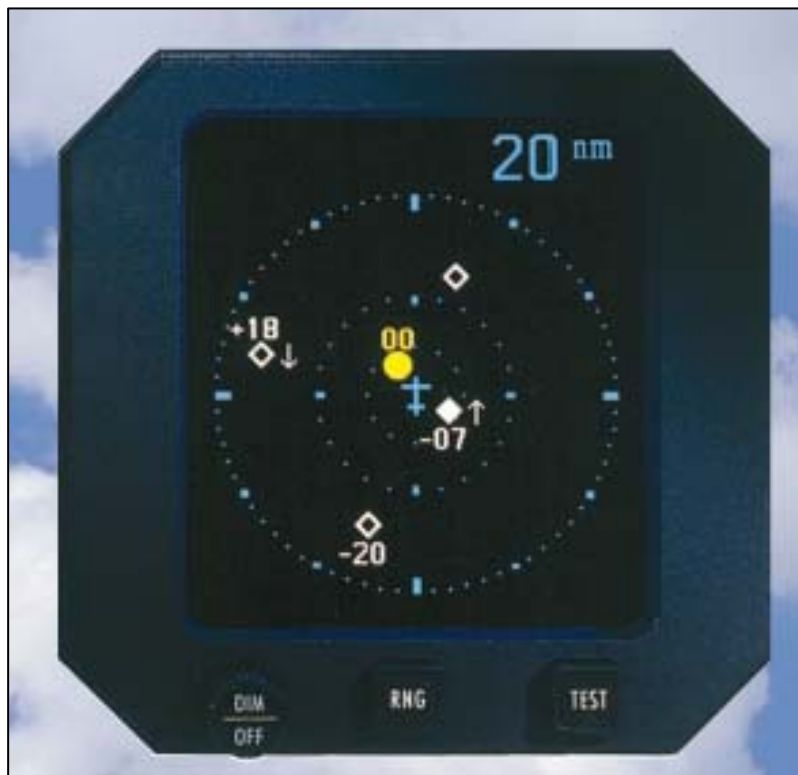


Figure 7. In one five-inch box, the pilot gets the database mapping and color terrain displays plus all the IFR navigation and communication features. In addition to aural and visual terrain alerts, an obstacles database helps pilots see and avoid towering manmade structures as well.

The TCAS gives you TAs (Traffic Advisories) and RAs (Resolution Advisories climb and descent commands). To review briefly, the system provides a map-like display of surrounding traffic, and a TA whenever another aircraft is within about 48 seconds of its closest point of approach. During a TA, a synthesized voice announces, "Traffic, traffic," and the symbol for the intruder aircraft changes from a white diamond shape to a solid yellow round dot. During an RA, the other aircraft symbol changes to a solid red square block, and the system will demand a maneuver such as "Climb, climb" or "Descend, descend," or it may tell the pilot not to maneuver. When a TCAS issues an RA involving another TCAS equipped aircraft, it coordinates with the other aircraft's TCAS to avoid mirror-image maneuvers, such as having both airplanes climb.



**Figure 8. Using standard TCAS symbols, easily identified by their color and shape, the range, bearing, and altitude of each intruder is shown relative to the aircraft**



**Table 3. (continued)**

02-15-2006	18:07	20:05	18:10	21:25	Cloud physics flight in convective clouds over the foothills and aerosol flight over the northern and central Sierra foothills. The flight started with a formation flight to Blodgett. Cloud physics data is good until 19:30 when the aircraft lost power.	✓x	✓x	✓x	✓x	✓x	✓x	✓	✓	✓	✓
02-16-2006	22:04	00:24	22:10	00:30	Cloud physics flight and aerosol flight over the northern Sierra foothills orographic clouds and coastal orographic clouds, starting with a formation flight to Blodgett. Cloud physics data is good until 23:52 when the aircraft lost power.	✓x	✓x	✓x	✓x	✓x	✓x	✓	✓	✓	✓
02-17-2006	no flight		22:57	00:10	Aerosol flight starting towards Blodgett. IFR conditions prevailed and aircraft had to return to base before reaching Blodgett. Flight in rain below cloud base.							✓	✓	✓	✓
02-18-2006	no flight		18:12	21:33	Aerosol flight starting towards Blodgett and continuing towards Monterey and San Francisco bay.							✓	✓	✓	✓
02-26-2006	18:40	20:14	20:20	22:15	Cloud physics measurements of synoptically driven Altocumulus with embedded weak convection west of the Sierra crest. Aerosol flight to Blodgett. Aerosol aircraft flew in virga and some rain.	✓	✓	✓	✓	✓	✓	✓	✓	✓	✓
02-27-2006	17:08	19:16	17:10	19:29	Cloud physics flight in ice precipitation over the Sierra and in convective clouds northeast of Oakland. Aerosol flight towards Blodgett continuing towards Oakland. The aerosol aircraft was in and out of precipitation until 1745Z. The cloud physics aircraft had false airspeed readings.	✓x	✓	✓	✓	✓x	✓x	✓	✓	✓	✓
	22:14	23:20	22:15	23:54	Both aircraft started in formation and broke off at Hangtown. The cloud physics aircraft flew through pre-frontal precipitation layers. Intermittent airspeed readings occurred again and it was decided to cancel the flight. Aerosol aircraft continued towards Stockton.	✓x	✓	✓	✓	✓x	✓x	✓	✓	✓	✓

**Table 3. (continued)**

02-28-2006	17:29	20:12	17:34	20:30	Cloud physics flight in the convective and orographic clouds over the Sierra foothills, coastal range and over the ocean. Aerosol aircraft flies in coordination with the cloud physics aircraft but remains over the central valley and the coastal range.	✓	✓	✓	✓	✓	✓	✓	✓	✓	✓	
	22:55	01:45	22:54	01:06	Cloud physics flight measuring convective clouds and aerosols in a mixed boundary layer in the central valley and off the coast. Aerosol aircraft flies in coordination along the approximate same flight track.	✓	x	✓	✓	✓	✓	✓	x	✓	✓	✓
03-01-2006	21:25	00:37	21:24	00:23	Both aircraft started in formation and broke off at Hangtown. Aircraft flew coordinated tracks taking aerosol and cloud measurements over the foothills, west towards Mendocino and over the ocean.	✓	✓	✓	✓	✓	✓	✓	✓	✓	✓	✓
03-02-2006	17:01	18:09	17:01	18:55	Cloud physics flight measuring orographic clouds and aerosols over the foothills and the windward side of the Sierra above Squaw Valley. Aerosol aircraft measures aerosols vertically.	✓	✓	✓	✓	✓	✓	✓	✓	✓	✓	✓
	19:37	20:57	19:47	21:00	Same as above to study the evolution of the front.	✓	✓	✓	✓	✓	✓	✓	✓	✓	✓	✓
	22:58	00:21	22:50	23:55	Same as above to study the evolution and the affects of mixing in the boundary layer.	✓	✓	✓	✓	✓	✓	✓	✓	✓	✓	✓
03-03-2006	17:32	19:43	17:31	18:43	Cloud physics flight in receding frontal cloud band over the Sierra. Aerosol aircraft flew in the Sacramento local area to document the aerosols with height.	✓	✓	x	✓	✓	✓	✓	✓	✓	✓	✓
	21:35	23:45	21:48	23:55	The frontal cloud band moved to the east and new vigorous convective clouds developed on the mountains and around Sacramento. Data system crashed from 23:27 to 23:35.	✓	✓	x	✓	✓	✓	✓	✓	✓	✓	✓

**Table 3. (continued)**

03-06-2006	17:46	19:28	17:40	18:44	Cloud physics aircraft flew on the west side of a receding frontal cloud band over the Sierra, conducting penetrations of orographic cloud tops. Aerosol aircraft flew in the Sacramento area below cloud base and near the foothills.	✓	✓	✓	✓	✓	✓	✓	✓	✓	✓	
03-07-2006	17:03	19:34	17:00	18:30	Cloud physics flight in very messy layered cloud with embedded deep convection. The aircraft tracked as far south as Fresno and climbed into the high Sierra.	✓	✓	✓	✓	✓	✓	✓	✓	✓	✓	
	22:03	23:29	22:03	23:56	Planned aerosol and cloud physics flight measuring clouds and aerosols north of Sacramento. Data system failure.	✓	✓	✓	✓	✓	✓	✓	✓	✓	✓	
03-09-2006	19:28	22:07	19:22	23:00	Cloud physics flight into the orographic clouds first towards Hangtown in the foothills and then south along Sierra towards Fresno. The aerosol aircraft flew below the cloud bases and up to 10,000 ft near the Blodgett site, then followed the cloud physics aircraft track south.	✓	✓	✓	✓	✓	✓	✓	✓	✓	✓	
03-10-2006	18:36	20:47	17:03	20:39	Cloud physics measurements climbing to the Sierra crest, along the Sierra crest, and descending with further measurements along the central valley. Good CN data on the aerosol aircraft but the CCN counter power fails.	✓	✓	✓	✓	✓	✓x	✓	✓	✓	x	
03-11-2006	17:26	19:43	17:21	19:15	With a cold through centered over the central valley, precipitation echoes were abundant. Cloud physics flight was conducted from Sacramento to Hangtown and then to the SSE along the foothills. Aerosol aircraft flew in the Sacramento area up to 10,000ft.	✓	✓	✓	✓	✓	✓x	✓	✓	✓x	✓	
03-13-2006	18:14	19:55	18:06	19:34	Cloud physics aircraft followed aerosol aircraft to Linden. Aerosol aircraft returned to Sacramento while the cloud physics aircraft climbed to the Sierra crest, flew along the crest and descended back towards the valley. Temperature unreliable.	✓	✓x	✓	✓	✓	✓	✓	✓	✓	✓x	✓
03-14-2006	17:49	21:50	17:45	20:39	Cloud physics flight in layered glaciated cloud over the Sierra foothills and crest above Squaw Valley. Convective cloud profiles over the foothills, over the coastal hills and the ocean. Temperature unreliable.	✓	✓x	✓	✓	✓	✓	✓	✓	✓	✓x	✓

## 8.0 Important Flight Information

During SUPRECIP-2, researchers flew 53 missions: 25 by the cloud physics aircraft and 28 by the Cessna 340 aerosol aircraft. A little over half (27 of 53) of the research missions were flown in March 2006. After a slow beginning with mostly unsuitable weather during February 2006, the weather improved greatly for the project's purposes, resulting in 10 flight days in March 2006. Table 4 provides a summary of all the missions flown in SUPRECIP-2.

**Table 4. SUPRECIP-2 sorties inventory**

Date	Takeoff Cloud	Landing Cloud	Takeoff Aero	Landing Aero	Summary of data collected on this flight
02-03-2006	22:20	23:30	22:27	23:39	Cloud physics aircraft flies in shallow Sc cloud in the central valley. Aerosol aircraft flies below the cloud bases of the Sc cloud measured by the cloud physics aircraft.
02-04-2006	21:10	23:40	21:10	23:55	Cloud physics flight in weak orographic clouds to a location south of Tahoe and north of Squaw Valley, continuing along the foothills towards Chico. Aerosol aircraft flies a coordinated flight track along the foothills.
02-08-2006	no flight		22:55	00:49	Aerosol measurements over the Blodgett Forest Research Station.
02-10-2006	23:33	00:30	23:33	02:33	Inter-comparison aerosol measurements between the two aircraft. Aerosol aircraft continues to measure aerosol concentrations around the San Francisco area.
02-15-2006	18:07	20:05	18:10	21:25	Cloud physics flight in convective clouds over the foothills and aerosol flight over the northern and central Sierra foothills. The flight started with a formation flight to Blodgett. Cloud physics data is good until 19:30 when the aircraft lost power.
02-16-2006	22:04	00:24	22:10	00:30	Cloud physics flight and aerosol flight over the northern Sierra foothills orographic clouds and coastal orographic clouds, starting with a formation flight to Blodgett. Cloud physics data is good until 23:52 when the aircraft lost power.
02-17-2006	no flight		22:57	00:10	Aerosol flight starting towards Blodgett. IFR conditions prevailed and aircraft had to return to base before reaching Blodgett. Flight in rain below cloud base.
02-18-2006	no flight		18:12	21:33	Aerosol flight starting towards Blodgett and continuing towards Monterey and San Francisco bay.
02-26-2006	18:40	20:14	20:20	22:15	Cloud physics measurements of synoptically driven Altocumulus with embedded weak convection west of the Sierra crest. Aerosol flight to Blodgett. Aerosol aircraft flew in virga and some rain.

**Table 4. (continued)**

02-27-2006	17:08	19:16	17:10	19:29	Cloud physics flight in ice precipitation over the Sierra and in convective clouds northeast of Oakland. Aerosol flight towards Blodgett continuing towards Oakland. The aerosol aircraft was in and out of precipitation until 1745Z. The cloud physics aircraft had false airspeed readings.
	22:14	23:20	22:15	23:54	Both aircraft started in formation and broke off at Hangtown. The cloud physics aircraft flew through pre-frontal precipitation layers. Intermittent airspeed readings occurred again and it was decided to cancel the flight. Aerosol aircraft continued towards Stockton.
02-28-2006	17:29	20:12	17:34	20:30	Cloud physics flight in the convective and orographic clouds over the Sierra foothills, coastal range and over the ocean. Aerosol aircraft flies in coordination with the cloud physics aircraft but remains over the central valley and the coastal range.
	22:55	01:45	22:54	01:06	Cloud physics flight measuring convective clouds and aerosols in a mixed boundary layer in the central valley and off the coast. Aerosol aircraft flies in coordination along the approximate same flight track.
03-01-2006	21:25	00:37	21:24	00:23	Both aircraft started in formation and broke off at Hangtown. Aircraft flew coordinated tracks taking aerosol and cloud measurements over the foothills, west towards Mendocino and over the ocean.
03-02-2006	17:01	18:09	17:01	18:55	Cloud physics flight measuring orographic clouds and aerosols over the foothills and the windward side of the Sierra above Squaw Valley. Aerosol aircraft measures aerosols vertically.
	19:37	20:57	19:47	21:00	Same as above to study the evolution of the front.
	22:58	00:21	22:50	23:55	Same as above to study the evolution and the affects of mixing in the boundary layer.
03-03-2006	17:32	19:43	17:31	18:43	Cloud physics flight in receding frontal cloud band over the Sierra. Aerosol aircraft flew in the Sacramento local area to document the aerosols with height.
	21:35	23:45	21:48	23:55	The frontal cloud band moved to the east and new vigorous convective clouds developed on the mountains and around Sacramento. Data system crashed from 23:27 to 23:35.
03-06-2006	17:46	19:28	17:40	18:44	Cloud physics aircraft flew on the west side of a receding frontal cloud band over the Sierra, conducting penetrations of orographic cloud tops. Aerosol aircraft flew in the Sacramento area below cloud base and near the foothills.

**Table 4. (continued)**

03-07-2006	17:03	19:34	17:00	18:30	Cloud physics flight in very messy layered cloud with embedded deep convection. The aircraft tracked as far south as Fresno and climbed into the high Sierra. Planned aerosol and cloud physics flight measuring clouds and aerosols north of Sacramento. Data system failure.
	22:03	23:29	22:03	23:56	
03-09-2006	19:28	22:07	19:22	23:00	Cloud physics flight into the orographic clouds first towards Hangtown in the foothills and then south along Sierra towards Fresno. The aerosol aircraft flew below the cloud bases and up to 10,000 ft near the Blodgett site, then followed the cloud physics aircraft track south.
03-10-2006	18:36	20:47	17:03	20:39	Cloud physics measurements climbing to the Sierra crest, along the Sierra crest, and descending with further measurements along the central valley. Good CN data on the aerosol aircraft but the CCN counter power fails.
03-11-2006	17:26	19:43	17:21	19:15	With a cold trough centered over the central valley, precipitation echoes were abundant. Cloud physics flight was conducted from Sacramento to Hangtown and then to the SSE along the foothills. Aerosol aircraft flew in the Sacramento area up to 10,000ft.
03-13-2006	18:14	19:55	18:06	19:34	Cloud physics aircraft followed aerosol aircraft to Linden. Aerosol aircraft returned to Sacramento while the cloud physics aircraft climbed to the Sierra crest, flew along the crest and descended back towards the valley. Temperature unreliable.
03-14-2006	17:49	21:50	17:45	20:39	Cloud physics flight in layered glaciated cloud over the Sierra foothills and crest above Squaw Valley. Convective cloud profiles over the foothills, over the coastal hills and the ocean. Temperature unreliable.

## 8.1 Adjustment of the CCN Measurements to 0.8% Supersaturation

The supersaturation to which the aerosols are exposed to in the CCN chamber is determined by the temperature difference between the plates inside the chamber. More aerosols are activated and form water droplets if exposed to a higher super saturation, but the nature of this relation may be affected by the chemical composition of the aerosols, their sizes and their concentrations. Therefore, when normally measuring CCN concentrations, the instrument is set to cycle through levels of supersaturations that can be found in natural clouds, thus leading to fluctuating measured CCN concentrations. The length of the supersaturation cycle in SUPRECIP-2 was about 7 minutes (equivalent to ~40 km flight path), during which the CCN characteristics varied significantly. The objective was to graphically display the CCN concentrations along the flight track, but in order to avoid fluctuating concentrations due to

changes in supersaturations, or to avoid neglecting a large part of the valuable data, it was decided to adjust the measurements at lower supersaturations to the highest supersaturation of 0.8% according to the following procedure:

1. Plot the measured CCN concentration ( $CCN$ ) versus the temperature difference between the plates (" $dT$ ", which represents a unique super saturation) for a whole flight.
2. Find the coefficients ( $a, b$ ) that best fit to the data in the form:  $CCN = a \cdot \exp(b \cdot dT)$
3. Since  $dT=12^\circ\text{C}$  is equivalent to 0.8% super saturation, apply the following adjustment to the measured CCN concentration:  $CCN_{0.8\%} = CCN \cdot \exp(b \cdot (12 - dT))$

Table 5 shows the values of the coefficient  $b$  for the various flights. Figure 9 shows an example for the dependence of the measured CCN concentration on  $dT$ .

The adjusted values are not precise since only one coefficient is used for a complete flight, during which aerosol properties can change, but they can give a good approximation of the changing CCN concentrations along a flight track.

**Table 5. The values of the coefficient  $b$  for various flights**

<b>Flight</b>	<b><math>b</math></b>
060215	0.159
060217	0.1097
060227a	0.069
060227b	0.073
060228a	0.111
060228b	0.083
060301	0.143
060302a	0.138
060302b	0.056
060302c	0.106
060303a	0.085
060303b	0.113
060306	0.111
060307a	0.116
060307b	0.113
060310	0.172
060311	0.065
060313	0.067
060314	0.066

060307b

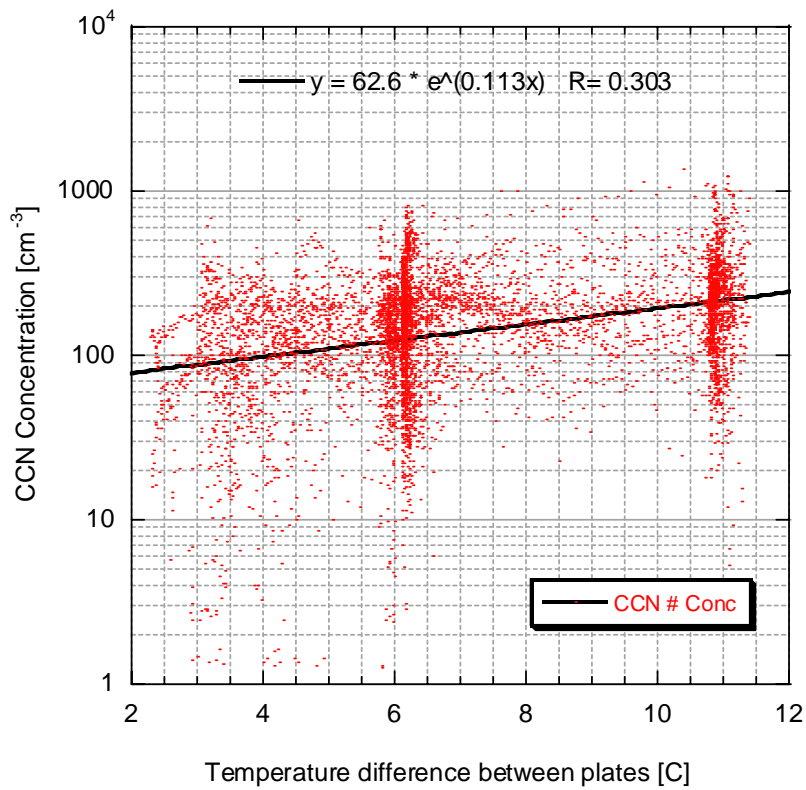


**Figure 9. Scatterplot and benefit line showing the dependence of the measured CCN concentration on the temperature difference (dT) between the plates in the CCN counter**

The collective daily flight tracks, the plots for the aerosol (Cloud 2) and for the cloud physics aircraft (Cloud 1) are given in Appendix E.

## **Appendix D**

### **The Satellite Methodology Used in the Research Effort**



## Appendix D

### The Satellite Methodology Used in the Research Effort

#### Background

The method of Rosenfeld and Lensky (1998) makes use of AVHRR multi-spectral data from polar orbiting satellites to infer the evolution of convective cloud particles and precipitation at various heights within the clouds. The method can be applied also to orographic clouds such as those occurring in California during the winter season in order to determine whether pollution is affecting these clouds. The very high resolution (i.e., 1 km) of the AVHRR imagery provided by the polar-orbiting NOAA-14 and NOAA-16 satellites will even make it possible to bring the focus down to specific areas of interest in California. That this can be done is demonstrated by Rosenfeld and Lensky (1998) and Rosenfeld (1999) for forest fires in Indonesia and by Rosenfeld (2000) for individual pollution sources in southeastern Australia.

#### How the Method Works

The method to deduce the microphysical structure of clouds from space makes use of data from the Advanced Very High Resolution Radiometer (AVHRR) onboard the NOAA operational weather satellites, which provide sub-satellite 1.1 km data in 5 channels centered at 0.65, 0.9, 3.7, 10.8, and 12.0  $\mu\text{m}$ . The visible wave band (0.65  $\mu\text{m}$ ) is used to select points with visibly bright clouds for the analyses. The thermal infrared (0.9  $\mu\text{m}$ ) is used to obtain cloud-top temperatures. Cloud-top particle size is inferred from the solar radiation component of the 3.7-micron wave band.

In making the inferences of cloud microphysical structure, the effective radius ( $r_e$ ) of fully cloudy pixels is retrieved in the manner described by Rosenfeld and Gutman (1994) and Lensky and Rosenfeld (1997). This is done by inverting a radiative transfer model developed by Nakajima and King (1990), using the solar reflectance component of the 3.7  $\mu\text{m}$  channel and the viewing geometry as inputs. Retrieval of particle size at cloud top is based on the fact that water absorbs part of the solar radiation at the 3.7  $\mu\text{m}$  wave band. While the back-scattered solar radiation is determined mainly by the surface area of the particles, the amount of absorption is determined by the volume of the particles. Therefore, larger particles absorb more and reflect less, so clouds that are made of larger droplets are seen darker in the reflected 3.7  $\mu\text{m}$  radiation.

Knowing the energy radiated from the sun and the portion of that energy reflected back to the satellite sensor, the fraction of the solar energy absorbed can be retrieved. This provides the basis for calculating the ratio between the integral volume and integral surface area of cloud particles in the satellite measurement volume. Conventionally, this ratio has been defined as the particle effective radius,  $r_e$ .

The initial research suggests that an  $r_e$  of 14  $\mu\text{m}$  is a threshold value above which clouds contain precipitation-size particles that can be detected by weather radar (Rosenfeld and Gutman, 1994). The maximum value of  $r_e$  that can be retrieved by this method is 30  $\mu\text{m}$ .

The evolution of  $r_e$  as a function of cloud-top height or temperature (T) of growing convective elements can reveal the microphysical evolution of the clouds as they grow vertically and undergo the various microphysical process that lead to the formation of precipitation. However, the satellites carrying high-resolution AVHRR sensors typically provide only a twice-daily snapshot image of a specific portion of the earth. Thus, a single cloud cannot be viewed continuously in the imagery. This difficulty is overcome by observing an area containing a convective cloud cluster composed of cloud elements at various stages of vertical growth. This allows compositing of the  $r_e$  calculations for many clouds as if they represented a single cloud at different times in its lifetime.

The actual composite is done in the following steps:

- a) Define a window, typically of several thousand pixels, encompassing convective cloud clusters with growing elements at various stages of development.
- b) Calculate the median and other percentiles of the  $r_e$  for pixels within each 1°C interval of cloud top temperature (T).
- c) Display graphically the T vs.  $r_e$  curves of the 10, 25, 50, 75, and 90 percentiles.
- d) Analyze the shape of the median (50th percentile) to find the microphysical zones as discussed below.

The shape of the T vs.  $r_e$  diagrams contains much information on the microphysical processes in the clouds. It is known that droplets grow by diffusion a small distance above the base of convective clouds while higher up in the clouds the hydrometeor growth rate is often accelerated by coalescence and ice processes. Because nearly all cloud droplets are nucleated at cloud base and cloud water-mass increases less than linearly with depth, it is found that the  $r_e$  in clouds with mostly diffusional growth increases by a power law of less than  $D^{1/3}$ , where D is depth above cloud base. D can be approximated using  $T_b - T$ , where T and  $T_b$  are cloud top and base temperatures, respectively. It can then be seen that  $r_e$  is proportional to  $(T_b - T)^{1/3}$  and a plot of  $r_e$  versus temperature will look like an upward convex curve. Therefore, a deviation from such a curve (i.e., an upward concave curve) indicates the existence of amplification mechanisms for the cloud-particle growth rate, such as coalescence and ice formation processes, which lead ultimately to precipitation.

Based on about a hundred analyzed cases well distributed over the globe, the evolution of convective cloud-top particles as a function of depth above cloud base and cloud-top temperature can be characterized into five distinct vertical zones, not all necessarily appearing in a given cloud system:

- 1) *Diffusional droplet growth zone*: Very slow growth of cloud droplets with depth above cloud base, indicated by shallow slope of  $dr_{eff}/dT$ .

- 2) *Droplet coalescence growth zone*: Large increase of the droplet growth rate  $dr_{\text{eff}}/dT$  at  $T > 0^\circ\text{C}$ , indicating rapid growth of the cloud droplets with depth above cloud base. This can only occur by drop coalescence.
- 3) *Rainout zone*: A zone where  $r_e$  remains stable at about  $20\ \mu\text{m}$ , probably determined by the maximum drop size that can be sustained by rising air near the cloud top, where the larger drops are precipitated to lower elevations and may eventually fall as rain from the cloud base. This zone is so named, because the clouds seem to be raining out much of their water while growing. The radius of the drops that actually rain out from cloud tops is much larger than the indicated  $r_e$  of  $20\ \mu\text{m}$ , being at the upper end of the drop size distribution.
- 4) *Mixed phase zone*: The large growth rate that may occur at  $T < 0^\circ\text{C}$  can be attributed to coalescence as well as to mixed phase precipitation formation processes. Therefore, the mixed phase and coalescence zones are ambiguous at temperatures below freezing. Because the first ice phase in growing continental clouds appears typically at  $T < -10^\circ\text{C}$ , the zones are separated arbitrarily at  $-10^\circ\text{C}$ .
- 5) *Glaciated zone*: A nearly stable  $r_e$  zone at below freezing temperatures at a value greater than that of the rainout zone. The value is probably determined by the maximum ice particle size that can be sustained near cloud top, where the larger particles are precipitated to lower elevations while aggregating and forming snowflakes. Several examples of the above cloud-microphysical zones as inferred from the AVHRR imagery are provided in the following case studies. Plotted are the 25%, 50%, 75% and 90% percentiles of the  $r_e$  for each  $1^\circ\text{C}$  interval. The median is indicated by the thick line. The numbers in the plots refer to the growth zones as numbered above.

The first two examples are from continental situations in Israel, where it can be seen that there was a deep diffusional growth zone capped by a zone of mixed-phase growth (Figures 1a and 3b). In the second example a glaciated zone lay above the mixed phase zone (Figure 1b).

In contrast to the first two examples are plots of  $r_e$  versus temperature for two AVHRR windows in an image covering the Bay of Bengal (Figure 2a) and Thailand (Figure 2b). In these plots the diffusional growth zone is virtually non-existent in clouds over the Bay of Bengal, where the droplet coalescence growth zone is already well developed a small distance above the bases of the maritime clouds. Even in the interior of Thailand (Figure 2b) the diffusional growth zone is shallower than in the examples shown for Israel above which there is a zone of droplet growth by coalescence.

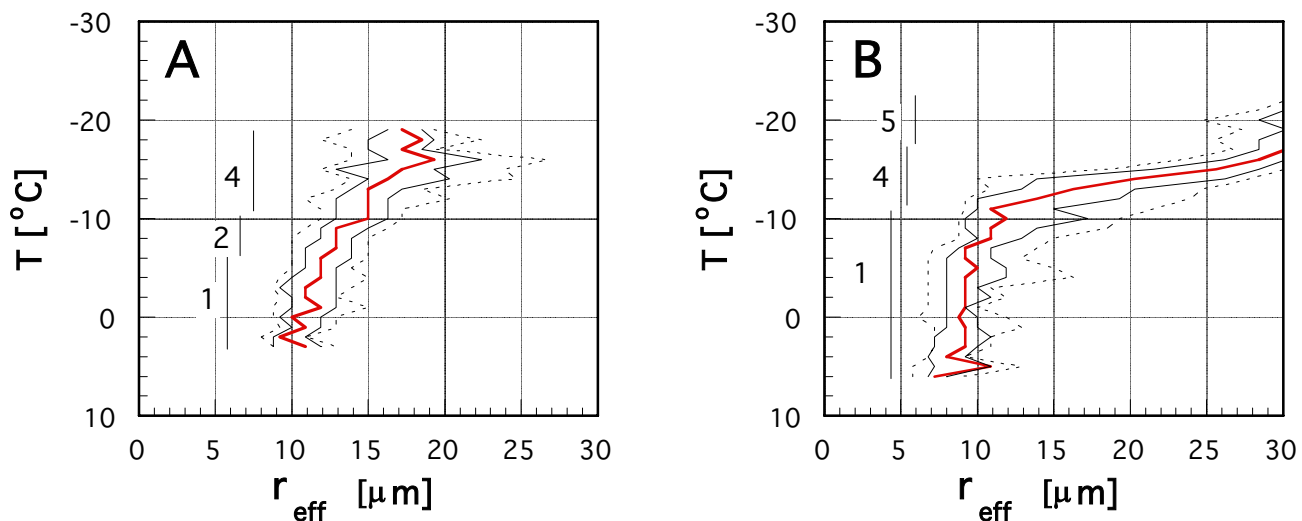


**Figure 1.** The effective radius as a function of cloud-top temperature for two AVHRR windows over Israel on 25 March (A) and 3 April 1995 (B). Plotted are the 10%, 25%, 50%, 75%, and 90% percentiles of the  $r_e$  for each  $1^{\circ}\text{C}$  interval. The thick line indicates the median. The vertical bars denote the different microphysical zones as numbered in the text.

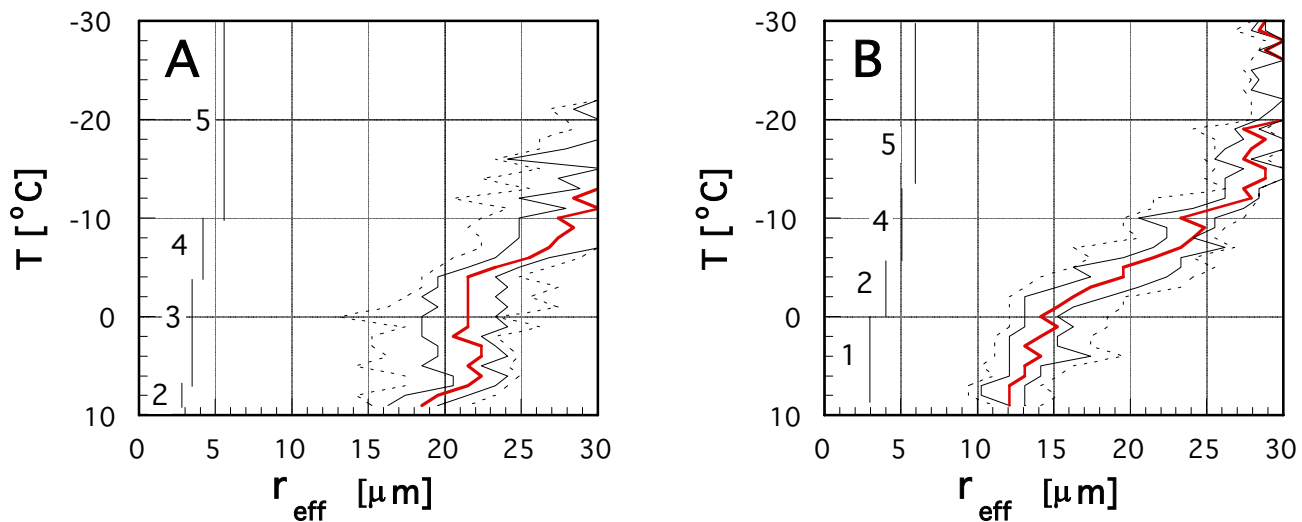


**Figure 2.** The same as Figure 1 but for two AVHRR windows containing clouds growing in monsoon flow on 12 November 1992. Window A covers a portion of the Bay of Bengal to the Burmese coastal areas and window B is in the interior of Thailand.

The rainout zone can exist only in clouds with well-developed coalescence that has progressed to the extent that further increase of drop size is compensated by the large drop fallout from the cloud tops. Therefore, the rainout zone exists just above the droplet coalescence growth zone. As can be seen (Figure 2a), the rainout zone is well-developed in maritime clouds, but its extent is reduced in less maritime clouds (Figure 2b) and completely vanishes in continental clouds (Figure 1a and 1b).

The mixed-phase zone exists above the glaciated zone. Often the coalescence and mixed phase zones overlap to one continuous region of rapid growth of  $r_e$  through the  $0^\circ\text{C}$  isotherm. In such cases the separation between the zones is set arbitrarily to  $-6^\circ\text{C}$  (Figure 2b). The transition from the rainout zone to the glaciated zone (Figure 2a) is also defined as a mixed-phase zone.

A glaciated cloud is one in which practically all of its water has turned into ice particles. Cloud-top glaciation occurs at temperatures of about  $-5^\circ\text{C}$  to  $-10^\circ\text{C}$  for clouds with well-developed coalescence, typical of maritime clouds (Figure 2a), in agreement with the laboratory experiments of Hallett and Mossop (1974). Glaciation occurs typically at about  $-15^\circ\text{C}$  for continental clouds with some coalescence (Figure 2b) or  $-20^\circ\text{C}$  for more continental clouds. In the extreme, glaciation can occur at temperatures as cold as  $-38^\circ\text{C}$  for highly continental clouds (Rosenfeld and Woodley 2000).

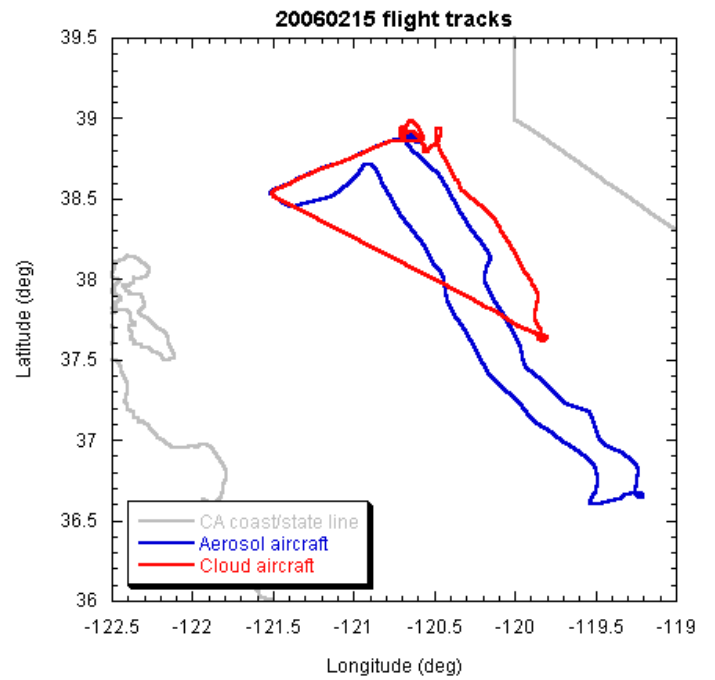
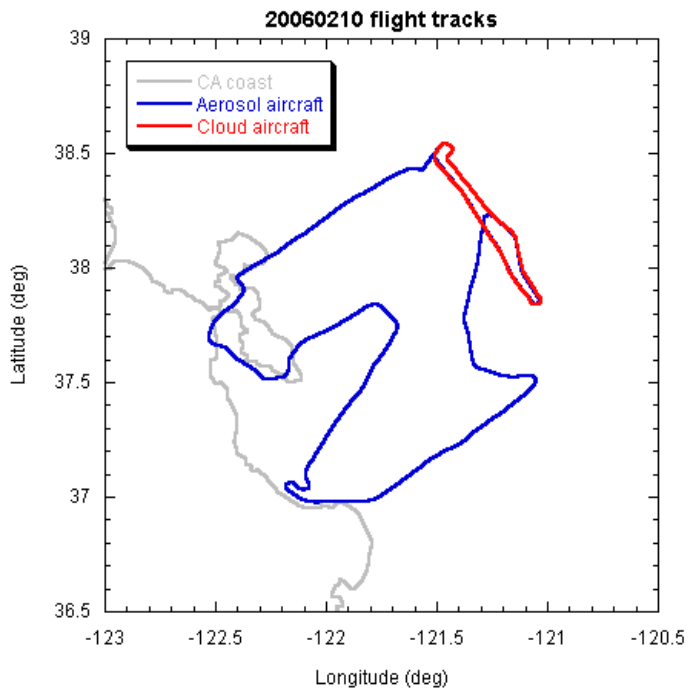
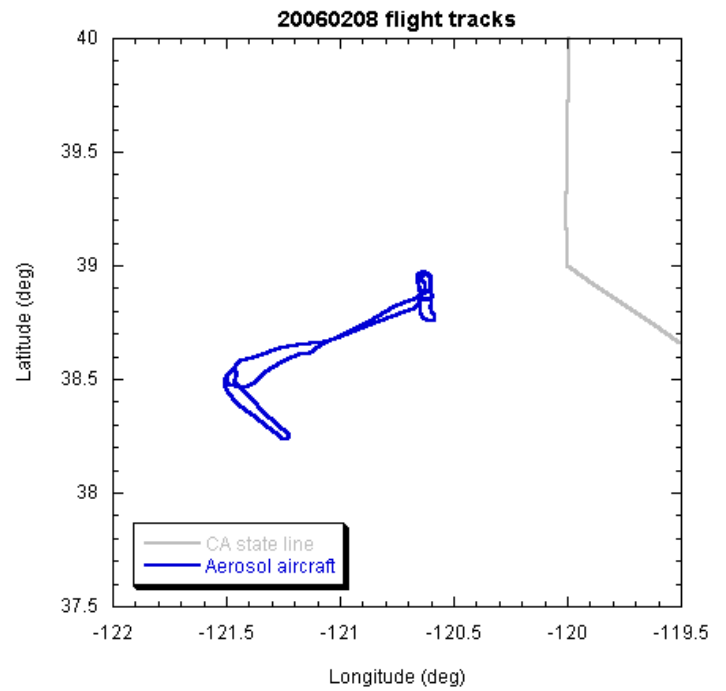
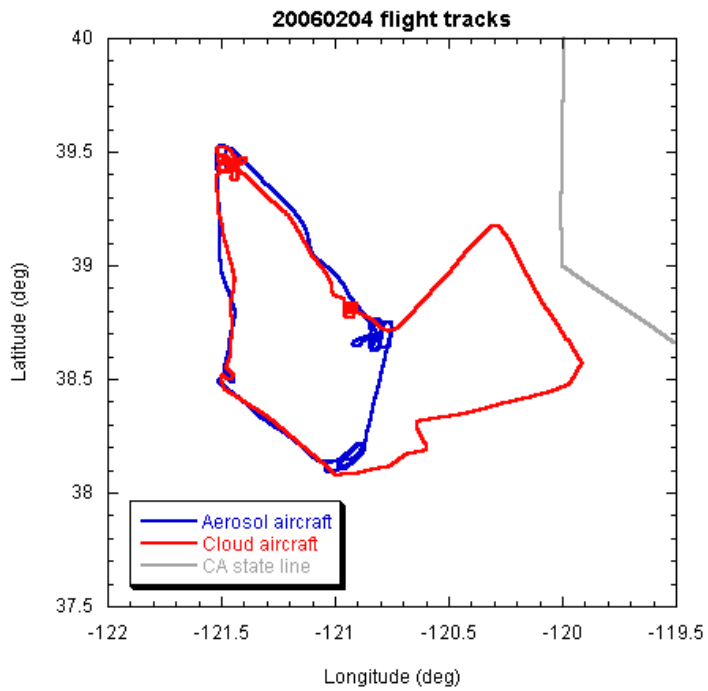
## References

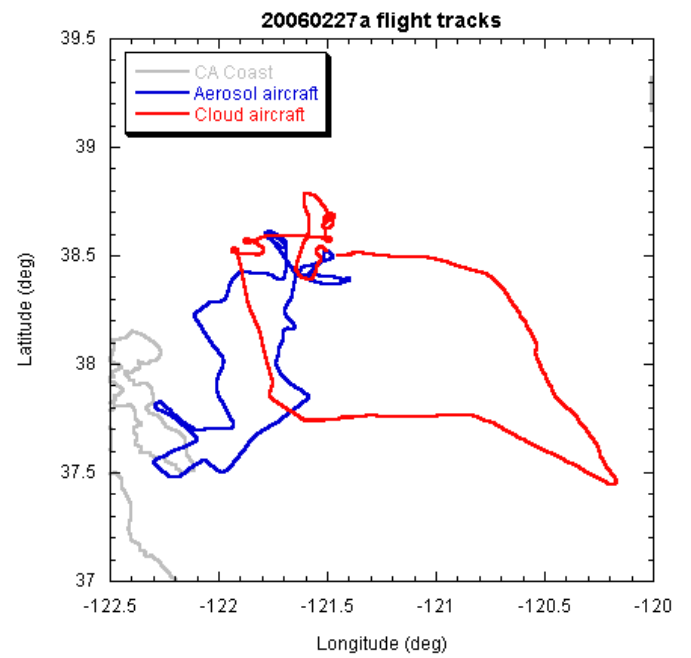
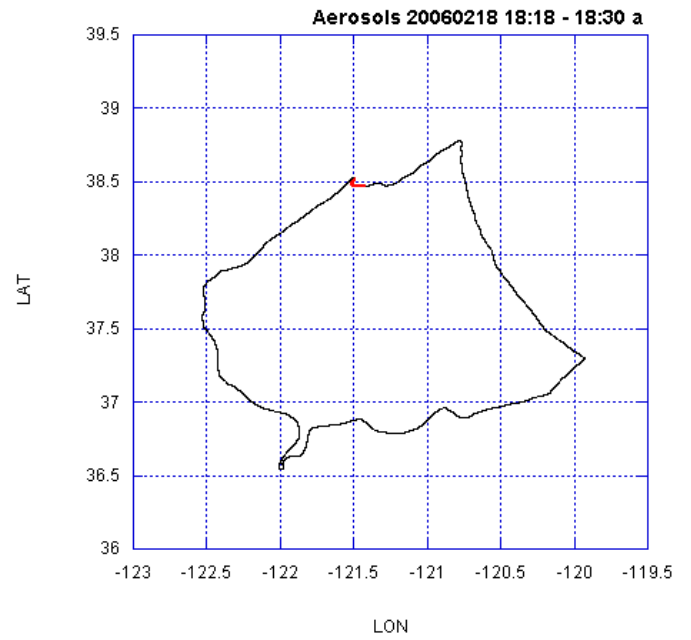
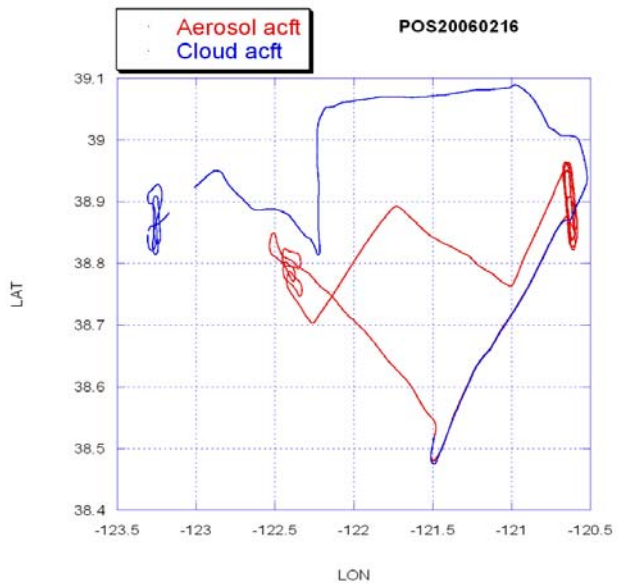
- Hallett J., and S. C. Mossopp. 1974. "Production of secondary ice particles during the riming process." *Nature* 249: 26–28.
- Lensky, I. M., and D. Rosenfeld. 1997. "Estimation of precipitation areas and rain intensity based on the microphysical properties retrieved from NOAA AVHRR data." *Journal of Applied Meteorology* 36: 234–242.
- Nakajima, T., and M. D. King. 1990. "Determination of the optical thickness and effective particle radius of clouds from reflected solar radiation measurements. Part I: Theory." *J. Atmos. Sci.* 47: 1878–1893.
- Rosenfeld D. 1999. "TRMM Observed First Direct Evidence of Smoke from Forest Fires Inhibiting Rainfall." *Geophysical Research Letters* 26(20): 3105–3108.
- Rosenfeld D. 2000. "Suppression of Rain and Snow by Urban and Industrial Air Pollution." *Science* 287(5459): 1793–1796.
- Rosenfeld, D., and G. Gutman. 1994. "Retrieving microphysical properties near the tops of potential rain clouds by multispectral analysis of AVHRR data." *Atmospheric Research* 34: 259–283.
- Rosenfeld D., and I. M. Lensky. 1998. "Satellite-based insights into precipitation formation processes in continental and maritime convective clouds." *The Bulletin of American Meteorological Society* 79: 2457–2476.
- Rosenfeld, D., and W. L. Woodley. 2000. "Deep convective clouds with sustained supercooled liquid water down to -37.5°C." *Nature* 405: 440–442.

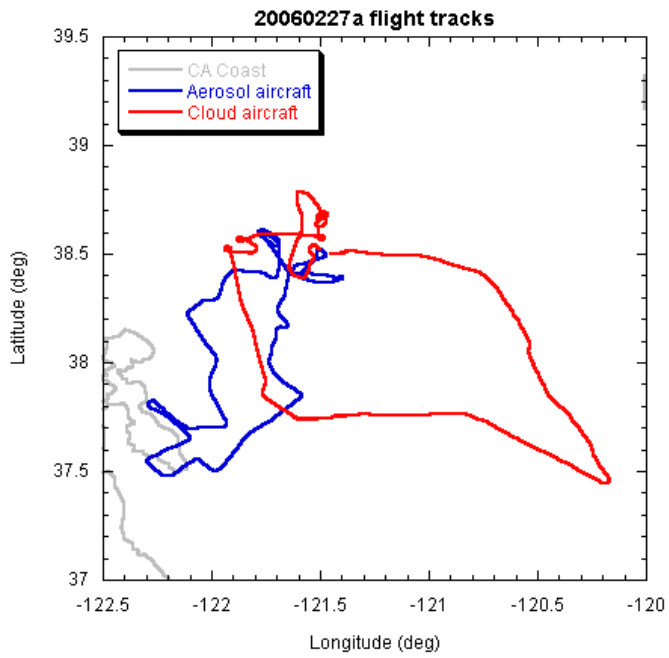
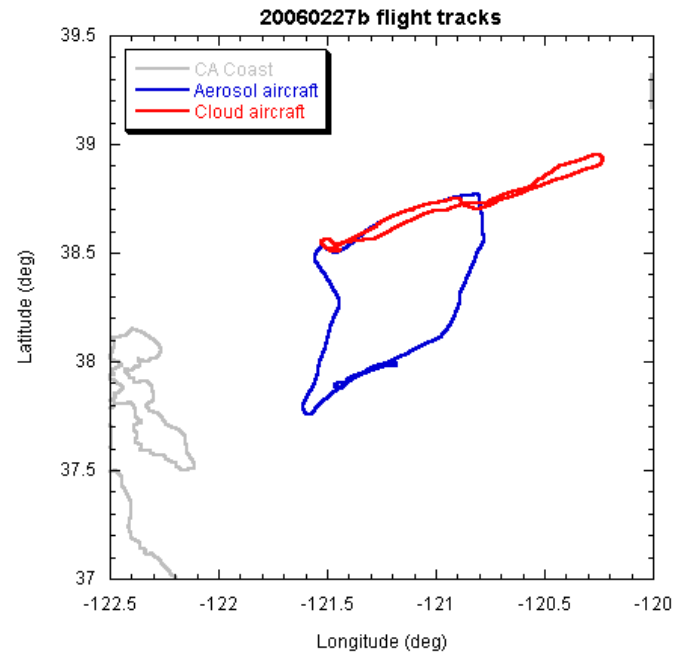
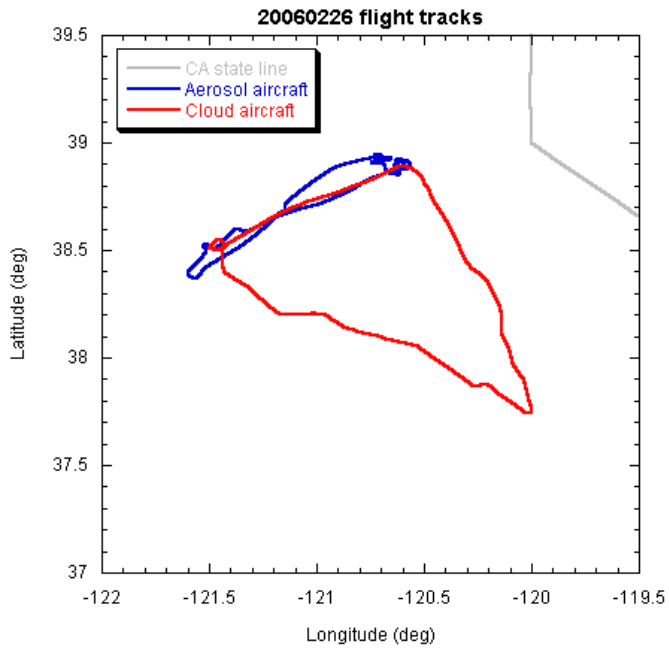
## **Appendix E**

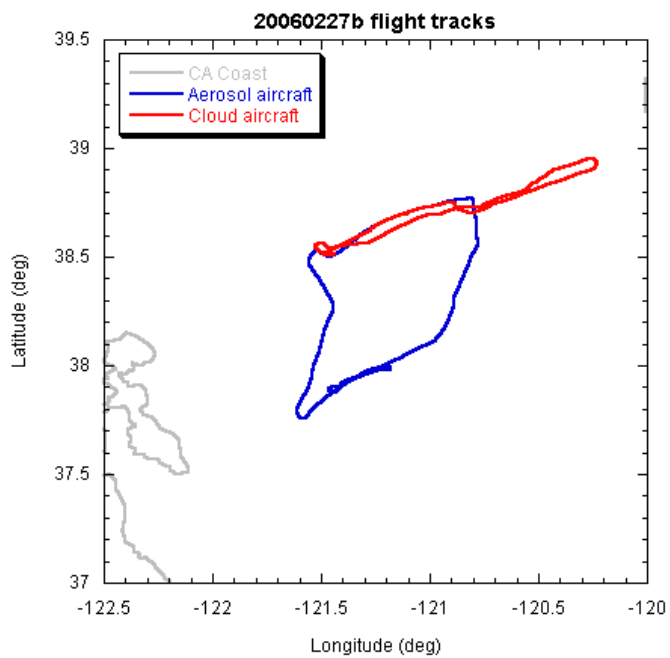
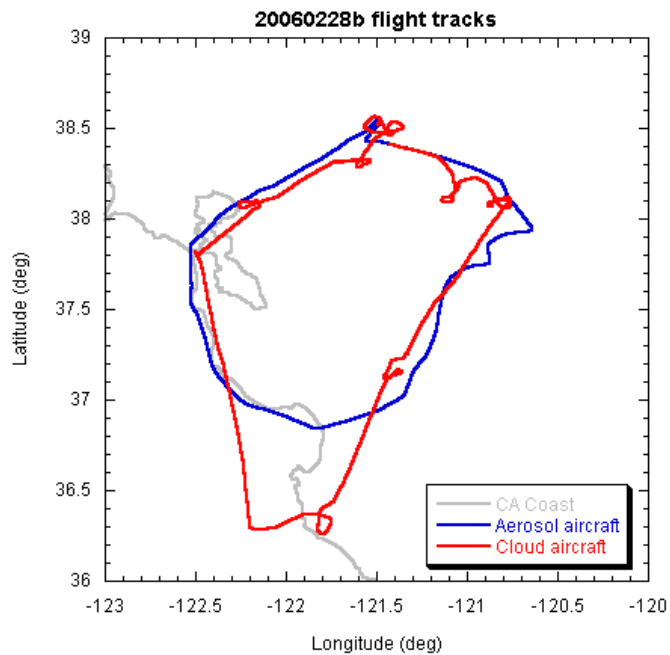
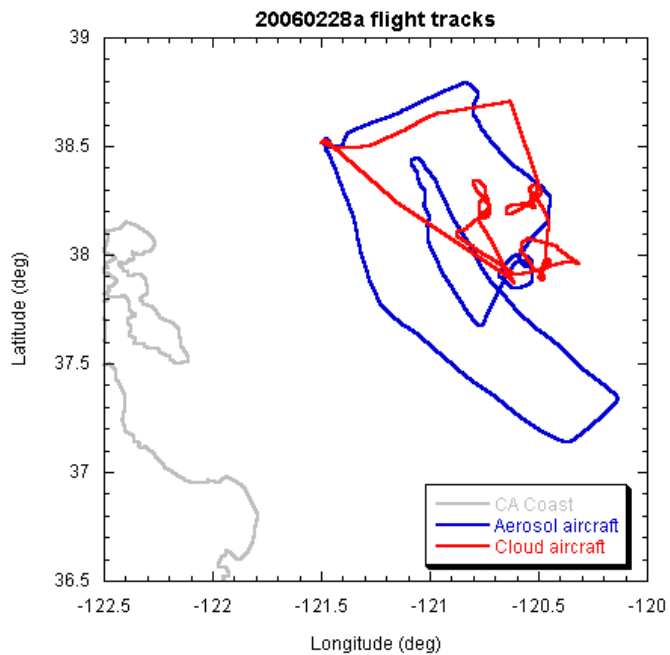
### **Presentation of Flight Tracks and Plotted Data for Flights of the Cloud Physics and Aerosol Aircraft**

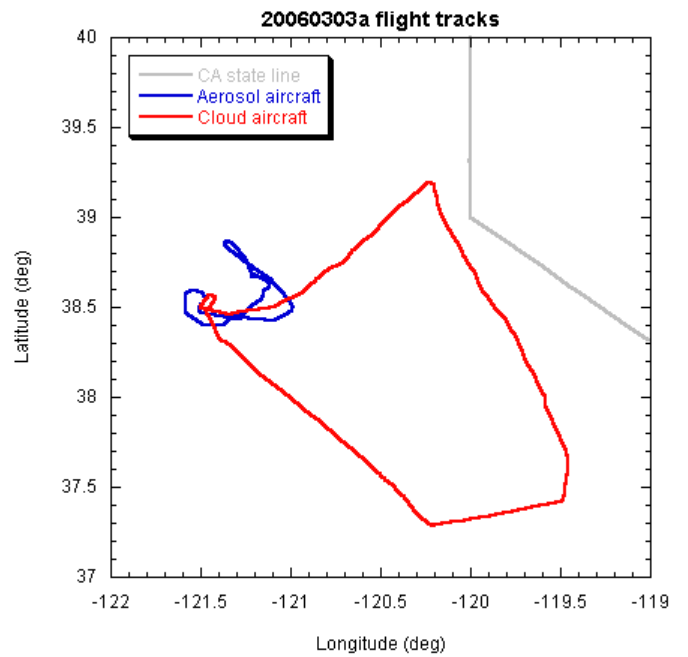
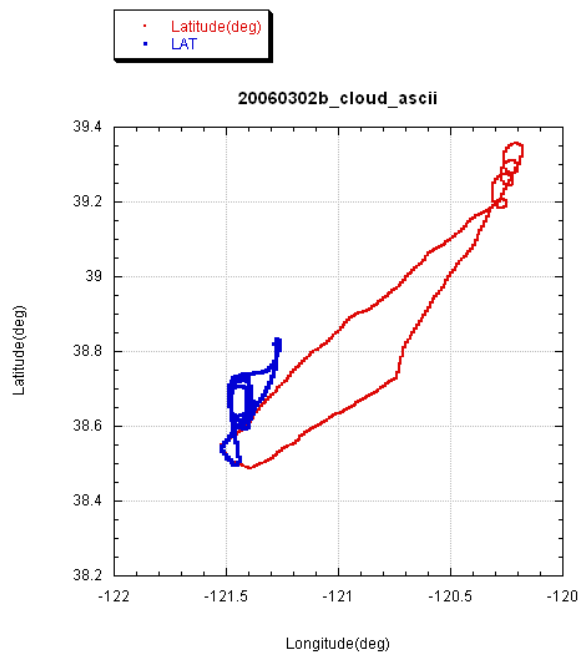
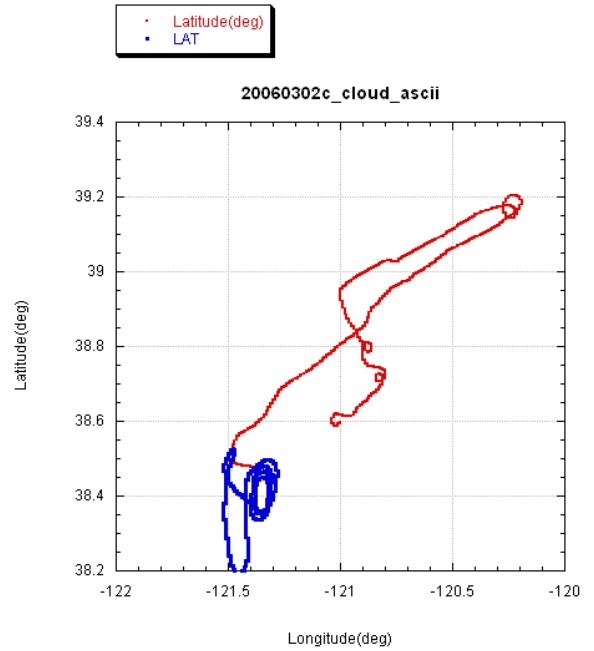
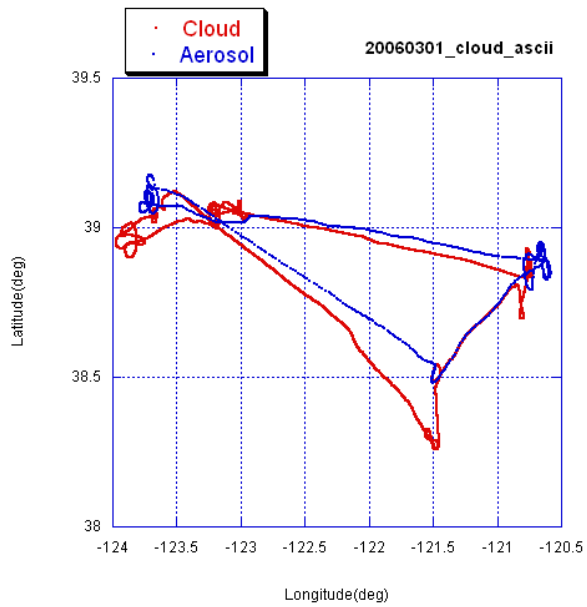


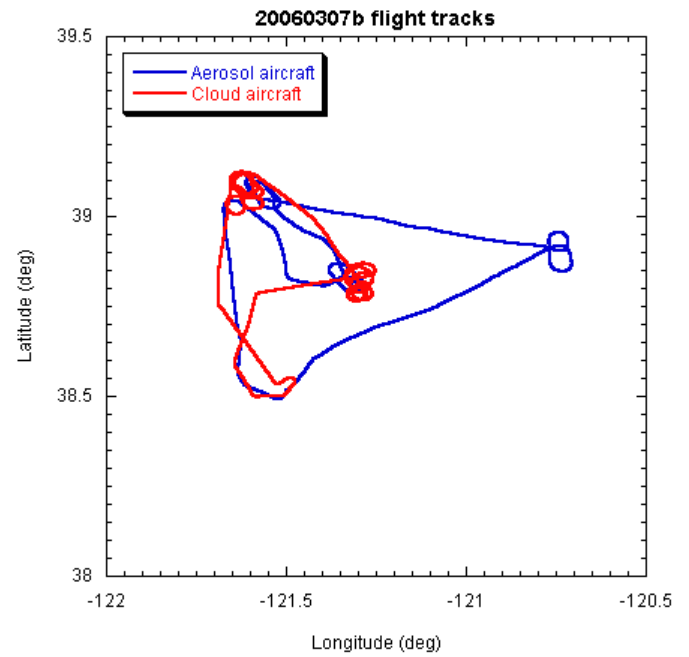
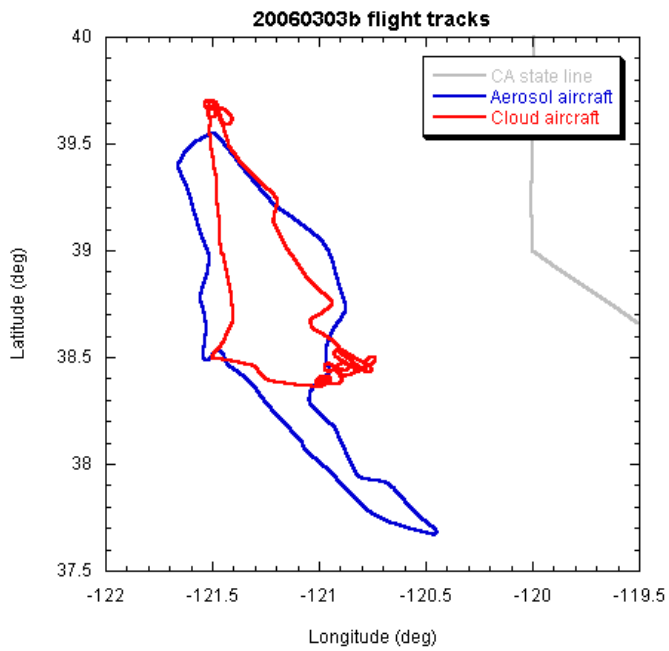
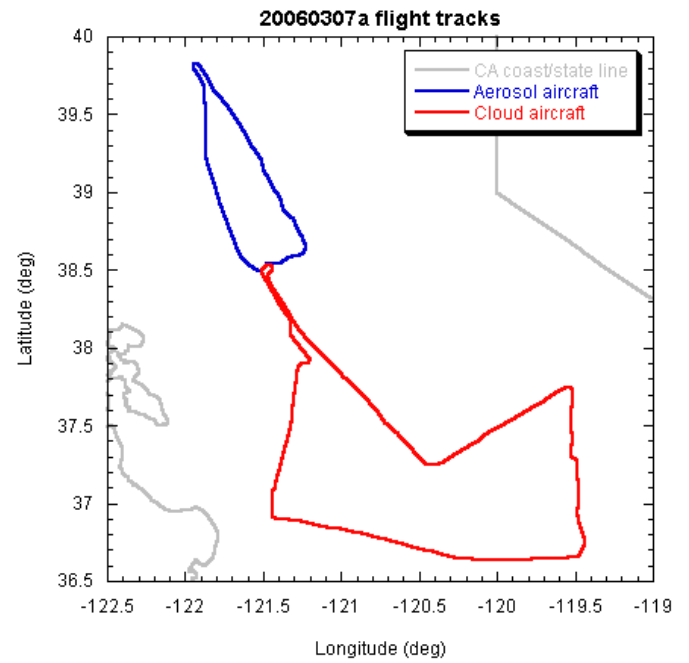
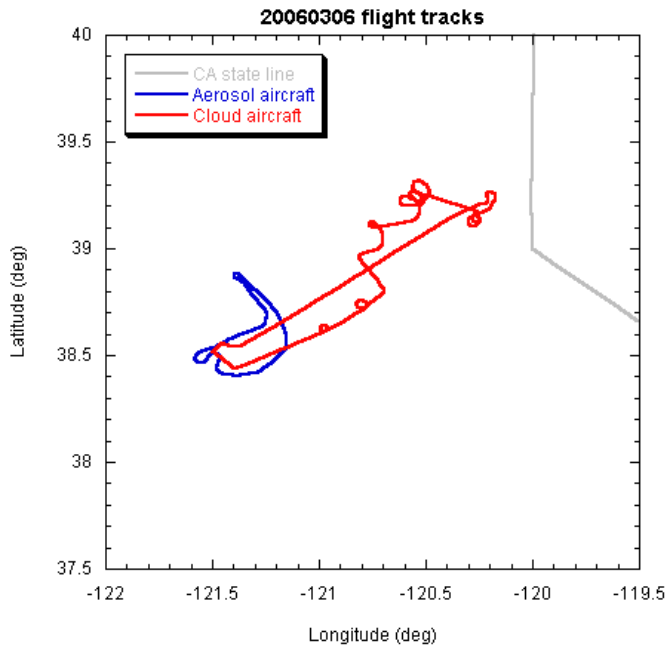


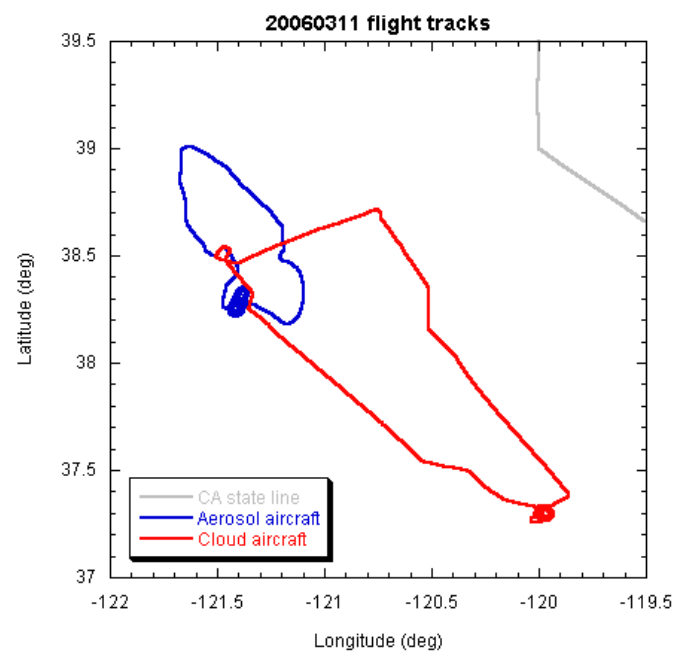
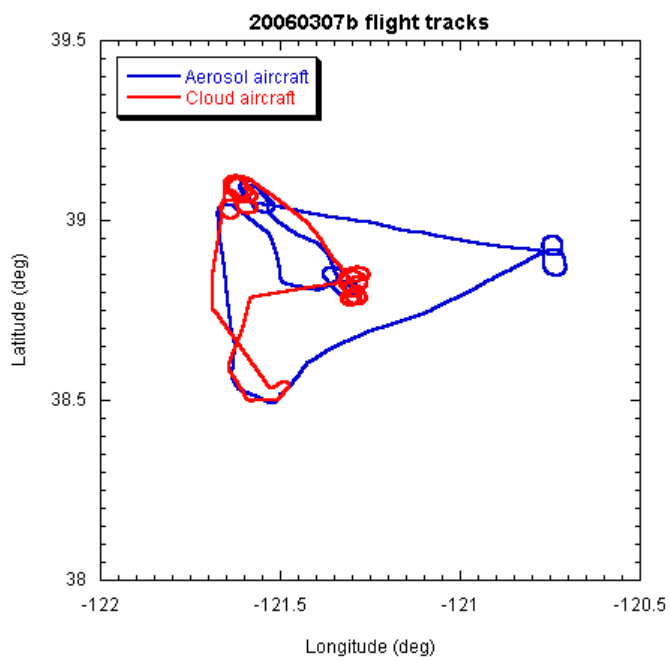
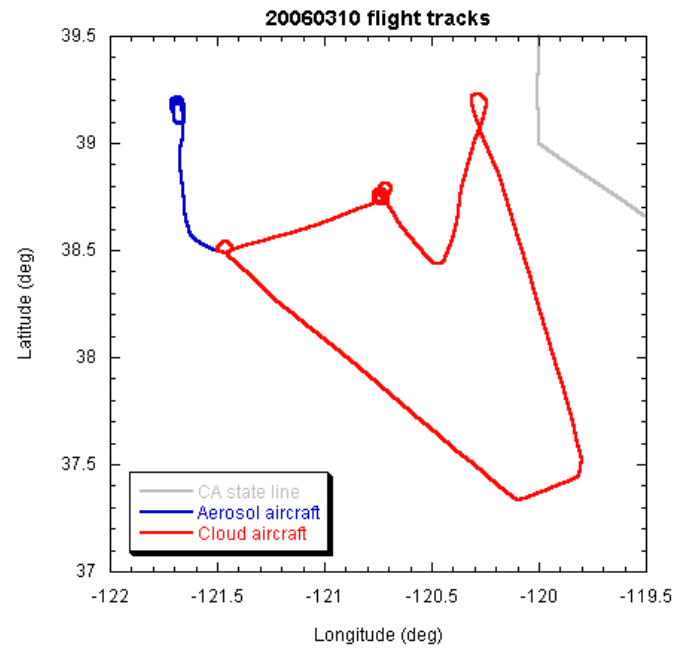
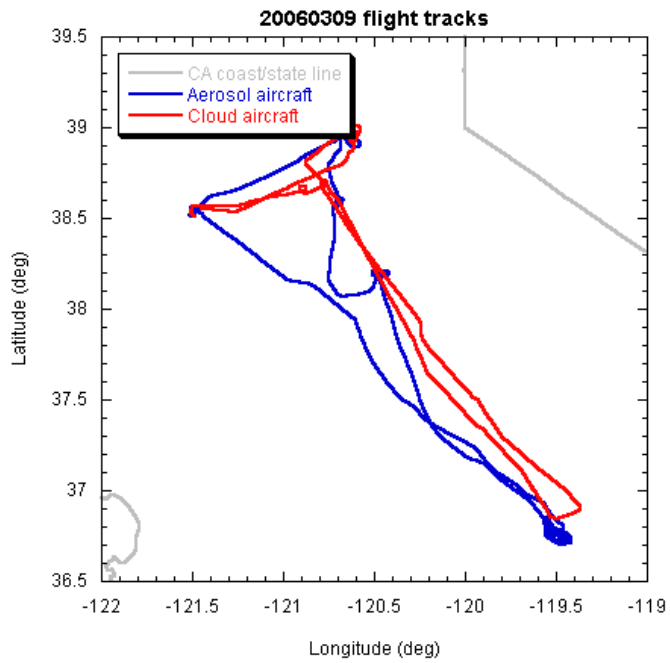


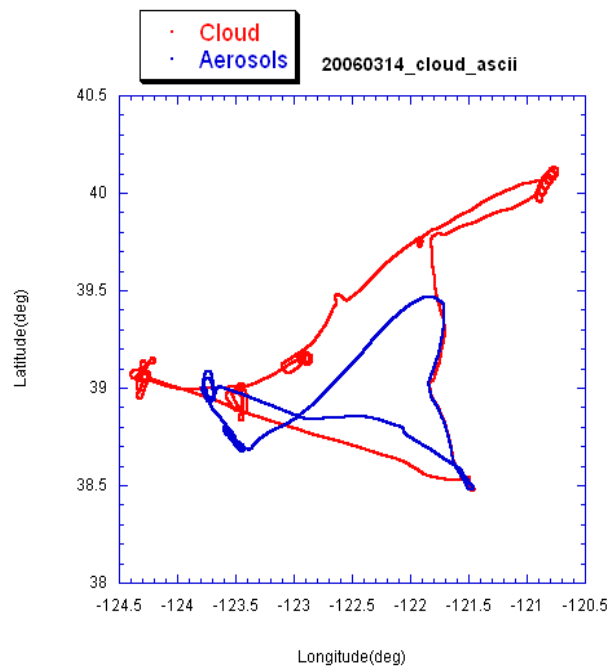
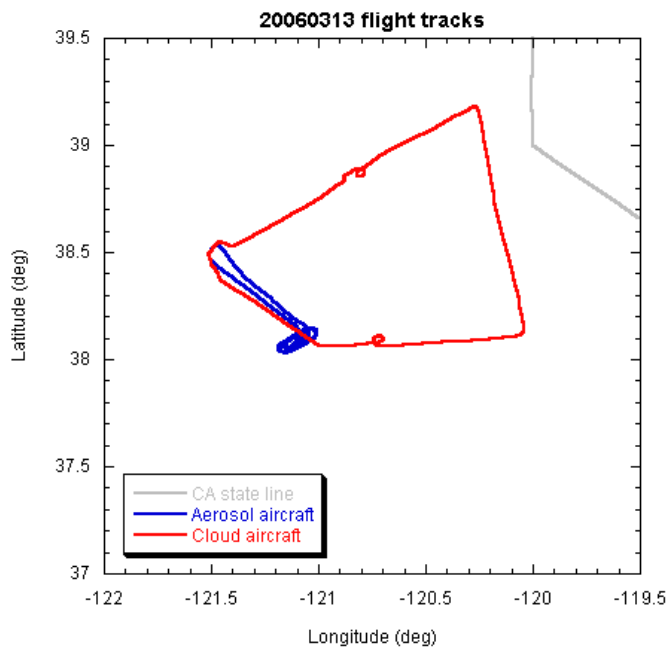


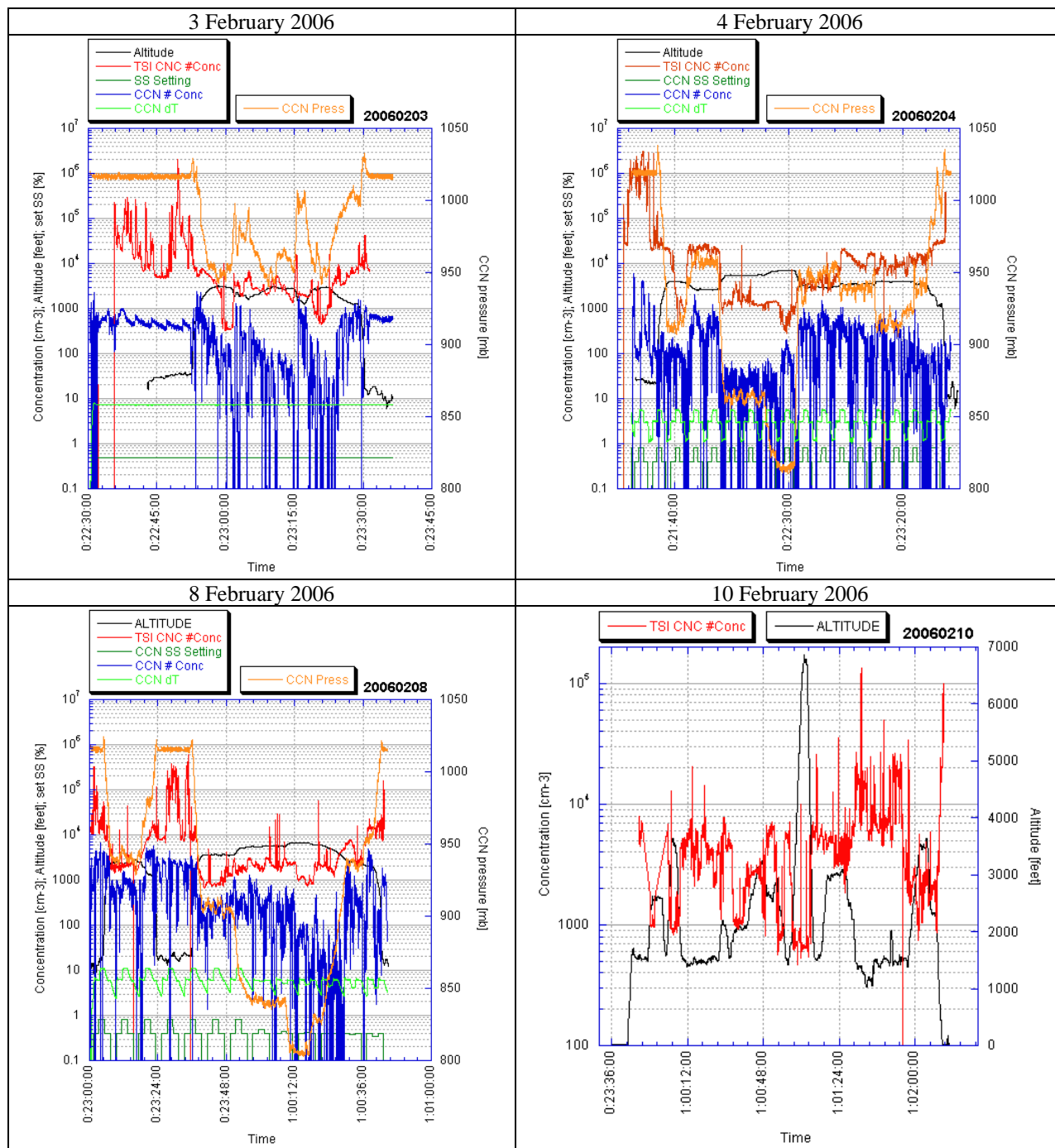


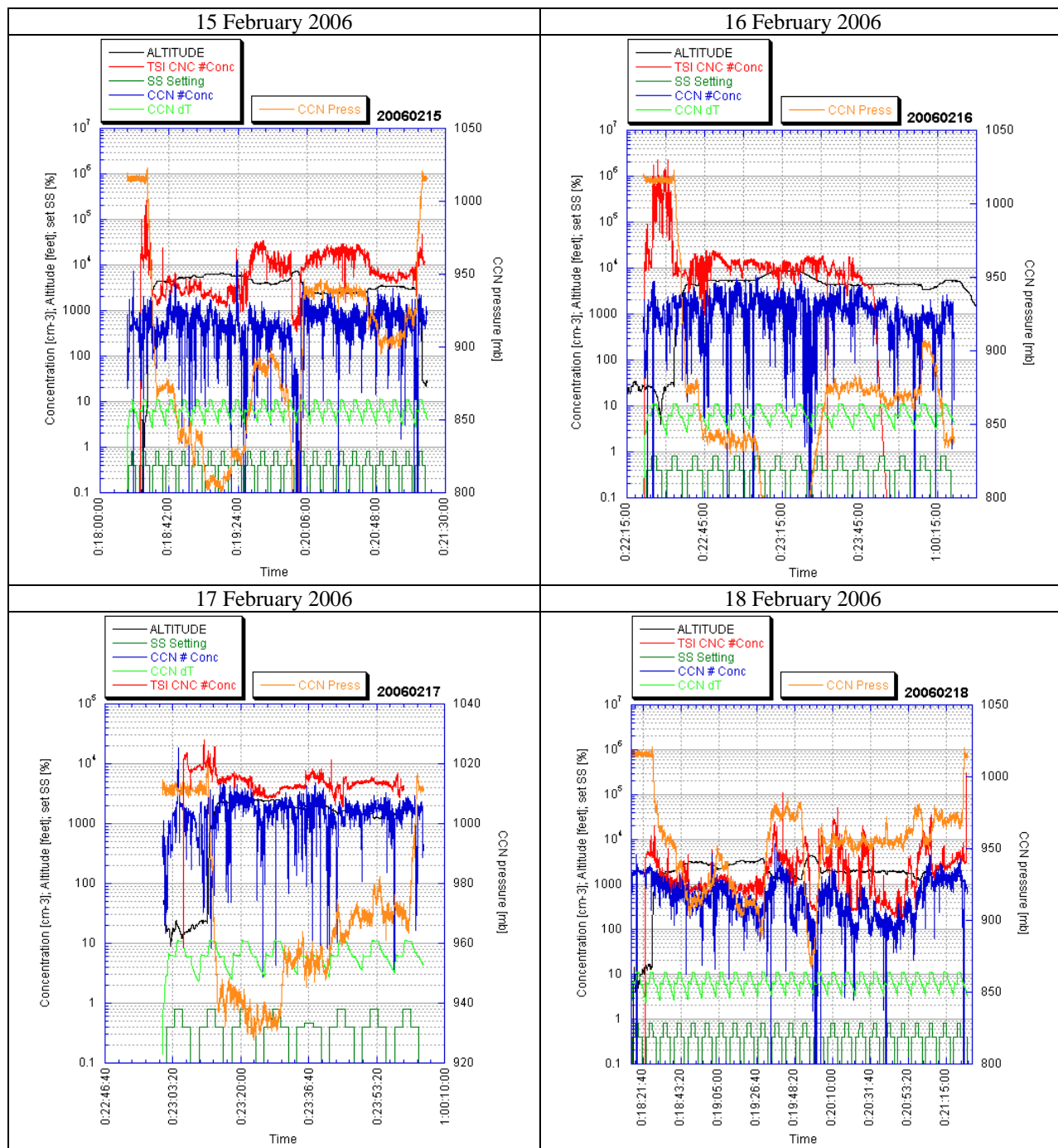


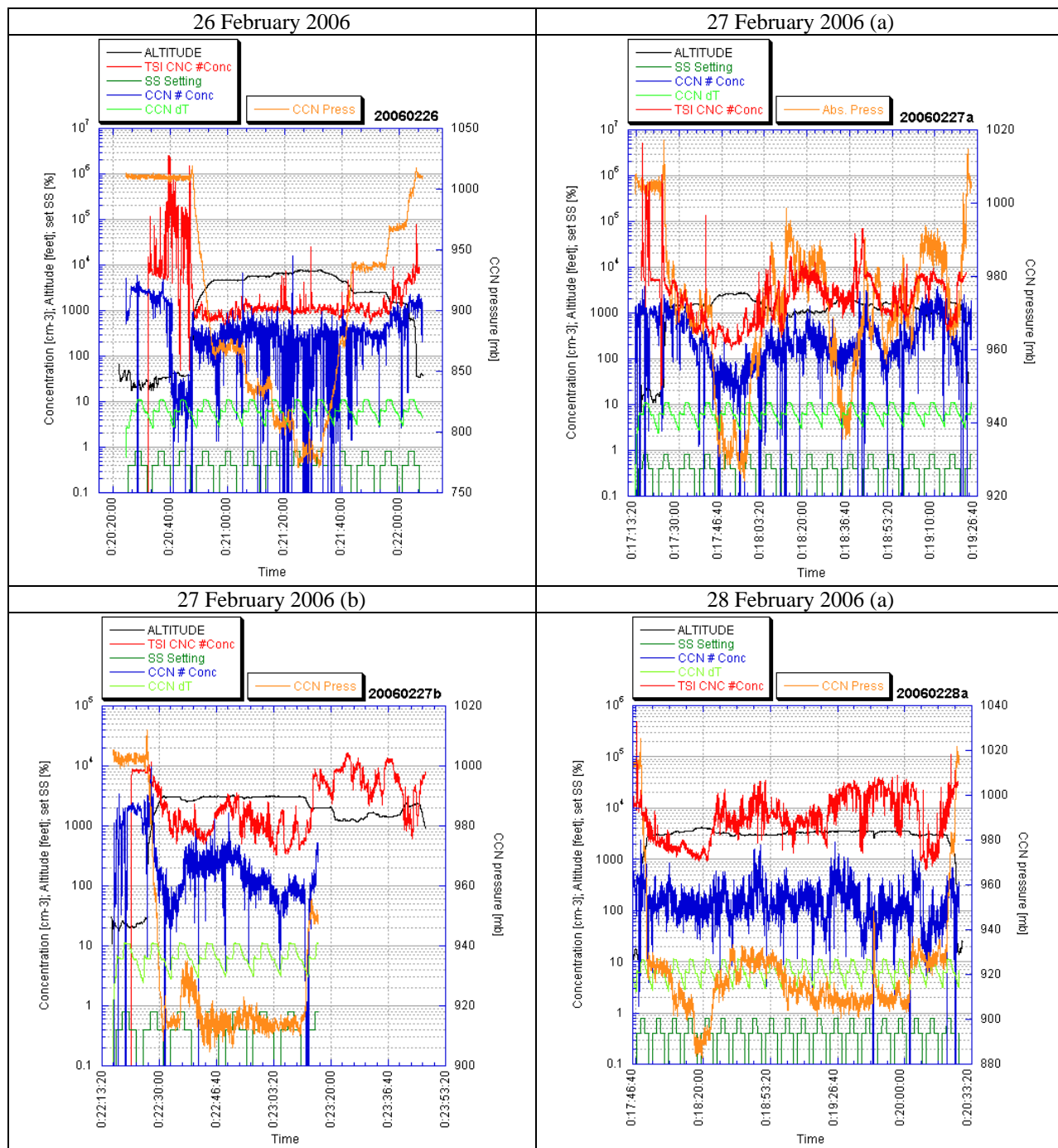


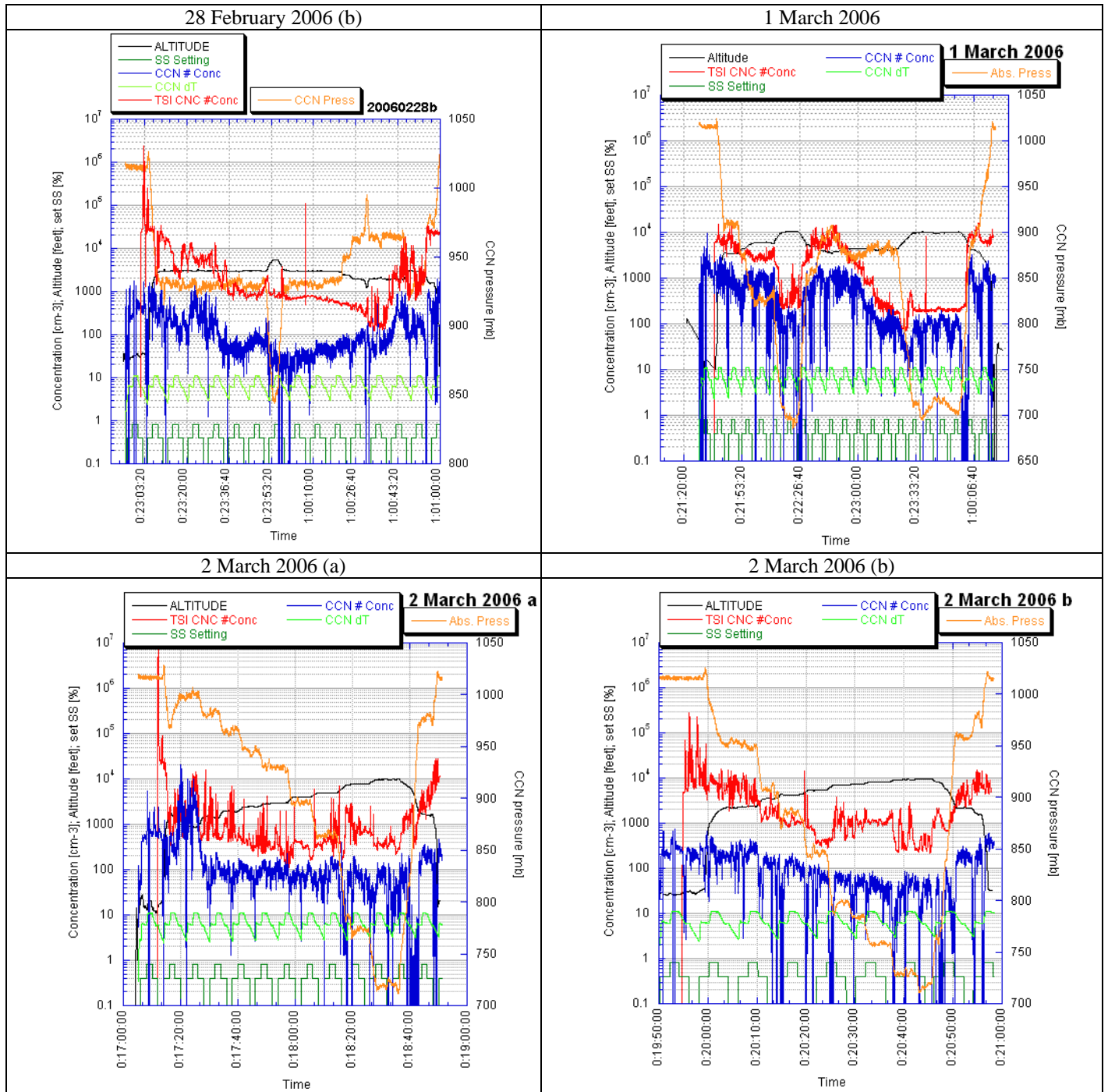


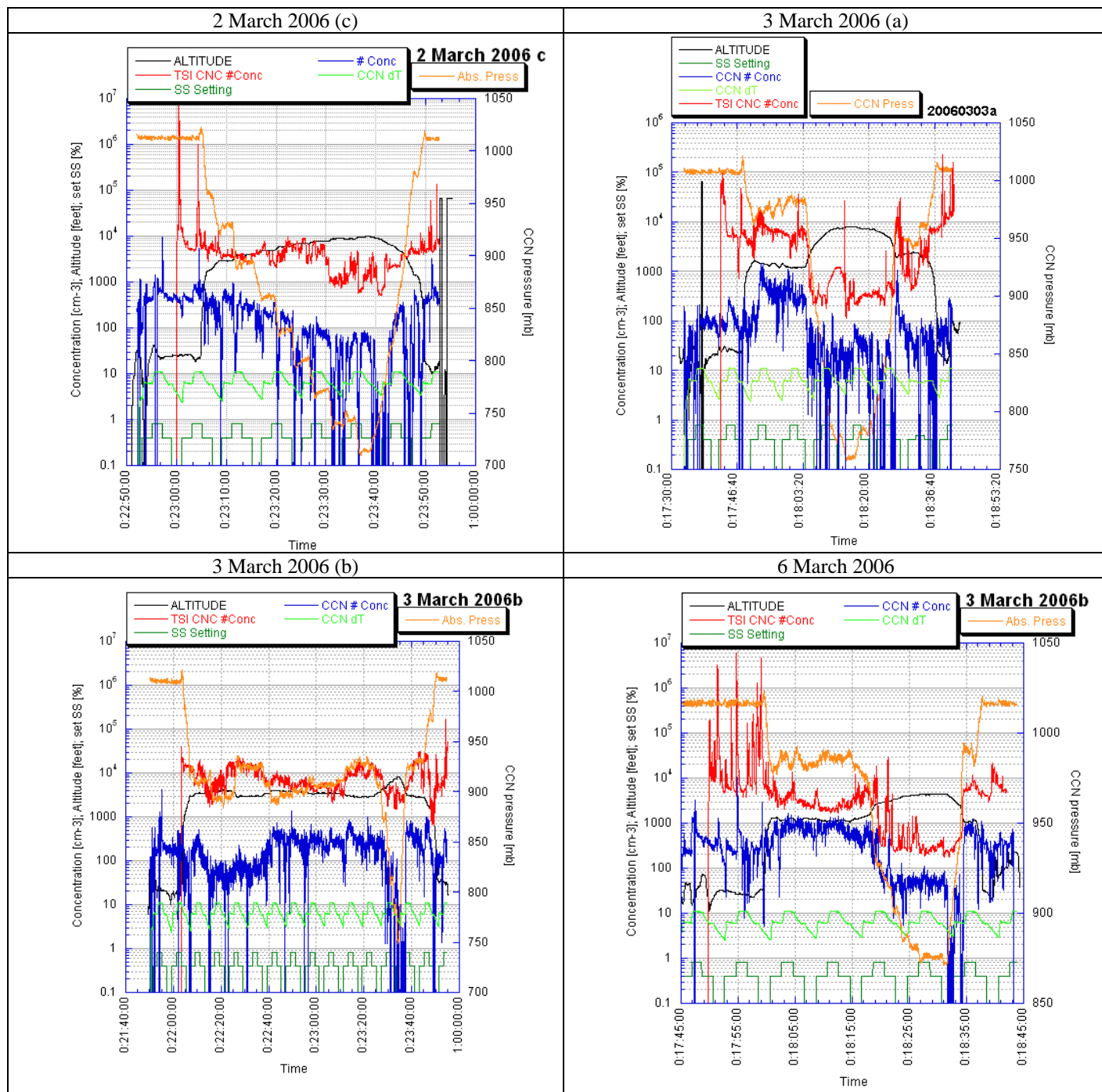


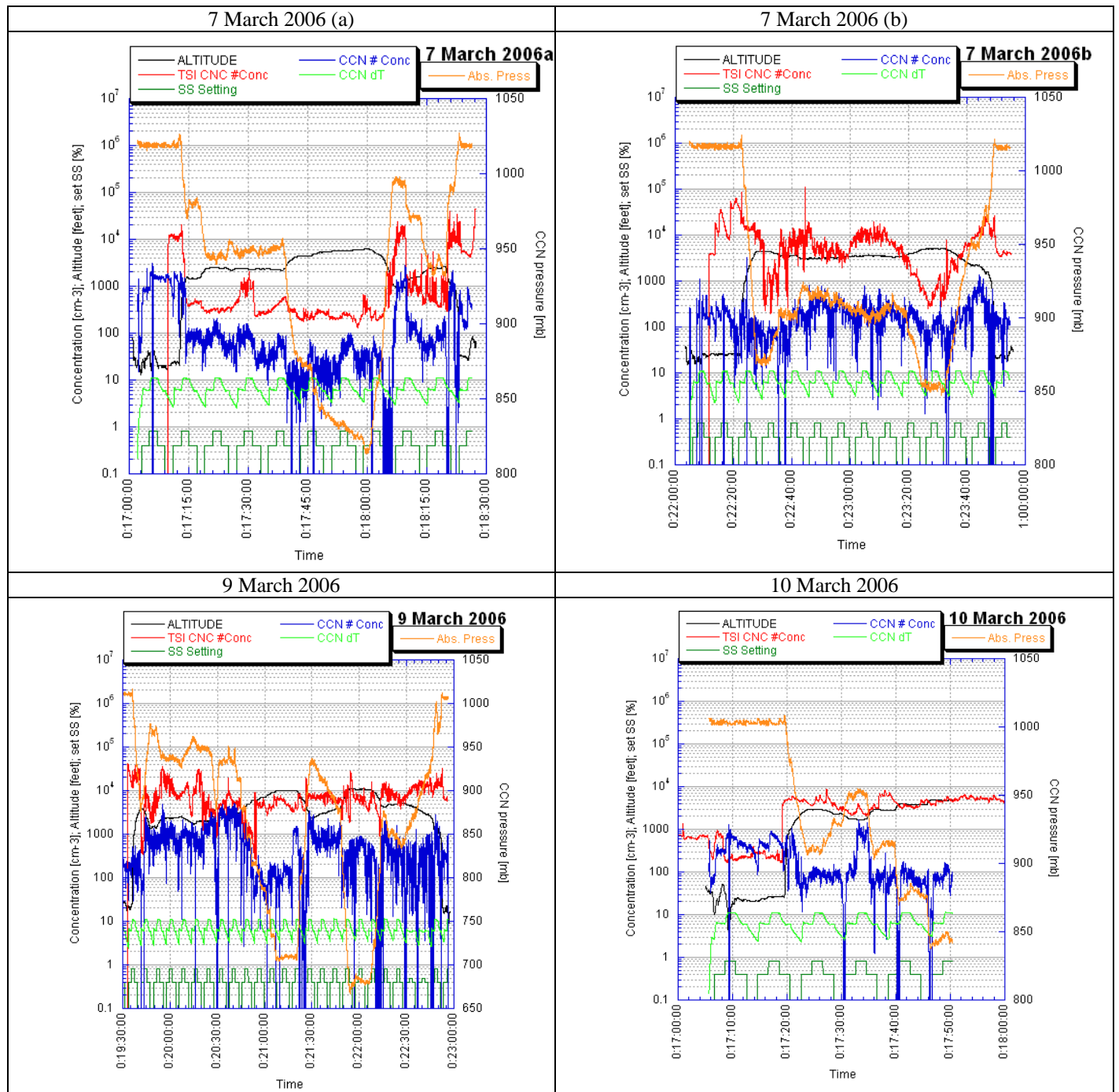




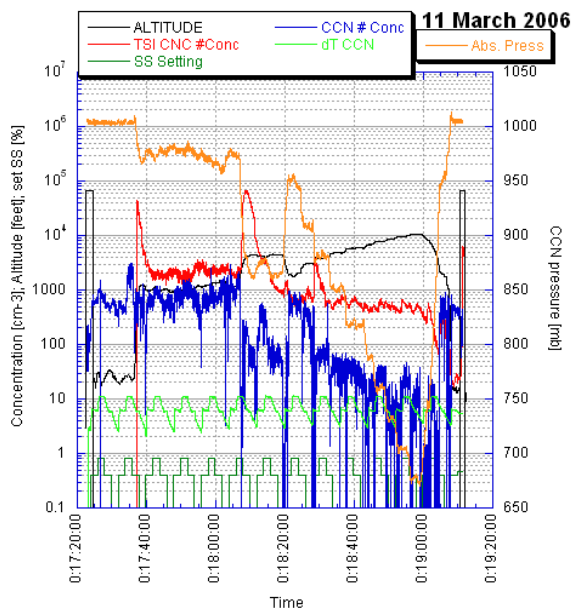




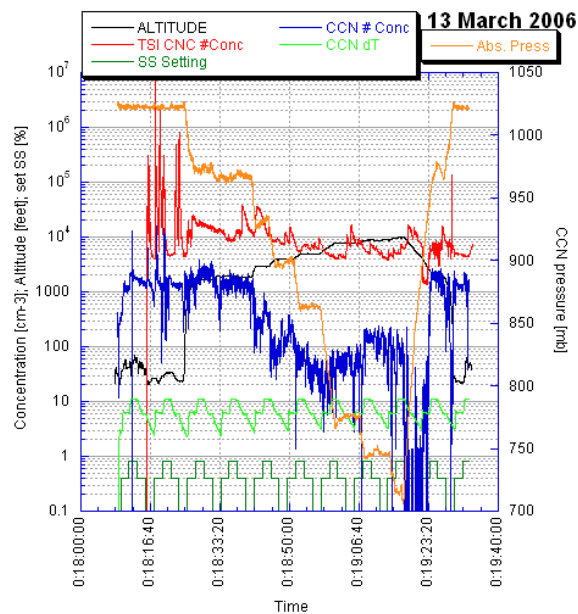




11 March 2006



13 March 2006



14 March 2006

